Synthesis, Characterization, and Gas Permeation Properties of Novel Cellulose Derivatives

Fareha Zafar KHAN

2008

To Mom and Daddy,

for their profound love and care.

To Filza, Faiza and Awais,

for their unflinching support and encouragement.

To Irfan,

for being there whenever I needed him, always.

Table of Contents

General Introduction

Research Background

Life is a marvelous and the most mesmerizing endowment by *Mother Nature* upon the lovely Earth planet witnessing its vital eminence in the wilderness of universe. The remarkable display of the ultimate impeccability undoubtedly seems to stem forth from the unexcelled selection of the building blocks; each and every form of life portrays an ample interplay of the integral entities commonly regarded as biopolymers, materials for life.

Billions of years ago, in fact all the way back to the dawn of all existence, nature has been playing with natural polymeric materials to make life possible; cellulose constituting the body covering of plants and providing apparel and shelter for humans; starch serving as a foodstuff; proteins composing our bodies, administering metabolic events, and furnishing fine ensemble; and finally of utmost significance are DNA and RNA, the biopolymers playing a vital role in our genetic and life processes.

Cellulose, the most abundant natural polymeric material on the earth, being endowed with an almost inexhaustible existence, an environmentally benign nature, and fascinating structural features, enjoys the most remarkable functional attributes ever conceivable beyond the realm of nature. As old as the history of mankind, cellulose has found a multitude of applications in the form of wood, cotton, and other plant fibers as a source of energy, building material and apparel; and has most significantly contributed to human culture and civilization in the form of paper.[1]

Cellulose is an organic polymer existing in the greatest abundance, comprising about 1.5×10^{12} tons of the total annual biomass production and is expected to foster the escalating demand for the low cost as well as environment-friendly and biocompatible polymeric products.[2] Wood pulp has served as the most significant raw material source for cellulose processing till today, being employed extensively for paper and cardboard manufacturing, while about 2% ($\geq$ 3 million tons) utilized for the production of regenerated cellulose fibers and films, and to synthesize various

cellulose derivatives via esterification and etherification. Wood cellulose exists as a native composite material with lignin and other polysaccharides seeking a passage through chemical pulping, separation, and purification for the sake of isolation while the seed hairs of cotton as another source of botanical origin offer an almost pure form of cellulose.

Depending upon the origin and/or mode of synthesis, there are four different pathways to access the most abundant natural polymeric material (Scheme 1) with plants being the most prominent source as mentioned earlier. Apart from plants, the second major source of cellulose also belongs to the natural habitat including bacteria, algae, and fungi, producing cellulose forms with specific supramolecular architecture employed as model substances for various research endeavors in the domains of organic as well as polymer chemistry. The past few decades of investigation have

Scheme 1. Principle Pathways to Cellulose Formation

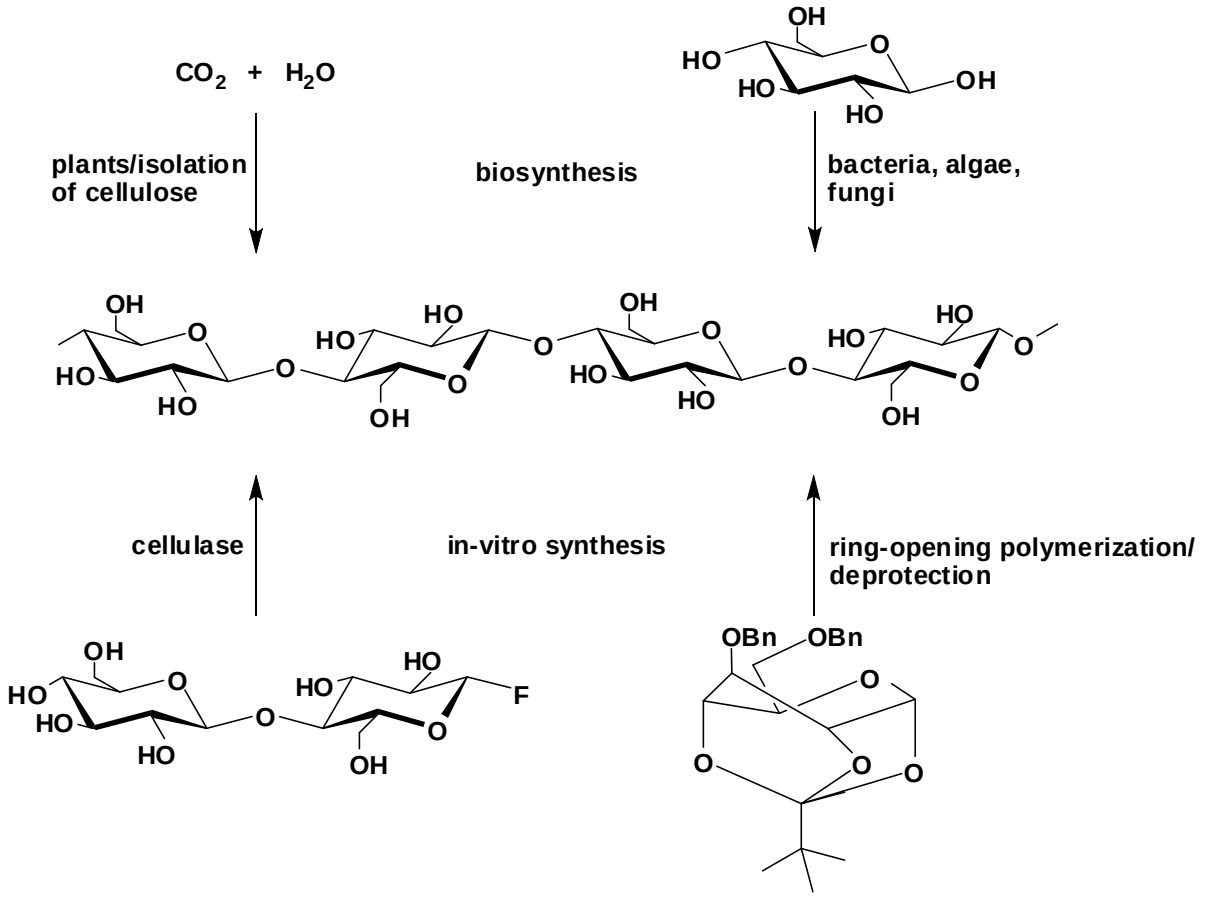

revealed that the biosynthesis of cellulose has been a part of the life cycle of cyanobacteria for over 3.5 billion years.[3]

Recent years have witnessed an exciting development in the synthesis of naturally occurring polymers, namely in-vitro synthesis of cellulose, opening up new vistas on the horizon of macromolecular architecture.[4] Kobayashi and co-workers were the first to report the cellulase-catalyzed synthesis of cellulose starting from cellobiosyl fluoride[5] while Nakatsubo et al furnished the first example of chemosynthesis of cellulose employing the ring-opening polymerization of substituted D-glucose derivatives.[6]

All the magnetism and beneficence of this fascinating biopolymer emanates from its specific structure, epitomizing an amazing conjunction of carbohydrate and polymer chemistry, drawing its roots from a low molecular weight carbohydrate, glucose, and emerging into the world of macromolecules with surprisingly specific and impressively diverse architectures, reactivity, and functions.

The repeated connection of D-glucose building blocks, constituting the idiosyncratic cellulosic framework, bestows this homopolymer with unique structural peculiarities of extensive linearity, chain stiffness, chirality, hydrophilicity, and biodegradability, high degree of functionality, broad derivatization/modification capability, versatile fiber morphologies, and supramolecular architecture.

Figure 1. Structure of Cellulose

The molecular structure of cellulose is illustrated in Figure 1 delineating a carbohydrate polymer, comprised of β-D-glucopyranose units with acetal functions accomplishing the β-1,4-glucan linkage (between the equatorial hydroxy groups on C4 and C1 carbon atoms) with every second unit rotated 180° in the plane in order to accommodate the acetal oxygen bridges in the preferred alignment, as it is

biogenetically formed. The presence of β-1,4-glycosidic linkage leads to an extensively linear polymeric structure with a large number of hydroxy groups (three per anhydroglucose (AGU) unit) present in the thermodynamically preferred $^4C_1$ conformation. The OH groups in cellulose are responsible for extensive hydrogen bonded networks imparting a variety of partially crystalline fiber structures and morphologies. The distinct polyfunctionality, high degree of chain stiffness, and sensitivity of the acetal linkages towards hydrolysis and oxidation are the most significant parameters in determining the role of cellulose in the world of synthesis and derivatization. Furthermore, the chemical reactivity and properties of cellulose are greatly influenced by the intermolecular interactions, chain lengths, chain-length distribution, and by the distribution of functional groups on the repeating units and along the polymer chains.

Cellulose has been exploited as a chemical raw material for about 150 years.

Scheme 2. Cellulose Esters of Commercial Significance

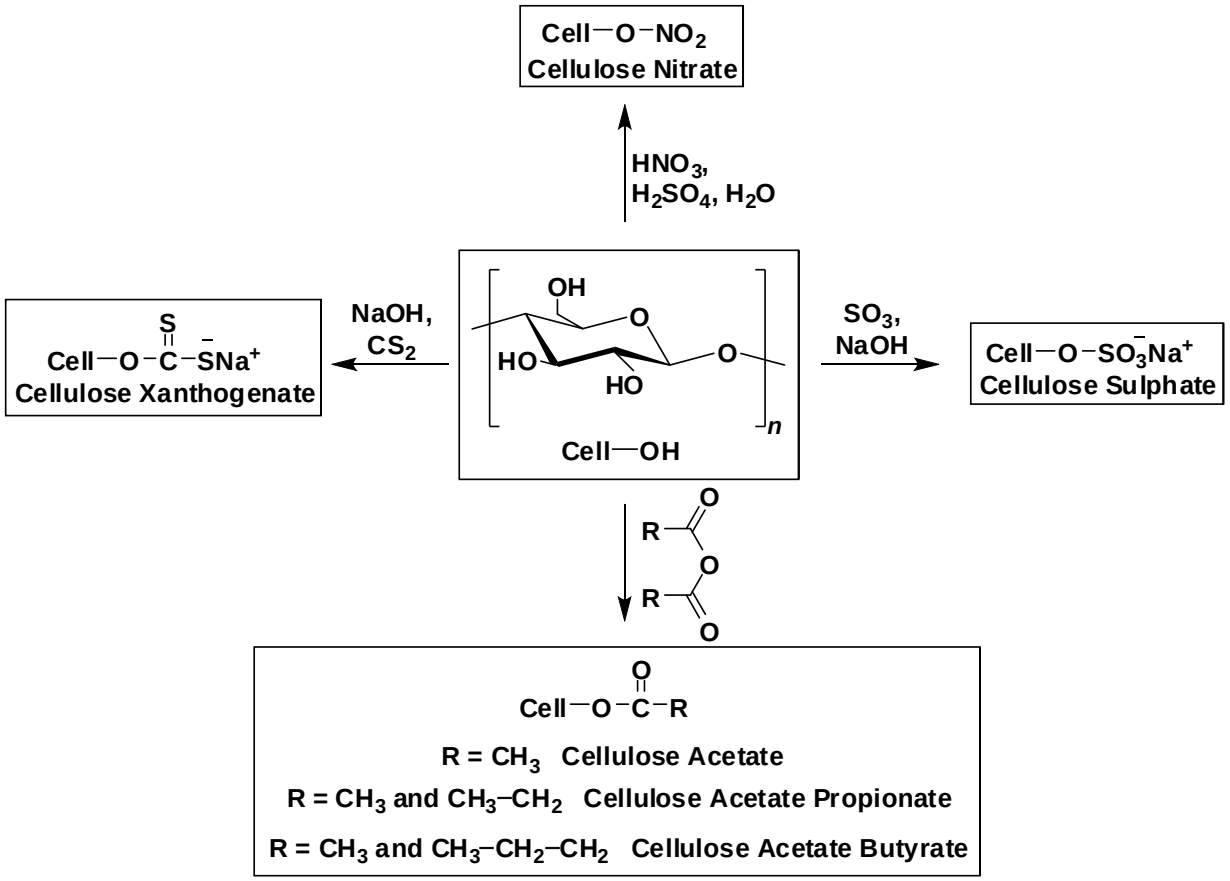

The synthesis of cellulose nitrate laid the foundations for the chemical derivatization of the inexhaustible natural polymer followed by the synthesis of first thermoplastic polymer called celluloid in 1870, marking a milestone in the history of polymer science that revolutionized our modern life style.[7,8] Since then there became an avalanche of man-made or regenerated cellulose fibers based on wood pulp rather than native cellulose fibers, for textiles and technical products. Rayon is the oldest regenerated cellulosic fiber having been in commercial production since 1880s in France, where it was originally developed as a cheap alternative to silk, followed by the viscose process, currently the most important large scale technical process in fiber production,[9] and finally by the Lyocell process, an industrial breakthrough opening new frontiers in the field of environment-friendly fiber technologies.[10,1a]

By far now, the ester and ether derivatives of cellulose (exemplified in Schemes 2 and 3) have been lauded as the trail-blazing candidates of cellulose

Scheme 3. A Few Examples of Commercial Ethers

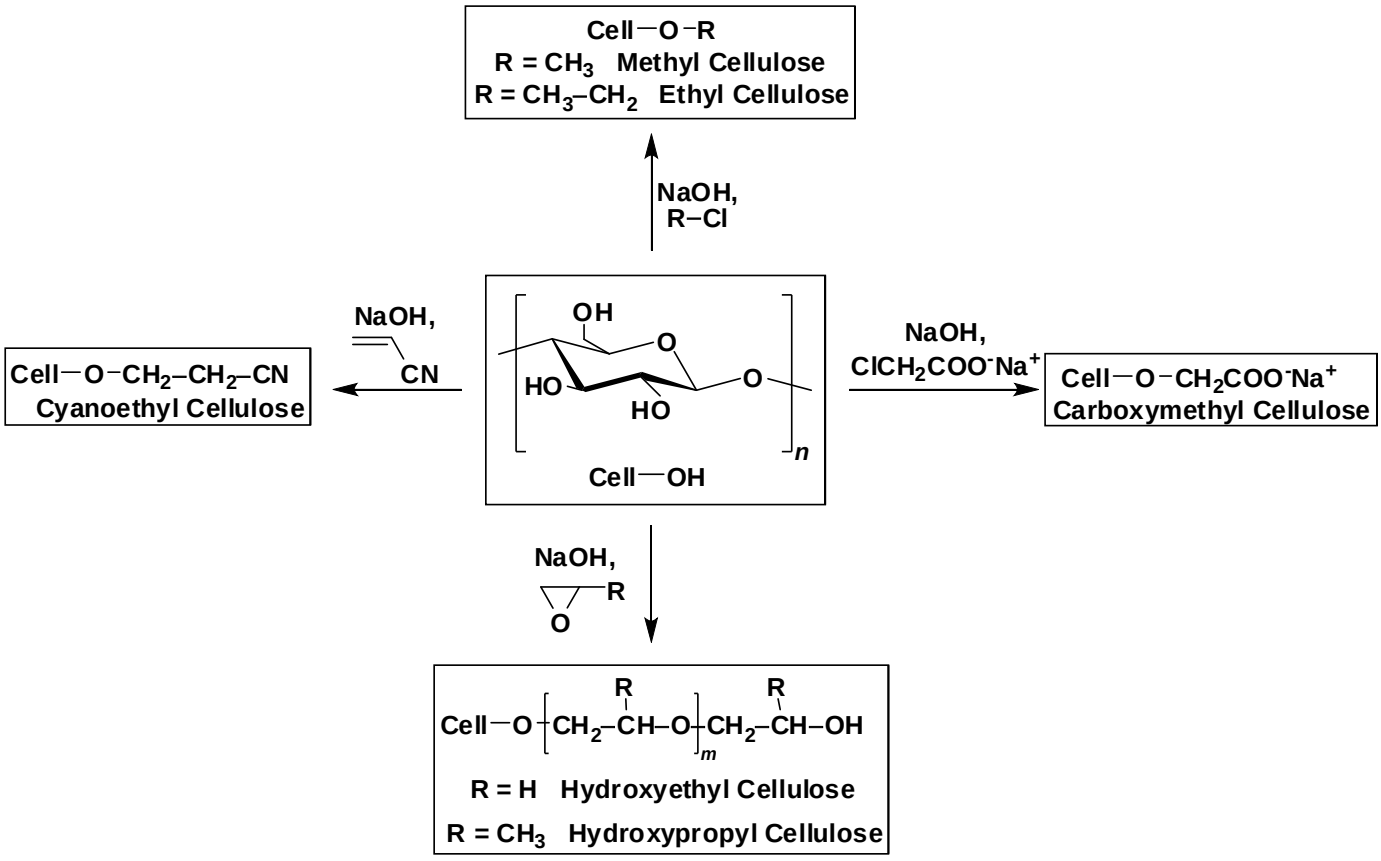

chemistry offering the most distinct and momentous applications of commercial and technical significance. Cellulose esters have found a variety of applications as classical material-coatings and controlled-release systems while recent developments include enteric coatings, hydrophobic matrices, and semipermeable membranes for applications in pharmacy, agriculture, and cosmetics. Furthermore, to serve the quest for high-performance materials based on renewable resources, cellulose esters are being widely employed as binders, fillers, and laminate layers in composites and laminates, as excellent material for photographic films, and as membrane-forming materials serving for gas separation, water purification, food and beverage processing, medicinal and bioscientific applications.[11] On the other hand, cellulose ethers on account of good solubility, high chemical resistance, and non-toxic nature are being utilized in drilling technology and building materials, as additives for drilling fluids to provide consistency control and to control the rheology and processing of plaster systems, and function as stabilizers in food, and constitute the principle ingredients of pharmaceutical and cosmetics formulations as well.[12]

Recently, there has been an intense interest to exploit the biocompatibility, biodegradability, and chirality of naturally occurring renewable sources of polymeric materials. The past few years have witnessed an extensive research activity to elucidate the new ways of synthesis and to unveil the unique properties of cellulose-based materials expected to find a myriad of applications as liquid crystalline materials,[13] as biomaterials,[14] in enantioselective separation,[15] as composites with synthetic as well as biopolymers,[16] for the immobilization of proteins,[17] antibodies,[18] and heparin,[19] as adsorbents for the extracorporeal blood purification,[20] and in medicines and cosmetics.[21]

Membranes for Gas Separation

Membrane separation technology has emerged into a new era of advanced functional materials owing to its exquisite separation principle of selective transport and unique features of isothermal operation, facile integration, and low energy

requisition. At present, a variety of novel membrane materials are employed for specific functions including the separation of small molecules like gases and vapors as well as relatively larger entities such as colloids and insoluble matter, the resolution of optical isomers, ions, or biological matter, and in catalytic membrane reactors and sensor systems, hence finding a multitude of potential applications in the domains of biomaterial, chemical, medicinal, and catalysis sciences.[22]

"Membrane" serves as an interphase between two adjacent phases acting as a selective barrier, administering the transport of substances between two compartments under the influence of the potential gradient in concentration or pressure, or the electrical imbalance across the selective integument.[23]

Regardless of the architectural diversities, the porous or non-porous nature and the pore size of the membrane are of vital significance in determining the transport and separation mechanisms. Therefore the membrane-based separation processes can be broadly classified as strainer filtration, microfiltration, ultrafiltration, nanofiltration, dialysis, reverse osmosis, pervaporation, and gas separation. Strainer filtration involves membranes possessing the pore-size of ≥ 5 μm and is used for the separation of large particulate matter in laboratories. The microfiltration (MF) and ultrafiltration (UF) techniques rely on molecular sieving through the pores; the former makes use of membranes of 0.1–5 μm pore-size to filter fine particles and bacteria from water while the latter with the membrane pore-diameter of 2–50 nm is employed for concentration, fractionation, or purification processes to separate water and microsolutes from colloids.[24] The pore-size of nanofiltration (NF) membranes ($\leq$ 2 nm) is somewhat intermediate of those of the ultrafiltration and reverse osmosis membranes. On the other hand, electrodialysis (ED), reverse osmosis (RO), and pervaporation (PV) membranes make use of both the polymer segmental gaps (~ 0.3–0.5 nm) and the micropores ($\leq$ 1 nm). RO, employed for sea-water desalination for drinking and process applications, and fine purification for medical and microelectronics industries,[25] is based on the solution-diffusion model; ED utilizes ion exchange membranes to effect separation and obeys the Donnan effect while PV follows the

solution-diffusion mechanism for the separation of liquid mixtures. The gas separation membranes are either non-porous or microporous with even smaller pore-size, finding applications in air separation, flue gas rectification, hydrogen purification, and natural gas sweetening.[26]

Membrane technology for gas separation has engrossed substantial prominence due to the lower energy consumption, mechanical simplicity, and smaller footprints in comparison with the conventional separation methodologies, and is likely to accomplish a significant contribution in alleviating the environmental and energy-related concerns. The use of polymeric membranes for gas separation dates back to the early 19th century with its foundations grounded in the findings of J. K. Mitchell,[27] T. Graham,[28] and S. von Wroblewski,[29] demonstrating the capability of gases to permeate through non-porous polymeric films like rubber. In 1855, Fick published a quantitative description of gas flux through the membranes,[30] and in 1866, Graham proposed the so-called solution-diffusion model, a milestone in the annals of gas permeation,[28] followed by the momentous endeavors of Bechhold and Karplus making the utility of microporous membranes widely accessible.[31,32]

The gas transport performance of a membrane is ascribed to its permeability *i.e.* gas flux and selectivity for a specific gas in a mixture; and gas separation membranes are broadly categorized as: (i) porous membranes (ii) non-porous membranes and (iii) asymmetric membranes. The porous membranes characterized by the presence of a large number of voids with interconnected pores are generally capable of displaying high gas permeability but relatively low permselectivity. Furthermore, the membrane properties are largely determined by the mode of preparation while solution casting, sintering, stretching, and phase separation are the most commonly used preparative techniques. On the other hand, the non-porous membranes, as the name implies, possess neither the large scale voids nor the interconnected pores but the remarkable capability of separating the individual components of the gas pairs even with similar sizes, only on the basis of the disparity in their solubility in the membrane. The non-porous membranes are generally

prepared by melt extrusion or solution casting and exhibit high permselectivity and rather low gas permeability. An asymmetric membrane is made up of two distinct layers, a thin non-porous one responsible for the separation performance and a porous one to provide the physical support.

In accordance with the type of the membrane, the membrane separation mechanisms for a binary gas mixture have been primarily classified into five categories, porous membranes (I–IV) and non-porous membranes (V), as illustrated in Figure 2.[22c,33] With porous membranes, in the absence of any interaction between the gas molecules and the membrane 'Knudsen flow' or Knudsen diffusion mechanism (I) is known to operate whereas 'surface diffusion' (II) takes place if the gas molecules interact with the surface inside the pores and 'capillary condensation' (III) acts for the transport of gases or vapors which tend to condense inside the pores. The molecular sieve mechanism (IV) prevails for the porous membranes, with average pore-size greater than the molecular size of one of the gases, thus exhibiting extremely high separation performance; however, it is quite difficult to prepare well-ordered angstrom-size (*i.e.*, gas size) pores in the polymer membranes.

Figure 2. Basic Mechanisms of Gas Permeation through Membranes

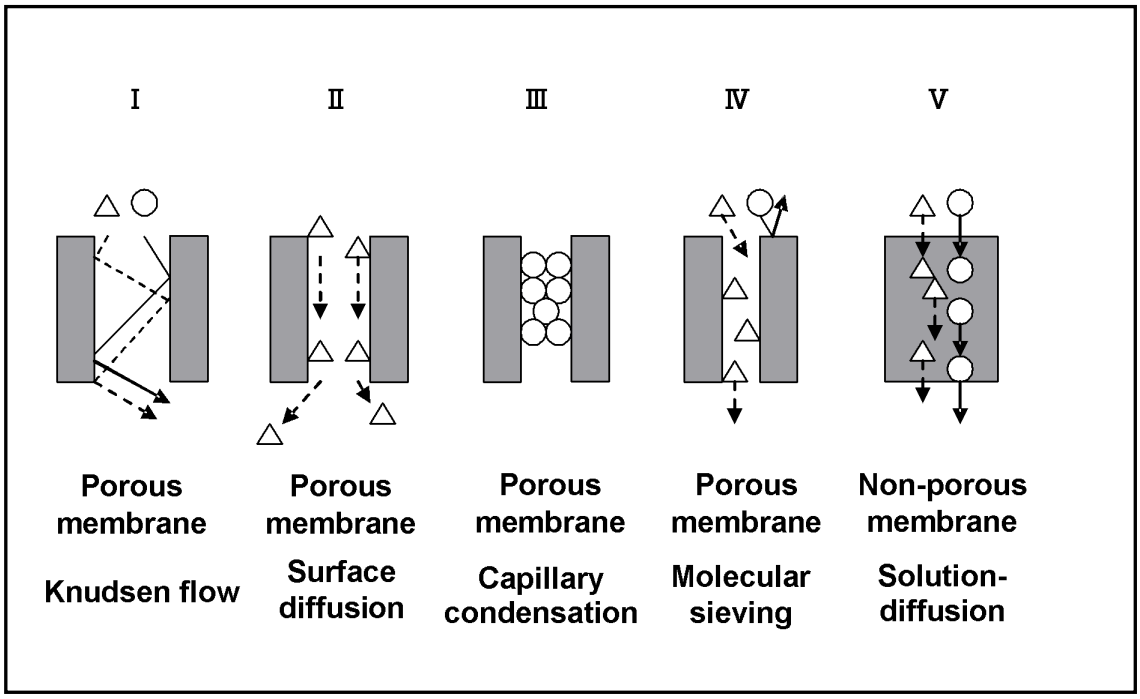

A simplified transport model is valid for all the porous membranes irrespective of their actual microporous structure. The gas permeance, *Q*, through a porous membrane can be described as:

$$Q\sqrt{MRT} = \alpha e^{\beta\left(V_c\sqrt{T_c}\right)} \quad (1)$$

where *M* is the molecular weight of the gas, *R* the gas constant, *T* the temperature, and V_c and T_c are the critical volume and critical temperature of the gas, respectively.[34] α is the Knudsen diffusion factor and β is the surface diffusion factor, both of which are independent of the *real* geometric pore structures.

On the other hand, the mechanism of gas separation by non-porous membranes is quite different from that of the porous integuments and is best explained by the solution-diffusion model,[35] attributing the diffusion and solubility of gases in the membranes to the molecular properties of diameter, shape, or volume and condensability or polarity, respectively.[22c,33b,33c,36] According to this mechanism, the gas molecules first dissolve in the surface of a *dense* membrane, and then the dissolved entities diffuse through the transient gaps between the polymer chains, hence, the permeation (*P*) of *gas A* through a polymer membrane is described as the product of gas solubility (*S*) in the upstream face of the membrane and effective average gas diffusion (*D*) through the membrane.

$$P_A = S_A \times D_A \quad (2)$$

In other words, *permeability*, the pressure- and thickness-normalized gas flux through the polymer film, depends upon two factors: a thermodynamic term, *S*, characterizing the number of gas molecules sorbed into and onto the polymer and a kinetic term, *D*, characterizing the mobility of gas molecules as they diffuse through the polymer.[37] The solubility coefficient, *S*, is determined by the condensability of the penetrants, the polymer-penetrant interactions, and the amount of free volume in

the glassy polymer. The average diffusion coefficient, *D*, is a measure of the mobility of the penetrant between the upstream and downstream faces of the membrane and depends on the packing and motion of the polymer segments and on the size and shape of the penetrating molecules.

The selectivity of *gas A* over *gas B* is defined as the ratio of the permeability coefficients of *gas A* and *gas B*, P_A/P_B.

$$\alpha_{A/B} = \frac{P_A}{P_B} = \left(\frac{S_A}{S_B}\right) \times \left(\frac{D_A}{D_B}\right) \tag{3}$$

Selectivity can thus be described as the product of the ratios of solubility coefficients, (S_A/S_B) and diffusivity coefficients (D_A/D_B); the first term referred to as the solubility selectivity and the latter the diffusivity selectivity, and an increase in either or both entails enhanced permselectivity.

Polymers with both high gas permeability and permeation selectivity are desirable for practical applications as higher permeability favors the curtailment of the required membrane area thereby reducing the capital cost of membrane units while higher selectivity results in the high purity product gas. However, a rather general tradeoff relation has been recognized between permeability and selectivity, *i.e.*, more permeable polymers generally tend to be less selective and *vice versa*.[38] On the basis of an exhaustive literature survey,[38b,39] Robeson proposed the so-called "upper bound" combinations of permeability and selectivity of known polymer membrane materials for various gas pairs and demonstrated this tradeoff relation empirically which was later on modeled by Freeman.[40]

The gas permeability (*P*) of glassy polymers exhibits a more vital dependence on the gas diffusion coefficients (*D*) in comparison with the solubility coefficients (*S*) as the latter display a much narrower range if compared with the former; for instance, the S_{CO_2} of most of the glassy polymers falls in the range of 1–10 (cm^3(STP)/(cm^3 polymer atm) while the D_{CO_2} varies from 10^{-6} to 10^{-11} (cm^2/s) and similar trends have

been observed for the permeation of other gases.[41] Moreover, in the presence of a slight or no interaction between the polymeric membrane and gas molecules, permselectivity has been observed to be primarily contingent upon the diffusivity selectivity rather than solubility selectivity,[22c,33b,33c,36] because the gas solubility is strongly dependent on the gas condensability (*e.g.*, boiling point, critical temperature, Lennard-Jones force constant) rather than the polymeric structure.[42]

Notwithstanding the primary structure of the polymer, the diffusion of gas molecules across a polymer membrane is correlated to its chain packing efficiency, *i.e.*, fractional free volume (FFV) as below:

$$D = A_D \exp\left(-\frac{B_D}{\mathrm{FFV}}\right) \tag{4}$$

where A_D and B_D are empirical constants varying from gas to gas and from one polymer to another and this relation holds if there is a little or no interaction between the gas molecules and the polymer chains. As aforementioned, the gas solubility coefficients in glassy polymer membranes vary over a much narrower range and are quite exiguously swayed by the varying free volume than does the diffusivity, FFV is often directly correlated to gas permeability coefficients,[43]

$$P = A_P \exp\left(-\frac{B_P}{\mathrm{FFV}}\right) \tag{5}$$

where A_P and B_P are adjustable parameters.

Although the D and P values tend to decrease with increasing reciprocal FFV as expected from the Equations 4 and 5, better linear correlation coefficients were reported only for the structurally related polymers when Bondi's method is used to estimate FFV. However, predictable correlations of general applicability could not be drawn presumably on account of the systematic errors in the van der Waals increments leading to such discrepancies among widely varying families of polymers or due to the

fact that not only the size of the free volume elements (empirical FFV values) rather the free volume size distribution inside the polymer matrix is of considerable significance, both of which can be estimated by positron annihilation lifetime spectroscopy (PALS).[44] Furthermore, the classical free volume theory does not take into account the effect of interchain interactions, however, the dielectric constant of polymer membranes is correlated to FFV which is strongly influenced by the polarity of polymers. Based on the Clausius-Mossottii equation, gas diffusivity and gas permeability defined as the functions of the dielectric constant (ε) are given as under:

$$P = A'\exp\left(\frac{-B'}{1-\alpha}\right) \tag{6}$$

$$D = A\exp\left(\frac{-B}{1-\alpha}\right) \tag{7}$$

where $\alpha = 1.3\frac{V_W}{P_{LL}}\frac{\varepsilon-1}{\varepsilon+2}$ *A*, *A'*, *B*, *B'* are adjustable constants, V_W is the specific van der Waals volume, and P_{LL} is the molar polarization.[45] As α takes into account the interaction between gas molecules and polymer chains, the $1-\alpha$ values of 6FDA-based polyimides have been reported to be 1.6–2.2 times larger than FFV.

Nevertheless, the solution-diffusion model is strictly valid for non-porous membranes of rubbery polymers and applies approximately to glassy polymers. The mechanism of gas permeation through glassy polymeric membranes is complicated by the presence of thermodynamic non-equilibrium or excess free volume, effectuating variable sorption behavior above or near the glass transition temperature (T_g) and when the polymer matrix is plasticized by the penetrant gases. However, the 'dual-mode model' serves as a well-established empirical correlation invoking a combination of Henry's law domains and unrelaxed (Langmuir-type) regions, the latter corresponding to the holes or 'microvoids' arising from the non-equilibrium nature of glassy

polymers.[41,46]

The solubility coefficient, *S*, for equilibrium gas sorption in glassy polymers is often described by the dual-mode model as:[46b]

$$S = \frac{C}{P} = k_D + \frac{C'_H b}{1 + bp} \tag{8}$$

where k_D is the Henry's law coefficient, C'_H is the Langmuir or hole-filling capacity of the glass, and b is the hole-affinity constant. On the other hand, the diffusion coefficient, D, interpreted in terms of the frequency (f) and jump length (λ) of the diffusive jumps across the membrane has been demonstrated by Bueche as:[47]

$$D = \frac{1}{6} f\lambda^2 \tag{9}$$

The dual-mode sorption and transport model has successfully explained the pressure dependence of permeability by taking into account two distinct diffusion coefficients ascribable to two separate sorption sites.[46a,46c] Hence, the permeability coefficient, P, of a glassy polymer is related to D_D (Henry' law diffusion coefficient), D_H (Langmuir diffusion coefficient), and the dual-mode parameters through the relationship:

$$P = k_D D_D + D_H \frac{C'_H b}{1 + bp} \tag{10}$$

In the case of non-porous membranes, the characteristics of gas permeation exhibit direct reliance on the subtle structural features of membrane materials, and over the past 25 years a wide array of synthetic polymeric architectures including polyacetylenes,[48] polycarbonates,[49] polyimides,[50] polysiloxanes,[51] polysulfones,[52] polyphosphazenes,[53] and a few of cellulose derivatives[54] have been employed as gas separation membrane materials. In the past two decades, considerable research effort

has been directed towards the development of membrane materials whose gas separation performance transcends the limits imposed by the upper bound. Despite such a voluminous activity revealing the subtle mechanistic aspects of gas transport and remarkably increasing commercial significance of environment-friendly and cost-effective membrane separation technology, a few polymeric membranes could be of industrial interest on account of the inherent drawbacks of low permeability/selectivity, high cost, lack of endurance under high temperature, and plasticization by the penetrant, etc.

Research Objectives

As demonstrated above, ethyl cellulose, cellulose acetate, and hydroxypropyl cellulose enjoying the remarkable attributes of chirality, thermal stability, biocompatibility, non-toxicity, and low cost along with the marvelous peculiarity of organosolubility reign the realm of cellulose chemistry on account of the most pivotal synthetic, technical, and commercial significance. Hence, the present dissertation highlights the derivatization of aforementioned organosoluble cellulosics accomplishing the synthesis of novel functional cellulose derivatives via etherfication/esterification/carbamoylation, and encompasses the elaborate elucidation of structure, properties, and innovative frontiers of potential applications.

The substitution of residual hydroxy groups by specific functionalities of varied chemical nature, size/bulk, and shape was envisaged to bear profound impact on the structural characteristics and properties of the derivatized polymers. Therefore, a variety of organic side groups like non polar and slightly bulky silyl moieties; various lengths of hydrophobic perfluoroalkanoyl groups; polar, bulky, and almost spherical amidoimide dendritic wedges; spherical and moderately polar carbamoyl pendants, and biocompatible aminoalkanoyl functionalities of varied polarity were incorporated into ethyl cellulose/cellulose acetate/hydroxypropyl cellulose, and considerable transformation of properties was witnessed accompanying the alteration of polymeric side chain structure regardless the presence of the same backbone.

Keeping in view, the commercial, environmental, and energy-related significance of membrane based separation to fulfill the desire for sustainable chemical processing and to meet the requisites of good separation performance together with low cost and durability, author has envisioned the development of gas separation membranes based on the most sustainable and promising biopolymer of 21st century.

Ethyl cellulose and cellulose acetate have been the subject of gas separation membranes for several years, however, no considerable attempts have been made to effect the derivatization of these low cost membrane-forming cellulosics or to elucidate the role of various pendants in the transformation of architectural characteristics and thus the gas transport performance of new functionalized derivatives. The present treatise narrates the profound impact of the incorporation of a number of pendants of varied chemical nature on the gas permeation parameters of ethyl cellulose and cellulose acetate. The history of polymeric gas separation membranes celebrates the presence of spherical silyl groups to bestow the acetylenic polymers with high gas permeability thus new silylated derivatives of ethyl cellulose were fabricated into free-standing membranes. The author reasoned the increased diffusion coefficients leading to higher gas permeability to emanate from the enhanced local mobility despite the decrement in the solubility coefficients on account of the attenuated fractional free volume. Owing to the high electronegativity of fluorine atoms, fluorinated polymers are known to display the unique characteristics of high gas permeability with reasonable permselectivity. The fluorinated derivatives of ethyl cellulose are inferred to possess higher gas diffusion and solubility thus improved gas permeability due to the enhanced FFV ensuing from the repulsive interaction between fluorine atoms, on the other hand, high chain stiffness helped preventing the expected loss of permselectivity. Moreover, polar functionalities such as poly(amidoamine) dendrimers exploited in the form of composite or immobilized liquid membranes have recently been revealed to offer excellent CO_2 separation capability. Therefore, amidoimide dendritic pendants were integrated to ethyl

cellulose to decipher the impact of polar substituents on the structural characteristics and hence the gas permeation parameters of the polymeric membranes. The attenuated FFV of the polymer matrices has been described to be at the helm of the decrement in the gas diffusion and solubility and consequently the decreased gas permeability of the membranes. However, the increase in CO_2 permselectivity was not so evident and has been explicated by the author to be due to the unavailability of the polar groups on the peripheries to interact with CO_2. As discussed above, spherical pendants are acknowledged to endow the polymers with enhanced local mobility; therefore a blend of polar and spherical substituents was envisioned to enhance permeability without loss in CO_2 permselectivity. The interpolation of moderately polar carbamoyl groups with spherical *t*-butyl periphery was accomplished to bring in the improved gas permeability which was much more pronounced for the carbamates of cellulose acetate while no significant decrease in CO_2 permselectivity of polymer membranes has been ascribed to the retained solubility selectivity.

The intricate features of synthetic strategies and mechanistic aspects of cellulosic membranes explored in the present study are anticipated to lead us to new frontiers of potential applications of this renewable energy resource.

Outline of the Thesis

The present dissertation delineates the synthesis of novel functional cellulose ethers/esters, their characterization and investigation of various properties, and is comprised of five chapters. A variety of functional substituents have been appended to the backbone of different organosoluble cellulosics, *i.e.,* ethyl cellulose, cellulose acetate, and hydroxypropyl cellulose while the core synthetic strategy was to exploit the residual hydroxy protons for the sake of derivatization. The incorporated moieties encompass various silyl, perfluoroacyl, dendryl, carbamoyl, and aminoalkanoyl groups, and the nature of the substituents was revealed to be of considerable significance in determining the solubility and thermal characteristics of

the derivatized polymers. Moreover, the role of functional appendages on the fabricability of free-standing membranes and in tailoring the gas permeation characteristics has been elucidated in detail.

Chapter 1 describes the synthesis of silyl ethers of ethyl cellulose (R = Me_3Si, **2a**; Et_3Si, **2b**; Me_2-*i*-PrSi, **2c**; Me_2-*t*-BuSi, **2d**; Me_2-*n*-OctSi, **2e**; Me_2PhSi, **2f**) and the effect of the incorporation of silyl substituents on the solubility, thermal stability, and gas permeation parameters of the starting polymer/ethyl cellulose. Silylation of ethyl cellulose (DS_{Et}, 2.69) was accomplished with halosilanes of diversified chemical nature (alkyl and aryl) and various chain lengths. The substitution of hydroxy groups with nonpolar bulky silyl moieties accompanied the enhanced solubility in relatively nonpolar solvents without any significant decrease in thermal stability. The gas permeability of all of the silylated derivatives was higher than that of ethyl cellulose and followed a decline with increasing size/bulk of the silyl pendants (**2a** > **2b** ≈ **2c** > **2d** > **2e** > **2f** > **1**) whereas **2a**–**c** were located above the *upper bound* for the CO_2/N_2 gas pair. The enhanced gas permeability was elucidated to ensue from the increment in the gas diffusion coefficients because of the increased FFV of the polymer membranes.

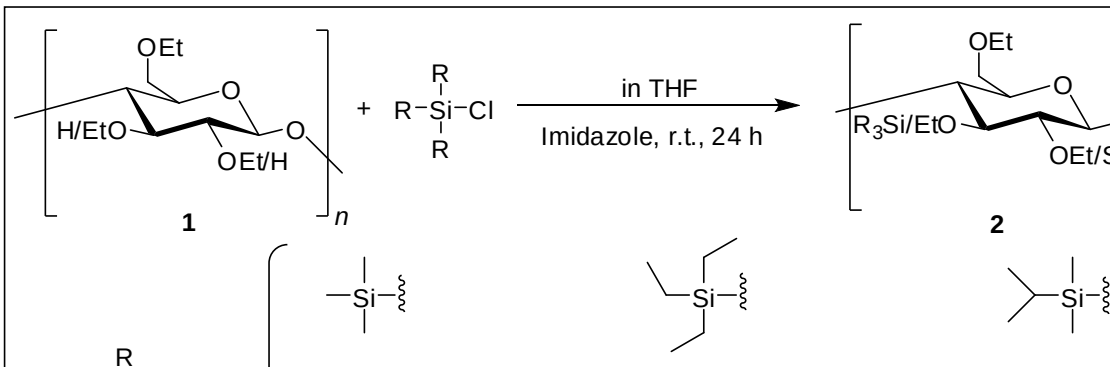

Chapter 2 reveals another contribution in the synthetic arena of novel cellulose derivatives demonstrating the quantitative esterification of ethyl cellulose (DS_{Et}, 2.69) with perfluoroalkanoyl substituents of various chain lengths and partial

incorporation of perfluorobenzoyl group (R = CF_3CO, **3a**; C_2F_5CO, **3b**; C_3F_7CO, **3c**; $C_7F_{15}CO$, **3d**; C_6F_5CO, **3e**). The substitution of perfluoroacyl pendants had an evident influence on various properties of ethyl cellulose, and the resulting polymers (**3a**–**e**) were more soluble in polar aprotic and nonpolar solvents while the completely acylated derivatives were soluble in fluorinated solvents as well. Perfluoroacylation resulted in the enhanced hydrophobicity and derivatized polymers exhibited higher contact angle with water on the surface. Trifluoroethanoyl derivative (**3a**) displayed the highest glass transition temperature which decreased with the increment in the length of the alkyl chain. Furthermore, the gas permeability of perfluoroalkanoylated derivatives was 2–3 times higher than that of ethyl cellulose by the virtue of the augmentation in the gas diffusion coefficients emanating from the repulsion between highly electronegative fluorine atoms thus leading to the enhanced FFV of the polymer matrices.

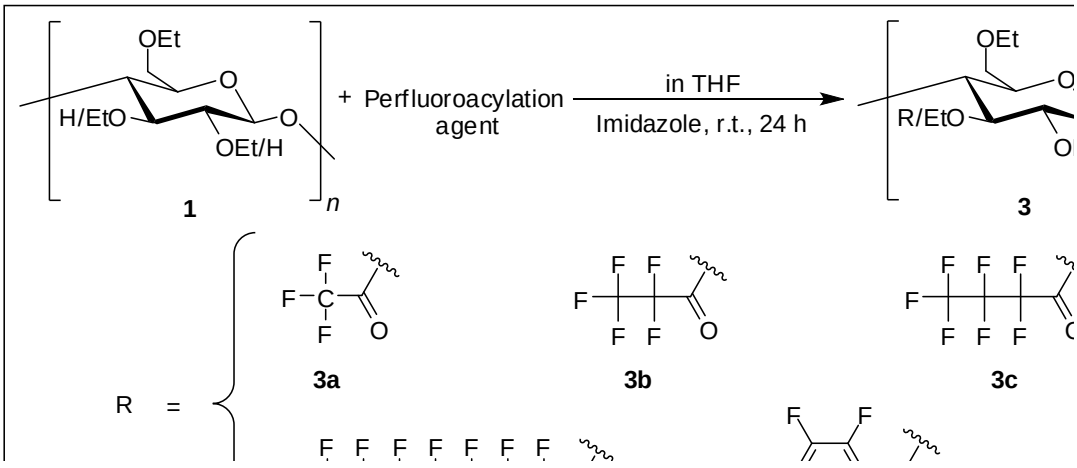

Chapter 3 is concerned with a successful merger of two unique families of macromolecular architectures delineating a pathway to dendronized cellulose derivatives and elucidates the effect of amidoimide dendritic substituents on the solubility behavior, thermal characteristics, and gas permeation properties of the dendron-functionalized polymers. G1 and G2 of amidoimide dendrons with branched alkyl periphery and focal carboxyl moiety were synthesized via a convergent

strategy (**G1-a-II**–**G1-c-II** and **G2-a-II**–**G2-c-II**) and coalesced with ethyl cellulose through ester linkage. All of the dendronized derivatives of ethyl cellulose (**4a**–**c**, **5a**–**c**) displayed fair thermal stability and a considerable lowering of glass transition temperature in comparison with the starting polymer, the latter being ascribable to the fairly bulky nonpolar alkyl peripheries. An appreciably good solubility of G1-functionalized polymers in $CHCl_3$ rendered the free-standing membranes' fabrication feasible by solution casting. The incorporation of bulky dendritic substituents into ethyl cellulose led to the more dense membrane structure with attenuated fractional free volume, thus decrement in the gas permeability of polymer membranes. However, an enhanced permselectivity for He/N_2, H_2/N_2, CO_2/N_2, and CO_2/CH_4 gas pairs was discerned.

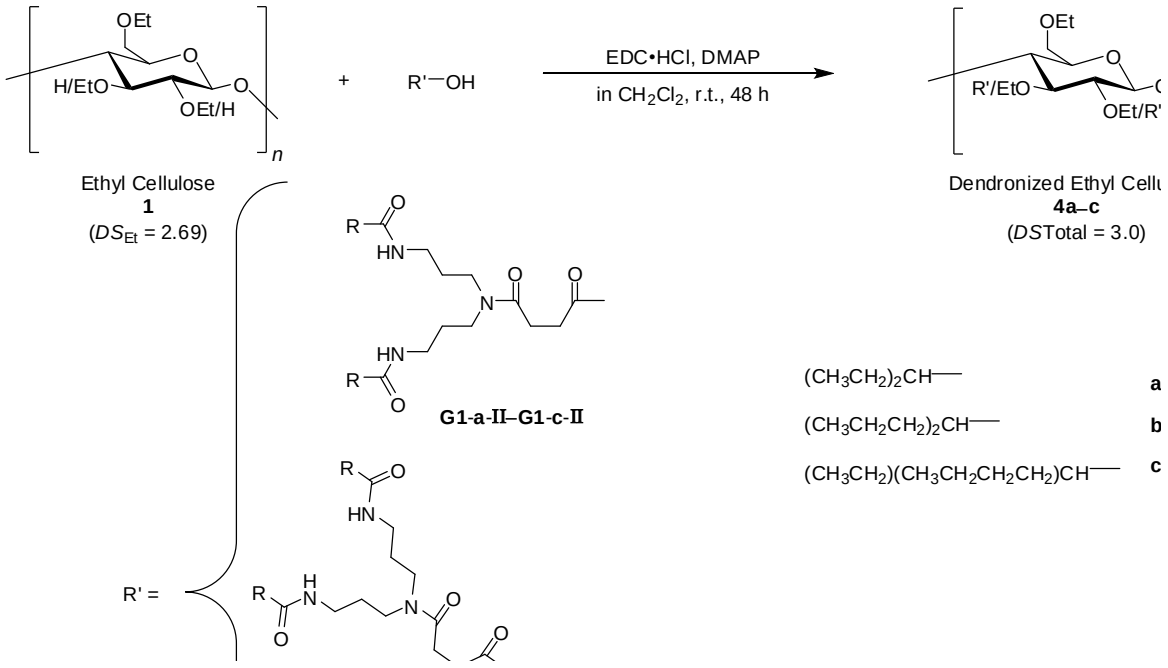

In **Chapter 4**, synthesis of *t*-butylcarbamates of ethyl cellulose (**1a**: DS_{Et}, 2.69, DS_{Carb}, 0.31; and **6a**: DS_{Et}, 2.50, DS_{Carb}, 0.50) and cellulose acetate (**7a**: DS_{Ac}, 2.46,

DS_{Carb}, 0.54; and **8a**: DS_{Ac}, 1.80, DS_{Carb}, 1.20) along with the solubility behavior, thermal characteristics, and gas permeation properties of the carbamoylated cellulosics has been discussed. The derivatization imparted the polymers with improved organosolubility especially for the *t*-butylcarbamate of cellulose acetate (**8a**), and a slight decrement in glass transition temperature was witnessed presumably due to the presence of bulky *t*-butyl moieties. The carbamate formation led to the enhanced gas permeability which was observed to ensue from the augmented gas diffusion emanating from the increased local mobility of the polymer matrix. The increase in the gas permeation and diffusion coefficients was much more remarkable for the *t*-butylcarbamates of cellulose acetate than those of ethyl cellulose. Nevertheless, the CO_2 solubility selectivity hence the CO_2/N_2 permselectivity was almost retained owing to the presence of polar carbamate linkages.

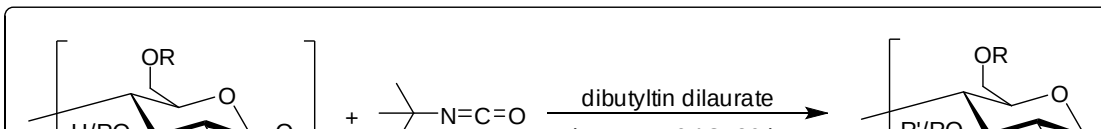

Chapter 5 deals with the derivatization of a physiologically inert, biocompatible, water soluble cellulose ether of remarkable commercial and pharmaceutical significance with amino acids, the basic building blocks of nature being widely employed in the domain of biocompatible architectures. Hydroxypropyl cellulose (HPC) was esterified with the *t*-Boc-protected amino acid functionalities of varied chemical nature, shape, and bulk and the degree of amino acid incorporation was deciphered to be prone to the steric hindrance imposed by the bulk of the substituent on the α-carbon of amino acids. The incorporation of aminoalkanoyl moieties accompanied the enhanced hydrophobicity (water insolubility) without any detriment of organosolubility and a significant increase in glass transition temperature thus transforming a rubbery starting material into almost glassy polymers.

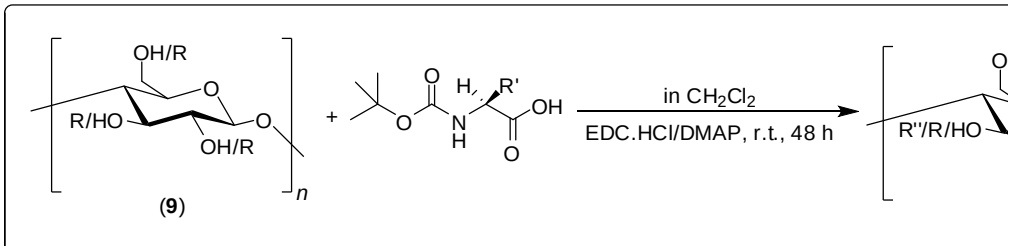

In conclusion, the author has successfully synthesized a number of novel cellulose derivatives appended with a variety of functional entities and has fully characterized the resulting polymers by making use of IR and NMR spectroscopic identification, elemental analysis, and molecular-weight determination etc. The nature of the substituent played a dominant role in determining the solubility and thermal characteristics of the polymers, for instance, the silylated and perfluoroacylated polymers displayed inclination towards nonpolar solvents, those with moderately polar G1 dendritic moieties were soluble in moderately polar solvents and highly polar protic solvents while the augmented polarity in going to G2-dendronized polymers imparted the relatively poor solubility characteristics. On the other hand, the carbamoyl- and amino acid-functionalized polymers exhibited very good organosolubility probably due to the presence of polar linkages along with the bulky alkyl peripheries. As far as the thermal characteristics are concerned, the dendron-functionalized ethyl cellulose derivatives exhibited the highest thermal stability (T_0, 295–325 °C) while the trifluoroacetylation conferred the polymers with the greatest chain stiffness (**3a**; T_g, 227 °C). Furthermore, the gas permeation characteristics were revealed to be a dynamic interplay of two intricate structural features, *i.e.*, local/segmental mobility and free space available inside the polymer matrix, both sensitive to the nature (polarity), shape, and bulk of the side groups in the present series of cellulose derivatives. In general, the trends in the permeability

coefficients showed more bearing on the gas diffusion through the polymer membranes displaying a considerable reliance on the local mobility of the substituents whereas the gas solubility seemed to be more affected by the polarity of the side groups and the FFV of the polymer matrix.

References

1. (a) Klemm, D.; Heublein, B.; Fink, H.-P.; Bohn, A. *Angew. Chem. Int. ed.* **2005**, *44*, 3358–3393. (b) Richter, A.; Klemm, D. *Cellulose* **2003**, *10*, 133–138. (c) Klemm, D.; Schmauder, H.-P.; Heinze, T. In *Biopolymers*; Vol. 6; Vandamme, E., Beats, S. D., Steinbüchel, A., Eds.; Wiley-VCH: Weinheim, 2002; pp 275–319. (d) Horii, F. In *Wood and Cellulosic Chemistry*; 2nd ed.; Hon, D. N.-S., Shiraishi, N., Eds.; Marcel Dekker: New York, 2001; pp 83–107. (e) Isogai, A. In *Wood and Cellulosic Chemistry*; 2nd ed.; Hon, D. N.-S., Shiraishi, N., Eds.; Marcel Dekker: New York, 2001; pp 599–625. (f) Vogl, O.; Matheson, R. R.; Matyjaszewski, K.; Jaycox, G. D. *Prog. Polym. Sci.* **2001**, *26*, 1337–1971. (g) Barton, D. H. R.; Nakanishi, K.; Meth-Cohn, O. *Comprehensive Natural Products Chemistry*; Elsevier Science: Oxford, 1999; Vol. 3. (h) Klemm, D.; Philipp, B.; Heinze, T.; Heinze, U.; Wagenknecht, W. *Comprehensive Cellulose Chemistry*; Wiley-VCH: Weinheim, 1998; Vol. 1, 2. (i) Hon, D. N.-S. In *Chemical Modification of Lignocellulosic Materials*; 1st ed.; Marcel Dekker: New York, 1996. (j) Krässig, H. A. In *Cellulose- Structure, Accessibility, and Reactivity*; Gordon and Breach: Amsterdam, 1993.
2. (a) Klemm, D.; Schmauder, H.-P.; Heinze, T. In *Biopolymers*; Vol. 6; Vandamme, E., Beats, S. D., Steinbüchel, A., Eds.; Wiley-VCH: Weinheim, 2002; pp 290–292. (b) Kaplan, D. L. In *Biopolymers from Renewable Resources*; Kaplan, D. L., Ed.; Springer: Berlin, 1998; pp 1–29.
3. (a) Klemm, D.; Schmauder, H.-P.; Heinze, T. In *Biopolymers*; Vol. 6; Vandamme, E., Beats, S. D., Steinbüchel, A., Eds.; Wiley-VCH: Weinheim, 2002; pp 285–290. (b) Kimura, S.; Kondo, T. *J. Plant Res.* **2002**, *115*, 297–302. (c) Roemling, U. *Res. Microbiol.* **2002**, *153*, 205–212. (d) Nobles, D.; Romanovicz, D.; Brown, J. R. M. *Plant Physiol.* **2001**, *127*, 529–542. (e) Saxena, I. M.; Brown, J. R. M. *Prog. Biotechnol.* **2001**, *18*, 69–76. (f) Kondo, T.; Togawa, E.; Brown, J. R. M. *Biomacromolecules* **2001**, *2*, 1324–1330. (g) Brown, J. R. M.; Saxena, I. M. *Plant Physiol. Biochem.* **2000**, *38*, 57–67. (h) Brown, J. R. M. *Pure Appl. Chem.* **1999**, *71*, 204–212. (i) Brown, J. R. M. *Science* **1999**, *71*, 204–212. (j) Brown, J. R. M. *J. Macromol. Sci. Pure Appl. Chem.* **1996**, *33*, 1345–1373.
4. Kobayashi, S.; Sakamoto, J.; Kimura, S. *Prog. Polym. Sci.* **2001**, *26*, 1525–1560.

5. (a) Kobayashi, S.; Uyama, H.; Ohmae, M. *Bull. Chem. Soc. Jpn.* **2001**, *74*, 613–635. (b) Kobayashi, S.; Shoda, S.; Uyama, H. *Adv. Polym. Sci.* **1995**, *121*, 1–30. (c) Kobayashi, S.; Kashiwa, K.; Shimada, J.; Kawasaki, T.; Shoda, S. *Mocromol. Symp.* **1992**, *54/55*, 509–518. (d) Kobayashi, S.; Kashiwa, K.; Kawasaki, T.; Shoda, S. *J. Am. Chem. Soc.* **1991**, *113*, 3079–3084.
6. Nakatsubo, F.; Kamitakahara, H.; Hori, M. *J. Am. Chem. Soc.* **1996**, *118*, 1677–1681.
7. Schönbein, C. F. *Ber. Naturforsch. Ges. Basel* **1847**, *7*, 27. (b) Schönbein, C. F. *Phil. Mag.* **1846**, *31*, 7.
8. Balser, K.; Hoppe, L.; Eichler, T.; Wendel, M.; Astheimer, A.-J. In *Ullmann's Encyclopedia of Industrial Chemistry*; Vol. A5; Gerhartz, W., Yamamoto, Y. S., Campbell, F. T., Pfefferkorn, R., Rounsaville, J. F. Eds.; VCH: Weinheim, 1986; p 419–459.
9. (a) Götze, K. *Chemiefasern nach dem Viskoseverfahren*; 3rd Ed.; Vol. 1; Springer: Heidelberg, 1967; pp. 1–778. (b) Cross, C. F.; Bevan, B. T.; Beadle, C. *Ber. Dtsch. Chem. Ges.* **1893**, *26*, 2520–2533. (c) Cross, C. F.; Bevan, B. T.; Beadle, C. *Ber. Dtsch. Chem. Ges.* **1893**, *26*, 1090–1097.
10. (a) Fink, H.-P.; Weigel, P.; Purz, H. J.; Ganster, J. *Prog. Polym. Sci.* **2001**, *26*, 1473–1524. (b) Dubé, M.; Blackwell, R. H. In *Proceedings of the International Dissolving and Speciality Pulps Conference*, Boston, Tappi Press, **1983**, S. 111–119. (c) Chanzy, H.; Dubé, M.; Marchessault, R. H. *J. Polym. Sci. Lett. Ed.* **1979**, *17*, 219–226.
11. (a) Nagai, Y.; Yoshimizu, H.; Tsujita, Y. *J. Membr. Sci.* **2005**, *256*, 72–77. (b) Kusumocahyo, S. P.; Ichikawa, T.; Shindo, T.; Iwatsubo, T.; Kameda, M.; Ohi, K. *J. Membr. Sci.* **2005**, *253*, 43–48. (c) Buchanan, C. M.; Buchanan, N. L.; Debenham, J. S.; Gatenholm, P.; Jacobsson, M.; Shelton, M. C.; Watterson, T. L.; Wood, M. D. *Carbohydr. Polym.* **2003**, 5*2*, 345–357. (d) Toriz, G.; Arvidsson, R.; Westin, M.; Gatenholm, P. *J. Appl. Polym. Sci.* **2003**, *88*, 337–345. (e) Vaca-Garcia, C.; Gozzelinoi, G.; Glasser, W. G.; Borredon, M. E. *J. Polym. Sci. Part B: Polym. Phys.* **2003**, *401*, 281–288. (f) Franko, A.; Seaveg, K. C.; Gumaer, J.; Glasser, W. G. *Cellulose* **2001**, *8*, 171–179. (g) Spricigo, C.B.; Bolzan, A.; Machado, R. A. F.; Carlson, L. H. C.; Petrus, J. C. C. *J. Membr. Sci.* **2001**, *188*, 173–179. (h) Edgar, K. J.; Buchanan, C. M.; Debenham, J. S.; Rundquist, P. A.; Seiler, B. D.; Shelton, M. C.; Tindall, D. *Prog. Polym. Sci.* **2001**, *26*, 1605–1688. (i) Matsumura, H.; Glasser, W. G. *J. Appl. Polym. Sci.* **2000**, *78*, 2254–2261. (j) Ghosh, I.; Jain, K. R. Glasser, W. G. *J. Appl. Polym. Sci.* **1999**, *74*, 448–457. (k) Glasser, W. G.; Taib, R.; Jain, R, K.; Kander, R. *J. Appl. Polym. Sci.* **1999**, *73*, 1329–1340. (l) Rahn, K.; Diamantoglou, M.; Klemm, D.; Berghmans, H.; Heinze,

T.; *Angew. Makromol. Chem.* **1996**, *238*, 143–163. (m) Heinze, T.; Rahn, K. *Papier* **1996**, *12*, 721–729. (n) Puleo, A. C.; Paul, D. R. *J. Membr. Sci.* **1989**, *47*, 301–332.

12. (a) Crowley, M. M.; Schroeder, B.; Fredersdorf, A.; Obara, S.; Talarico, M.; Kucera, S.; McGinity, J. W. *Int. J. Pharm.* **2004**, *269*, 509–522. (b) Poersch-Parcke, H.-G.; Kirchner, R. *Solutions*; 2nd Ed.; Wolff Cellulosics GmbH: Walsrode, 2003. (c) Brandt, L. In *Industrial Polymers Handbook*; Vol. 3; Wilks, E. S., Ed.; Wiley-VCH: Weinheim, 2001; pp 1569–1613.
13. (a) Yoshida, Y.; Isogai, A. *Cellulose* **2006**, *13*, 637–645. (b) Figueirinhas, J. L.; Almeida, P. L.; Godinho, M. H. In *Polysaccharides*; 2nd Ed.; Dumitriu, S., Ed.; Marcel Dekker: New York, 2005**;** pp 1123–1139. (c) Kondo, T.; Kasai, W.; Brown, R. M. *Cellulose* **2004**, *11*, 463–474. (d) Greiner, A.; Hou, H.; Reuning, A.; Thomas, A.; Wendorff, J. H.; Zimmermann, S. *Cellulose* **2003**, *10*, 37–52. (e) Chiba, R.; Nishio, Y.; Miyashita, Y. *Macromolecules* **2003**, *36*, 1706–1712. (f) Sato, T.; Shimizu, T.; Kasabo, F.; Teramoto, A. *Macromolecules* **2003**, *36*, 2939–2943. (g) Yue, Z.; Cowie, J. M. G. *Macromolecules* **2002**, *35*, 6572–6577. (h) Edgar, C. D.; Gray, D. G. *Cellulose* **2001**, *8*, 5–12. (i) Thies, J. C.; Cowie, J. M. G. *Polymer* **2001**, *42*, 1297–1301. (j) Müller, M.; Zentel, R. *Macromol. Chem. Phys.* **2000**, *201*, 2055–2063. (k) Hou, H.; Reuning, A.; Wendorff, J. H.; Greiner, A. *Macromol. Chem. Phys.* **2000**, *201*, 2050–2054. (l) Zugenmaier, P. In *Handbook of Liquid Crystals;* Vol. 3; Demus, D., Ed.; Wiley-VCH: Weinheim, 1998**;** pp 453–482. (m) Derleth, C.; Zugenmaier, P. *Macromol. Chem. Phys.* **1997**, *198*, 3799–3814. (n) Guo, J.-X.; Gray, D. G. In *Cellulosic Polymers, Blends and Composites*; Gilbert, R. D., Ed.; Hanser: Munich, 1994**;** pp 25–45. (o) Gray, D. G. *Carbohydr. Polym.* **1994**, *14*, 277–284. (p) Zugenmaier, P. In *Cellulosic Polymers, Blends and Composites*; Gilbert, R. D., Ed.; Hanser: Munich, 1994**;** pp 71–94. (q) Gilbert, R. D. *ACS Symp. Ser.* **1990**, *433*, 259–272. (r) Siekmeyer, M.; Zugenmaier, P. *Makromol. Chem.* **1990**, *191*, 1177–1196. (s) Siekmeyer, M.; Steinmeier, H.; Zugenmaier, P. *Macromol. Chem.* **1989**, *190*, 1037–1045. (t) Gray, D. G. *Faraday Discuss. Chem. Soc.* **1985**, *79*, 257–264. (u) Vogt, U.; Zugenmaier, P. *Makromol. Chem. Rapid Commun.* **1983**, *4*, 759–765. (v) Zugenmaier, P.; Vogt, U. *Makromol. Chem.* **1983**, *184*, 1749–1760. (w) Werbowyj, R. S.; Gray, D. G. *Macromolecules* **1980**, *13*, 69–73. (x) Werbowyj, R. S.; Gray, D. G. *Mol. Cryst. Liq. Cryst.* **1976**, *34*, 97–103.
14. (a) Seifert, M.; Hesse, S.; Kabrelian, V.; Klemm, D. *J. Polym. Sci. Part A: Polym. Chem.* **2004**, *42*, 463–470. (b) Liu, C.; Baumann, H. *Carbohydr. Res.* **2002**, *337*, 1297–1307. (c) Klemm, D.; Schumann, D.; Udhardt, U.; Marsch, S. *Prog. Polym. Sci.* **2001**, *26*, 1561–1603.

15. (a) Goetmar, G.; Zhou, D.; Stanley, B. J.; Guiochon, G. *Anal. Chem.* **2004**, *76*, 197–202. (b) Ling, F.; Bramachary, E.; Xu, M.; Svec, F.; Fréchet, J. M. J. *J. Sep. Sci.* **2003**, *26*, 1337–1346. (c) Toga, Y.; Tachibana, K.; Ichida, A. *J. Liq. Chromatogr. Relat. Techn.* **2003**, *26*, 3235–3248. (d) Okamoto, Y.; Yashima, E.; Yamamoto, C. *Top. Stereochem.* **2003**, *24*, 157–208. (e) Kubota, T.; Yamamoto, C.; Okamoto, Y. *Chirality* **2003**, *15*, 77–82. (f) Kubota, T.; Yamamoto, C.; Okamoto, Y. *Chirality* **2002**, *14*, 372–376. (g) Franco, P.; Senso, A.; Oliveros, L.; Minguillon, C. *J. Chromatogr. A.* **2001**, *906*, 155–170. (h) Felix, G. *J. Chromatogr.* **2001**, *906*, 171–184. (i) Kubota, T.; Yamamoto, C.; Okamoto, Y. *J. Am. Chem. Soc.* **2000**, *122*, 4056–4059. (j) Spitzer, T.; Yashima, E.; Okamoto, Y. *Chirality* **1999**, *11*, 195–200. (k) Okamoto, Y.; Yashima, E. *Angew. Chem. Int. Ed.* **1998**, *37*, 1020–1043. (l) Acemoglu, M.; Kusters, E.; Baumann, J.; Hernandez, I.; Mak, C. P. *Chirality* **1998**, *10*, 294–306.
16. (a) Nishio, Y. *Adv. Polym. Sci.* **2006**, *205*, 97–151. (b) Linder, A. P.; Bergman, R.; Bodin, A.; Gatenholm, P. *Langmuir* **2003**, *19*, 5072–5077. (c) Amash, A.; Hildebrandt, F.-I.; Zugenmaier, P. *Desig. Monom. Polym.* **2002**, *5*, 385–399. (d) Karlsson, J. O.; Henriksson, A.; Michalek, J.; Gatenholm, P. *Polymer* **2000**, *41*, 1551–1559. (e) Amash, A.; Zugenmaier, P. *Polymer* **2000**, *41*, 1589–1596. (f) Nishio, Y. In *Cellulosic Polymers, Blends and Composites*; Gilbert, R. D., Ed.; Hanser: Munich, 1994**;** pp 95–113.
17. (a) Martinez, A. J.; Manolache, S.; Gonzalez, V.; Young, R. A.; Denes, F. J. *J. Biomater. Sci. Polym. Ed.* **2000**, *11*, 415–438. (b) Kauffmann, C.; Shoseyov, O.; Shpigel, E.; Bayer, E. A.; Lamed, R.; Shoham, Y.; Mandelbaum, R. T. *Environ. Sci. Technol.* **2000**, *34*, 1292–1296.
18. Loescher, F.; Ruckstuhl, T.; Seeger, S. *Adv. Mater.* **1998**, *10*, 1005–1009.
19. Erdtmann, M.; Keller, R.; Baumann, H. *Biomaterials* **1994**, *15*, 1043–1048.
20. Knaus, S.; Mais, U.; Binder, W. H. *Cellulose* **2003**, *10*, 139–150.
21. (a) Mutafov, S.; Angelova, B.; Schmauder, H.-P.; Avramowa, T.; Boyadijeva, L. *Biotechnol. Bioeng.* **2003**, *84*, 160–169. (b) Hornung, M.; Ludwig, M.; Schmauder, H.-P. *Chem. Ing. Tech.* **2002**, *74*, 667.
22. (a) Yampolskii, Y.; Pinnau, I.; Freeman, B. D., Eds.; *Materials Science of Membranes for Gas and Vapor Separation*; Wiley: Chichester, 2006. (b) Pinnau, I.; Freeman, B. D., Eds.; *Advanced Materials for Membrane Separations*; ACS Symposium Series 876; American Chemical Society: Washington, DC, 2004. (c) Baker, R. W. *Membrane Technology and Applications*, 2nd ed.; Wiley: New York, 2004. (d) Nunes, S.; Peinemann, K. V., Eds.; *Membrane Technology in the Chemical Industry*; Wiley-VCH: Weinheim, 2001. (e) Paul, D. R.; Yampol'skii, Y. P., Eds.; *Polymeric Gas Separation Membranes*; CRC Press: Boca Raton, FL,

1994.

23. Mulder, M. *Basic Principles of Membrane Technology*, 2nd ed.; Kulwer Academic Publishers: Dordrecht, 1996.
24. (a) Rana, D.; Matsuura, T.; Narbaitz, R. M.; Feng, C. *J. Membr. Sci.* **2005**, *249*, 103–112. (b) Rivas, B. L.; Pereira, E. D.; Moreno-Villoslada, I. *Prog. Polym. Sci.* **2003**, *28*, 173–208. (c) van Reis, R.; Zydney, A. L. *Curr. Opin. Biotechnol.* **2001**, *12*, 208–211. (d) Girard, B.; Fukumoto, L. R. *Crit. Rev. Biotechnol.* **2000**, *20*, 109–175. (e) Wienk, I. M.; Boom, R. M.; Beerlage, M. A. M.; Bulte, A. M. W.; Smolder, C. A.; Strathmann, H. *J. Membr. Sci.* **1996**, *113*, 361–371. (f) Zeman, L. J.; Zydney, A. L. *Microfiltration and Ultrafiltration*; Marcel Dekker: New York, 1996.
25. (a) Petersen, R. J. *J. Membr. Sci.* **1993**, *83*, 81–150. (b) Pusch, W. *Desalination* **1990**, *77*, 35–54. (c) Loeb, S.; Sourirajan, S. *ACS Adv. Chem. Ser.* **1963**, *38*, 117–132.
26. (a) Henis, J. M. S. *Commercial and Practical Aspects of Gas Separation Membranes*; CRC Press: Boca Raton, FL, 1994. (b) Kesting, R. E.; Fritzcsche, A. K. *Polymeric gas separation membranes*; New York: Wiley, 1993; pp 64. (c) Zolandz, R. R.; Fleming, G. K. In Ho, W. S. W.; Sirkar, K. K. Eds., Membrane Handbook; Chapman and Hall: New York, 1992, pp. 78–94.
27. Mitchell, J. K. *J. Membr. Sci.* **1995**, *100*, 11–16.
28. Graham, T. *Phil. Mag.* **1866**, *32*, 401–420.
29. von Wroblewski, S. *Ann. Phys. Chem.* **1879**, *8*, 29–52.
30. Fick, A. *Ann. Phys. Chem.* **1855**, *94*, 59–86.
31. Bechhold, H. *Biochem. Z.* **1908**, *6*, 379–408.
32. Erbe, F. *Kolloid. Z.* **1933**, *63*, 277–285.
33. (a) Sato, S.; Nagai, K. *Maku* **2005**, *30*, 20–28. (b) Koros, W. J.; Fleming, G. K. *J. Membr. Sci.* **1993**, *83*, 1–80. (c) Tsujita, Y. In *Membrane Science and Technology*; Osada, Y.; Nakagawa, T., Eds.; Marcel Dekker: New York, 1992; pp 3.
34. Hirata, T.; Sato, S.; Nagai, K. *Sep. Sci. Technol.* **2005**, *40*, 2819–2839.
35. (a) Wijmans, J. G.; Baker, R. W. In *Materials Science of Membranes for Gas and Vapor Separation*; Yampolskii, Y.; Pinnau, I.; Freeman, B. D., Eds.; Wiley: Chichester, 2006; pp 159–189. (b) Wijmans, J. G.; Baker, R. W. *J. Membr. Sci.* **1995**, *107*, 1–21. (c) Stannett, V. T.; Koros, W. J.; Paul, D. R.; Lonsdale, H. K. *Adv. Polym. Sci.* **1979**, *32*, 69–121.
36. (a) Lin, H.; Freeman, B. D. *J. Mol. Struct.* **2005**, *739*, 57–74. (b) Dixon-Garrett, S. V.; Nagai, K.; Freeman, B. D. *J. Polym. Sci. Part B: Polym. Phys.* **2000**, *38*, 1461–1473. (c) Freeman, B. D.; Pinnau, I. In *Polymer Membranes for Gas and Vapor Separation*; Freeman, B. D.; Pinnau, I., Eds.; ACS Symposium Series 733;

American Chemical Society: Washington, DC, 1999; p 1–27. (d) Nakagawa, T. In *Membrane Science and Technology*; Osada, Y.; Nakagawa, T., Eds.; Marcel Dekker: New York, 1992; pp 239.

37. Matteucci, S.; Yampolskii, Y.; Freeman, B. D.; Pinnau, I. In *Materials Science of Membranes for Gas and Vapor Separation*; Yampolskii, Y.; Pinnau, I.; Freeman, B. D., Eds.; Wiley: Chichester, 2006; pp 1–4.
38. (a) Stern, S. A. *J. Membr. Sci.* **1994**, *94*, 1–65. (b) Robeson, L. M. *J. Membr. Sci.* **1991**, *62*, 165–168.
39. Robeson, L. M.; Burgoyne, W. F.; Langsam, M.; Savoca, A. C.; Tien, C. F. *Polymer* **1994**, *35*, 4970–4978.
40. Freeman, B. D. *Macromolecules* **1999**, *32*, 375–380.
41. Kanehashi, S.; Nagai, K. *J. Membr. Sci.* **2005**, *253*, 117–138.
42. van Krevelen, D. W. *Properties of Polymers: Their Correlation with Chemical Structure; Their Numerical Estimation and Prediction from Additive Group Contributions*, 3rd ed.; Elsevier Science: Amsterdam, 1990; pp 71–107.
43. Lee, W. M. *Polym. Eng. Sci.* **1980**, *20*, 65–69.
44. (a) Yampolskii, Y.; Shantarovich, V. In *Materials Science of Membranes for Gas and Vapor Separation*; Yampolskii, Y.; Pinnau, I.; Freeman, B. D., Eds.; Wiley: Chichester, 2006; pp 191–210. (b) Freeman, B. D.; Hill, A. J. In *Structure and Properties of Glassy Polymers*; Tant, M. R.; Hill, A. J., Eds.; ACS Symposium Series 710; American Chemical Society: Washington, DC, 1998. (c) Hill, A. In *High Temperature Properties and Applications of Polymeric Materials*; Tant, M. R.; Connell, J. W.; McManus, H. L. N., Eds.; ACS Symposium Series 603; American Chemical Society: Washington, DC, 1995; p 63–80. (d) Shrader, D. M.; Jean, Y. C., Eds.; *Positron and Positronium Chemistry*; Elsevier: Amsterdam, 1988.
45. Nagai, K.; Lee, Y. M.; Masuda, T. In *Macromolecular Engineering: Precise Synthesis, Materials Properties, Applications*; Matyjaszewski, K.; Gnanou, Y.; Leibler, L., Eds.; Wiley-VCH: Weinheim, 2007; vol. 4, pp 2451–2491.
46. (a) Paul, D. R. In *Applied Polymer Science*; Tess, R. W.; Poehlein, G. W., Eds.; American Chemical Society: Washington, DC, 1985; pp 253–275. (b) Vieth, W. R.; Howell, J. M.; Hsieh, J. H. *J. Membr. Sci.* **1976**, *1*, 177–220. (c) Paul, D. R.; Koros, W. J. *J. Polym. Sci. Part B: Polym. Phys. Ed.* **1976**, *14*, 675–685.
47. Bueche, F. *Physical Properties of Polymers*; John Wiley: New York, 1962.
48. (a) Hu, Y.; Shiotsuki, M.; Sanda, F.; Masuda, T. *Chem. Commun.* **2007**, 4269–4270. (b) Sakaguchi, T.; Shiotsuki, M.; Sanda, F.; Freeman, B. D.; Masuda, T. *Macromolecules* **2005**, *38*, 8327–8332. (c) Shida, Y.; Sakaguchi, T.; Shiotsuki, M.; Sanda, F.; Freeman, B. D.; Masuda, T. *Macromolecules* **2005**, *38*, 4096–4102. (d)

Pinnau, I.; Morisato, A.; He, Z. *Macromolecules* **2004**, *37*, 2823–2828. (e) Khotimsky, V. S.; Tchirkova, M. V.; Litvinova, E. G.; Rebrov, A. I.; Bondarenko, G. N. *J. Polym. Sci., Part A: Polym. Chem.* **2003**, *41*, 2133–2155. (f) Nagai, K.; Masuda, T.; Nakagawa, T.; Freeman, B. D.; Pinnau, I. *Prog. Polym. Sci.* **2001**, *26*, 721–798. (g) Shantarovich, V. P.; Kevdina, I. B.; Yampolskii, Yu. P.; Alentiev, A. Yu. *Macromolecules* **2000**, *33*, 7453–7466. (h) Toy, L. G.; Nagai, K.; Freeman, B. D.; Pinnau, I.; He, Z.; Masuda, T.; Teraguchi, M.; Yampolskii, Yu. P. *Macromolecules* **2000**, *33*, 2516–2524. (i) Fujita, Y.; Misumi, Y.; Tabata, M.; Masuda, T. *J. Polym. Sci., Part A: Polym. Chem.* **1998**, *36*, 3157–3163.

49. (a) Sen, D.; Kalipcilar, H.; Yilmaz, L. *J. Membr. Sci.* **2007**, *303*, 194–203. (b) Hacarlioglu, P.; Toppare, L.; Yilmaz, L. *J. Appl. Polym. Sci.* **2003**, *90*, 776–785. (c) Hacarlioglu, P.; Toppare, L.; Yilmaz, L. *J. Membr. Sci.* **2003**, *225*, 51–62. (d) Laot, C. M.; Marand, E.; Schmittmann, B.; Zia, R. K. P. *Macromolecules* **2003**, *36*, 8673–8684. (e) Lopez-Gonzalez, M.; Saiz, E.; Guzman, J.; Riande, E. *Macromolecules* **2001**, *34*, 4999–5004. (f) Ruaan, R.-C.; Chen, S.-H.; Lai, J.-Y. *J. Membr. Sci.* **1997**, *135*, 9–18. (g) Chen, S.-H.; Ruaan, R.-C.; Lai, J.-Y. *J. Membr. Sci.* **1997**, *134*, 143–150. (h) Aguilar-Vega, M.; Paul, D. R. *J. Polym. Sci., Part B: Polym. Phys.* **1993**, *31*, 991–1004.
50. (a) Hillock, A. M. W.; Koros, W. J. *Macromolecules* **2007**, *40*, 583–587. (b) Wang, Y.-C.; Huang, S.-H.; Hu, C.-C.; Li, C.-L.; Lee, K.-R.; Liaw, D.-J.; Lai, J.-Y. *J. Membr. Sci.* **2005**, *248*, 15–25. (c) Wind, J. D.; Paul, D. R.; Koros, W. J. *J. Membr. Sci.* **2004**, *228*, 227–236. (d) Heuchel, M.; Hofmann, D.; Pullumbi, P. *Macromolecules* **2004**, *37*, 201–214. (e) Ayala, D.; Lozano, A. E.; de Abajo, J.; Garcia-Perez, C.; de la Campa, J. G.; Peinemann, K.-V.; Freeman, B. D.; Prabhakar, R. *J. Membr. Sci.* **2003**, *215*, 61–73. (f) Wind, J. D.; Sirard, S. M.; Paul, D. R.; Green, P. F.; Johnston, K. P.; Koros, W. J. *Macromolecules* **2003**, *36*, 6433–6441. (g) Burns, R. L.; Koros, W. J. *Macromolecules* **2003**, *36*, 2374–2381. (h) Wind, J. D.; Staudt-Bickel, C.; Paul, D. R.; Koros, W. J. *Macromolecules* **2003**, *36*, 1882–1888. (i) Niwa, M.; Kawakami, H.; Kanamori, T.; Shinbo, T.; Kaito, A.; Nagaoka, S. *Macromolecules* **2001**, *34*, 9039–9044.
51. (a) Raharjo, R. D.; Freeman, B. D.; Paul, D. R.; Sarti, G. C.; Sanders, E. S. *J. Membr. Sci.* **2007**, *306*, 75–92. (b) Roualdes, S.; Sanchez, J.; Durand, J. *J. Membr. Sci.* **2002**, *198*, 299–310. (c) Merkel, T. C.; Bondar, V. I.; Nagai, K.; Freeman, B. D.; Pinnau, I. *J. Polym. Sci., Part B: Polym. Phys.* **2000**, *38*, 415–434. (d) Singh, A.; Freeman, B. D.; Pinnau, I. *J. Polym. Sci., Part B: Polym. Phys.* **1998**, *36*, 289–301. (e) Kawakami, H.; Mori, Y.; Abe, H.; Nagaoka, S. *J. Membr. Sci.* **1997**, *133*, 245–253.
52. (a) Dai, Y.; Guiver, M. D.; Robertson, G. P.; Kang, Y. S.; Lee, K. J.; Jho, J. Y.

Macromolecules **2004**, *37*, 1403–1410. (b) Wang, D.; Teo, W. K.; Li, K. *J. Membr. Sci.* **2002**, *204*, 247–256. (c) Kim, I.-W.; Lee, K. J.; Jho, J. Y.; Park, H. C.; Won, J.; Kang, Y. S.; Guiver, M. D.; Robertson, G. P.; Dai, Y. *Macromolecules* **2001**, *34*, 2908–2913. (d) Ghosal, K.; Chem, R. T.; Freeman, B. D.; Daly, W. H.; Negulescu, I. I. *Macromolecules* **1996**, *29*, 4360–4369. (e) Aitken, C. L.; Koros, W. J.; Paul, D. R. *Macromolecules* **1992**, *25*, 3651–3658. (f) Aitken, C. L.; Koros, W. J.; Paul, D. R. *Macromolecules* **1992**, *25*, 3424–3434.

53. (a) Jha, P.; Mason, L. W.; Way, J. D. *Ind. Eng. Chem. Res.* **2006**, *45*, 6570–6577. (b) Orme, C. J.; Klaehn, J. R.; Harrup, M. K.; Luther, T. A.; Peterson, E. S.; Stewart, F. F. *J. Membr. Sci.* **2006**, *280*, 175–184. (c) Orme, C. J.; Stewart, F. F. *J. Membr. Sci.* **2005**, *253*, 243–249. (d) Orme, C. J.; Klaehn, J. R.; Stewart, F. F. *J. Membr. Sci.* **2004**, *238*, 47–55. (e) Orme, C. J.; Harrup, M. K.; Luther, T. A.; Lash, R. P.; Houston, K. S.; Weinkauf, D. H.; Stewart, F. F. *J. Membr. Sci.* **2001**, *186*, 249–256. (f) Nagai, K.; Freeman, B. D.; Cannon, A.; Allcock, H. R. *J. Membr. Sci.* **2000**, *172*, 167–176. (g) Wisian-Neilson, P.; Xu, G.-F. *Macromolecules* **1996**, *29*, 3457–3461. (h) Allcock, H. R.; Nelson, C. J.; Coggio, W. D.; Manners, I.; Koros, W. J.; Walker, D. R. B.; Pessan, L. A. *Macromolecules* **1993**, *26*, 1493–1502. (i) Hirose, T.; Mizoguchi, K. *J. Appl. Polym. Sci.* **1991**, *43*, 891–900.
54. (a) Nakai, Y.; Yoshimizu, H.; Tsujita, Y. *J. Membr. Sci.* **2005**, *256*, 72–77. (b) Wu, J.; Yuan, Q. *J. Membr. Sci.* **2002**, *204*, 185–194. (c) Li, X.-G.; Kresse, I.; Xu, Z.-K.; Springer, J. *Polymer* **2001**, *42*, 6801–6810. (d) Yang, J. P.; Huang, P. C. *J. Appl. Polym. Sci.* **2000**, *77*, 484–488. (e) Hu, L.; Zhang, X.; Zhang, H.; Niu, J.; Wang, X. *J. Appl. Polym. Sci.* **1997**, *65*, 1837–1841. (f) Suto, S.; Niimi, T.; Sugiura, T. *J. Appl. Polym. Sci.* **1996**, *61*, 1621–1630. (g) Bixon, B.; Nelson, J. K.; Muruganandam, N. *J. Membr. Sci.* **1994**, *94*, 313–328.

Chapter 1

Synthesis, Characterization, and Gas Permeation Properties of Silylated Derivatives of Ethyl Cellulose

Abstract

Silyl ethers of ethyl cellulose (**2a**–**f**) were synthesized in good yield by the reaction of various chlorosilanes with residual hydroxy groups of ethyl cellulose (**1**; DS_{Et}, 2.69). ^{1}H NMR and FTIR spectra of the silylated polymers furnished the evidence for complete substitution of hydroxy protons by the silyl groups. Silylated derivatives of ethyl cellulose (**2a**–**f**) were soluble in common organic solvents and displayed enhanced solubility in relatively nonpolar solvents due to the substitution of hydroxy groups. The onset temperatures of weight loss of the silylated derivatives (**2a**–**f**) in air were higher than 270 ºC, indicating fair thermal stability. Free-standing membranes of **1** and **2a**–**f** were fabricated by casting their toluene solution and all the silylated derivatives (**2a**–**f**) exhibited enhanced gas permeability (*P*) as compared to ethyl cellulose (**1**). An increment in the size of the silyl group led to the decrement in gas permeability of the polymers, and trimethylsilyl derivative (**2a**) exhibited the highest *P* value. The P_{CO_2}/P_{N_2} values of the polymers (**2a**–**f**) were observed to be in the range of 15–19, and the data for **2a**, **2b**, and **2c** were located above the upper bound in the plot of permselectivity versus permeability for CO_2/N_2 gas pair. For all the six gases under study, gas diffusion coefficients (*D*) increased upon silylation while gas solubility coefficients (*S*) underwent a decline.

Introduction

Polymeric gas separation membranes have engrossed substantial prominence, contributing to sustainable chemical processing in the past two decades and are being exploited in a wide array of commercial applications.[1] At present, a variety of gas mixtures of industrial interest are being separated by the selective permeation of the components through non-porous membranes made of glassy polymers such as polyacetylenes, polyimides, and polysulfones.[2] Among them silylated polyacetylenes are a class of highly gas-permeable glassy materials as they possess many microvoids in the polymer matrix due to their stiff main chain composed of alternating double bonds and the steric effect of the spherical pendant groups.[1b,3] One of them, poly(1-trimethylsilyl-1-propyne) [poly(TMSP)] is the most gas-permeable material and many studies concerning the gas permeation properties of this polymer have been reported till today.[1b,4] Most of poly(1-aryl-2-phenylacetylenes) having spherical substituents on the phenyl moiety also exhibit high gas permeability.[3a,5] For instance, the oxygen permeability coefficient (P_{O_2}) of poly[1-phenyl-2-(*p*-trimethylsilyl)phenylacetylene] [poly(TMSDPA)] is 1500 barrers,[5a] which is quite high among all the synthetic polymers. However, there remains a strong need to develop high flux membranes with high selectivity and fouling-resistant properties for large-scale applications. Physical or chemical modification of polymers is an attractive alternative to tailor the gas permeability and permselectivity of membrane-forming materials, as desired for specific applications.

Ethyl cellulose is derived from an inexhaustible natural polymeric material, cellulose, and possesses the fascinating structure and properties such as extensive linearity, chain stiffness, good solubility in organic solvents, adequate membrane-forming ability, moderate gas permeation/pervaporation capability, excellent durability, good film-flexibility, chemical resistance, mechanical strength, hydrophobicity, non-toxicity and low cost.[6] Ethyl cellulose has been the subject of research activity for oxygen enrichment for several years;[7] however, only a few studies concerning the systematic investigation of gas/vapor transport through ethyl cellulose

membranes have been reported.[8] Despite the fact that the carbon dioxide permeability exhibited by ethyl cellulose (P_{CO_2} is ~110 barrers) is not as high as those of silylated polyacetylenes, the carbon dioxide/nitrogen permselectivity (P_{CO_2}/P_{N_2} is ~22) is fairly high.[7f] Since silyl groups often favor high gas permeability,[1b,3,4,5] silylated derivatives of ethyl cellulose are expected to be interesting candidates for gas separation membranes.

The present chapter deals with the synthesis of various silyl ethers of ethyl cellulose (**2a**–**f**), their characterization, and elucidation of various properties. Free-standing membranes of the starting as well as silylated polymers were fabricated and their density, fractional free volume, and gas permeation parameters were determined. Furthermore, the diffusion and solubility coefficients of polymer membranes for O_2, N_2, CO_2, and CH_4 were also revealed.

Scheme 1. Silylation of Ethyl Cellulose with Various Chlorosilanes.

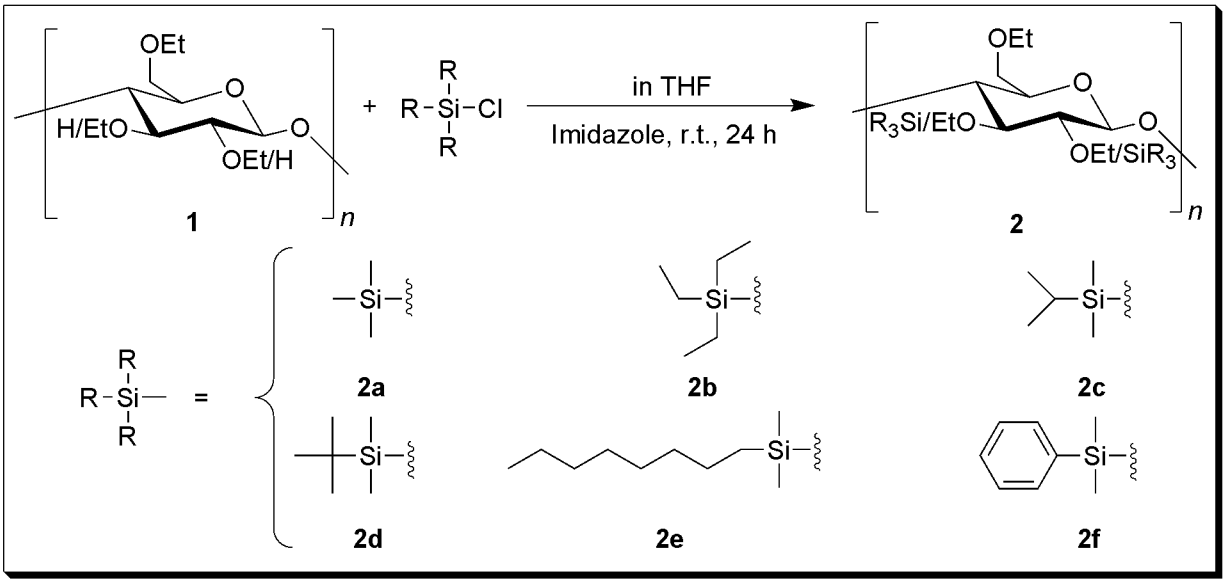

Experimental Section

Measurements. ^{1}H NMR spectra were recorded on a JEOL EX-400 spectrometer and the residual proton signal of the deutrated solvent was used as internal standard. The samples for the NMR measurements were prepared at a concentration of approximately 10 mg/mL and chemical shifts are reported in parts per

million (ppm). Infrared spectra were recorded on a Jasco FTIR-4100 spectrophotometer. The number- and weight-average molecular weights (M_n and M_w, respectively) and polydispersity indices (M_w/M_n) of polymers were measured by GPC at 40 ºC with a Jasco PU-980/RI-930 chromatograph (eluent THF, columns KF-805 (Shodex) × 3, molecular weight range up to 4×10^6, flow rate 1 mL/min). The elution times were converted into molecular weights using a calibration curve based on polystyrene standards in combination with the information obtained from the refractive index detector. Thermogravimetric analyses (TGA) were conducted in air with a Perkin-Elmer TGA7 thermal analyzer by heating the samples (3–5 mg) from 100–700 ºC at a scanning rate of 10 ºC min^{-1}. Membrane thickness was estimated by using a Mitutoyo micrometer. The gas permeability coefficients (P) were measured with a Rikaseiki K-315-N gas permeability apparatus using a constant volume/variable-pressure system. All of the measurements were carried out at 25 ºC and a feed pressure of 0.1 MPa (1 atm) while the system was being evacuated on the downstream side of the membrane.

Materials. Ethyl cellulose (**1**; ethoxy content, 49 wt%) and imidazole were purchased from Aldrich and Wako (Japan), respectively, and used as received. Chlorotrimethylsilane, chlorotriethylsilane, chlorodimethylisopropylsilane, chlorodimethyl-*n*-octylsilane, chlorodimethylphenylsilane (Tokyo Kasei, Japan), and chloro-*t*-butyldimethylsilane (Aldrich) were obtained commercially and used without further purification. Tetrahydrofuran, used as reaction solvent, was purchased from Wako (Japan) and employed after distillation.

Silylated derivatives of ethyl cellulose (**2a**–**f**) were synthesized according to Scheme 1. The details of the synthetic procedure and analytical data are as follows:

Trimethylsilyl Derivative of Ethyl Cellulose (2a). A 200 mL one-necked flask was equipped with a dropping funnel, a three-way stopcock, and a magnetic stirring bar. Ethyl cellulose (1.43 g, 6.10 mmol) and imidazole (2.49 g, 36.6 mmol) were placed in the flask, evacuated for half an hour, flushed with nitrogen, and dissolved in THF (50 mL) at room temperature. Then, chlorotrimethylsilane (2.31

mL, 18.3 mmol) was added dropwise and stirring was continued for 24 h at room temperature. Product was isolated by precipitation in methanol (1000 mL), filtered with a membrane filter, washed repeatedly with methanol and acetone successively and dried under vacuum to constant weight to afford the desired product (89%) as white solid. IR (ATR, cm^{-1}): 2972, 2870, 1375, 1249, 1088, 1049, 879, 842; ^{1}H NMR (400 MHz, $CDCl_3$, 25 ºC, ppm): 4.31–3.00 (m, 12.4H, OCH_2CH_3, OCH, OCH_2), 1.12 (brs, 8.07H, OCH_2CH_3), 0.094 (s, 2.79H, $SiCH_3$).

Triethylsilyl Derivative of Ethyl Cellulose (2b). This derivative was prepared by following the same procedure as for **2a** using chlorotriethylsilane instead of chlorotrimethylsilane. Yield 92%, white solid, IR (ATR, cm^{-1}): 2977, 2873, 1375, 1090, 1050, 819, 738; ^{1}H NMR (400 MHz, $CDCl_3$, 25 ºC, ppm): 4.30–2.89 (m, 12.4H, OCH_2CH_3, OCH, OCH_2), 1.12 (brs, 8.07H, OCH_2CH_3), 0.93 (brs, 2.79H, $SiCH_2CH_3$), 0.64 (brs, 1.86H, $SiCH_2CH_3$).

Dimethylisopropylsilyl Derivative of Ethyl Cellulose (2c). This derivative was prepared by following the same procedure as for **2a** using chlorodimethylisopropylsilane instead of chlorotrimethylsilane. Yield 90%, white solid, IR (ATR, cm^{-1}): 2972, 2867, 1374, 1253, 1089, 1050, 922, 850, 829, 802, 777; ^{1}H NMR (400 MHz, $CDCl_3$, 25 ºC, ppm): 4.30–2.98 (m, 12.4H, OCH_2CH_3, OCH, OCH_2), 1.12 (brs, 8.07H, OCH_2CH_3), 0.92 (brs, 1.86H, $SiCH(CH_3)_2$), 0.05 (brs, 2.17H, $SiCH_3$, $SiCH(CH_3)_2$).

Dimethyl-*t*-butylsilyl Derivative of Ethyl Cellulose (2d). This derivative was prepared by following the same procedure as for **2a** using chlorodimethyl-*t*-butylsilane instead of chlorotrimethylsilane and precipitation was carried out using water in place of methanol. Yield 88%, white solid, IR (ATR, cm^{-1}): 2974, 2868, 1375, 1092, 1056, 1000, 839; ^{1}H NMR (400 MHz, $CDCl_3$, 25 ºC, ppm): 4.30–3.00 (m, 12.4H, OCH_2CH_3, OCH, OCH_2), 1.13 (brs, 8.07H, OCH_2CH_3), 0.85 (brs, 2.79H, $SiC(CH_3)_3$), 0.05 (brs, 1.86H, $SiCH_3$).

Dimethyl-*n*-octylsilyl Derivative of Ethyl Cellulose (2e). This derivative was prepared by following the same procedure as for **2a** using

chlorodimethyl-*n*-octylsilane instead of chlorotrimethylsilane. Yield 92%, white solid, IR (ATR, cm^{-1}): 2971, 2922, 1375, 1089, 1050, 922, 839; ^1H NMR (400 MHz, $CDCl_3$, 25 ºC, ppm): 4.31–2.89 (m, 12.4H, OCH_2CH_3, OCH, OCH_2), 1.24 (brs, 3.72H, $CH_2(CH_2)_6$), 1.12 (brs, 8.07H, OCH_2CH_3), 0.86 (t, 0.93H, CH_2CH_3), 0.6 (brs, 0.62H, $SiCH_2$), 0.08 (s, 1.86H, $SiCH_3$).

Dimethylphenylsilyl Derivative of Ethyl Cellulose (2f). This derivative was prepared by following the same procedure as for **2a** using chlorodimethylphenylsilane instead of chlorotrimethylsilane. Yield 87%, white solid, IR (ATR, cm^{-1}): 2972, 2870, 1443, 1428, 1375, 1251, 923, 855, 830, 787, 741, 700; ^1H NMR (400 MHz, $CDCl_3$, 25 ºC, ppm): 7.61–7.24 (m, 1.55H, SiC_6H_5), 4.25–2.98 (m, 12.4H, OCH_2CH_3, OCH, OCH_2), 1.12 (brs, 8.07H, OCH_2CH_3), 0.39 (s, 1.86H, $SiCH_3$).

Determination of the Degree of Substitution. The degree of substitution with ethyl group (DS_{Et}) of the starting material, ethyl cellulose, and the degree of substitution with silyl group (DS_{Si}) of the silylated derivatives (**2a**–**f)** were determined by ^1H NMR (Figure 1). The total degree of substitution (DS_{total}) of **2a**–**f** was calculated by the following equation:

$$DS_{total} = DS_{Et} + DS_{Si}$$

Membrane Fabrication. Membranes (thickness ca. 40–80 μm) of polymers **1** and **2a**–**f** were fabricated by casting their toluene solution (concentration ca. 0.50–1.0 wt%) onto a Petri dish. The dish was covered with a glass vessel to retard the rate of solvent evaporation (3–5 days).

Membrane Density. Membrane densities (ρ) were determined by hydrostatic weighing using a Mettler Toledo balance (model AG204, Switzerland) and a density determination kit.[9] This method makes use of a liquid with known density (ρ_0), and membrane density (ρ) is calculated by the following equation:

$$\rho = \rho_0 M_A/(M_A - M_L)$$

where M_A is the weight of membrane in air and M_L is that in the auxiliary liquid. Aqueous $NaNO_3$ solution was used as an auxiliary liquid.

Fractional Free Volume (FFV) of Polymer Membranes. FFV (cm^3 of free volume/cm^3 of polymer) is commonly used to estimate the efficiency of chain packing and the amount of space (free volume) available for gas permeation in the polymer matrix. FFV is calculated by the following equation:[10]

$$\text{FFV} = (v_{sp} - v_0)/\, v_{sp} \approx (v_{sp} - 1.3\, v_w)/\, v_{sp}$$

where v_{sp} and v_0 are the specific volume and occupied volume (or zero-point volume at 0 K) of the polymer, respectively. Typically, occupied volume (v_0) is estimated as 1.3 times the van der Waals volume (v_w), which is calculated by the group contribution method.[11]

Measurement of Gas Permeation Parameters. The *P* values were calculated from the slopes of time-pressure curves in the steady state where Fick's law holds.[12] The *D* values were determined by the time lag method using the following equation:

$$D = l^2/6\theta$$

here, l is the membrane thickness and θ is the time lag, which is given by the intercept of the asymptotic line of the time-pressure curve to the time axis. The membrane thickness was controlled so that the time lag would be in the range of 10–300 s, preferably 30–150 s. When the time lag was < 10 s, the error of measurement became relatively large. If the time lag was, on the contrary, > 300 s, the error arising from the baseline drift became serious. The gas solubility coefficients (*S*) were calculated by using the equation, $S = P/D$.

Results and Discussion

Silylation of Ethyl Cellulose. Silylation of ethyl cellulose was carried out by employing various chlorosilanes as silylating agents, THF as a solvent, and imidazole as a base as shown in Scheme 1, and the results are summarized in Table 1.

Table 1. Degree of Substitution and Molecular Weight of Polymers 1 and 2a–f

polymer	DS_{Si} [a]	DS_{total} [a]	M_w [b]	M_w/M_n [b]
1	0.00	2.69	195 000	3.46
2a	0.32	3.01	187 000	2.26
2b	0.31	3.00	237 000	2.90
2c	0.33	3.02	289 000	4.24
2d	0.31	3.00	206 000	3.11
2e	0.34	3.03	264 000	2.20
2f	0.38	3.07	168 000	2.59

[a] DS_{Si}: Degree of silylation, DS_{total}: Total degree of substitution. Calculated from ^{1}H NMR. [b] Determined by GPC (THF, PSt).

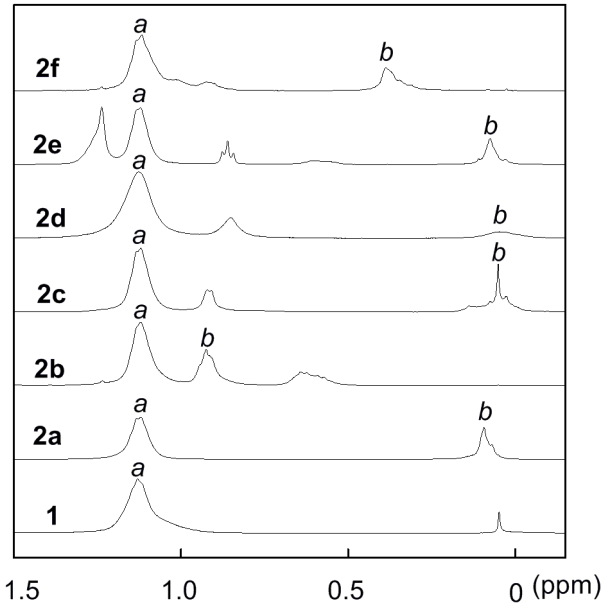

Figure 1. ^{1}H NMR spectra of polymers **1** and **2a**–**f** in $CDCl_3$ at 25 ºC.

The DS_{Et} of ethyl cellulose was estimated to be 2.69, by calculating the integration ratio of methyl protons (labeled as *a*, in Figure 1) to the rest of the protons in ethyl cellulose, indicating the presence of 0.31 hydroxy groups per anhydroglucose unit. Degree of silylation (DS_{Si}) of polymers (**2a**–**f**) was determined by calculating the integration ratio of the methyl protons of ethyl (labeled as *a*, in Figure 1) to those of silyl content (labeled as *b*, in Figure 1) and complete silylation of the residual hydroxy groups of ethyl cellulose was observed. IR spectra of the polymers (as exemplified in Figure 2) furnished further evidence for quantitative silylation due to the presence of the peaks characteristic of the silyl group (1375–1425 cm^{-1}, 775–850 cm^{-1}) and the absence of the broad band characteristic of the hydroxy group (3200–3600 cm^{-1}). According to GPC data of the polymers (Table 1), weight-average molecular weights (M_w) and polydispersity indices (M_w/M_n) of the silyl ethers were not quite different from those of **1**. For instance, the M_w and M_w/M_n of **1** were observed to be 195,000 and 3.46 while those of **2a** were 187,000 and 2.26, respectively. These facts rule out any sort of polymer chain cleavage in the course of silylation.

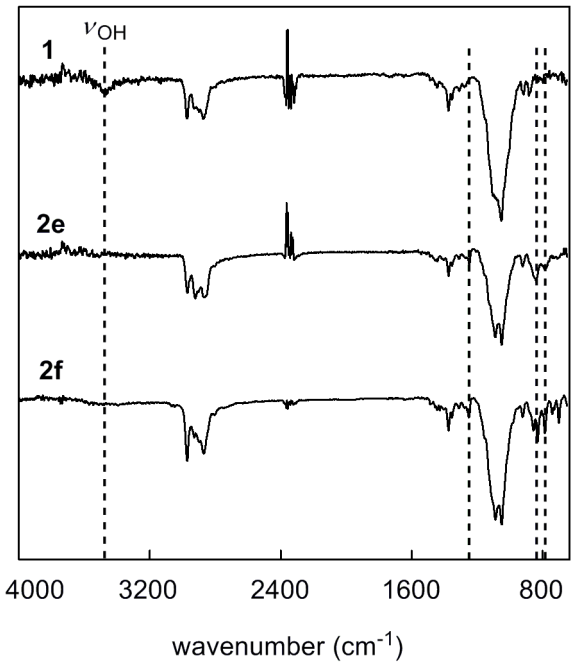

Figure 2. ATR-FTIR spectra of polymers **1, 2e** and **2f**.

Solubility and Thermal Stability of Polymers. The solubility properties of polymers **1** and **2a**–**f** are summarized in Table 2. The silylated ethyl cellulose derivatives (**2a**–**f)** displayed enhanced solubility in nonpolar solvents. Ethyl cellulose (**1)** was soluble in DMF, while its silylated derivatives were either insoluble or partly soluble. Similarly, **1** exhibited solubility in methanol, while its silylated derivatives were insoluble except **2d** which was partly soluble. On the other hand, all of the silylated polymers were soluble (**2d** was partly soluble) in hexane, a nonpolar solvent, while ethyl cellulose was insoluble. This augmented nonpolar character of silylated derivatives of ethyl cellulose finds its explanation in the less polar character of siloxy groups as compared to the hydroxy groups present in ethyl cellulose.

Table 2. Solubility[a] of Polymers 1 and 2a–f

polymer	**1**	**2a**	**2b**	**2c**	**2d**	**2e**	**2f**
hexane	–	+	+	+	±	+	+
toluene	+	+	+	+	+	+	+
$CHCl_3$	+	+	+	+	+	+	+
THF	+	+	+	+	+	+	+
acetone	–	–	–	–	+	–	+
methanol	+	–	–	–	±	–	–
DMF	+	–	±	±	±	±	–

[a] Symbols: +, soluble; ±, partly soluble; –, insoluble.

The thermal stability of polymers **1** and **2a**–**f** was examined by thermogravimetric analysis (TGA) in air (Figure 3). The onset temperatures of weight loss (T_0) of **2a**–**d** were in the range of 280–300 ºC (Table 3). As the bulk of the silyl group increased, the onset temperature of weight loss became higher. The T_0 value of **2e** was lower than the rest owing to the presence of the silyl group having longer alkyl chain. Polymer **2f** displayed the highest thermal stability among **2a**–**f**, probably imparted by the phenyl moiety in the silyl group. These results imply that the thermal stability increases with increase in the stiffness of the silyl substituent and undergoes a decrease as the length of the alkyl chain in the silyl group increases.

Although the thermal stability of the silylated derivatives of ethyl cellulose (**2a**–**f**), except **2f**, is slightly lower than that of the starting material (**1)**, it is still appreciably reasonable for practical applications as membrane-forming materials.

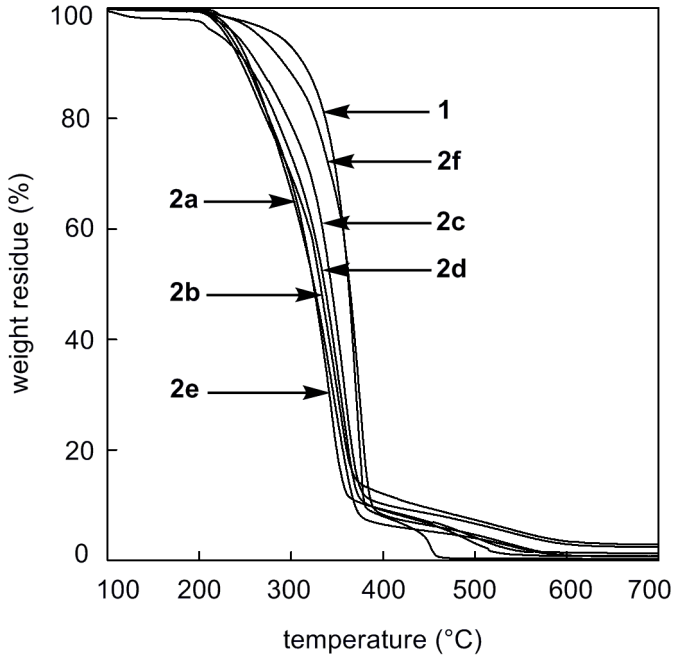

Figure 3. TGA curves of polymers **1** and **2a**–**f** (in air, heating rate 10 ºC min^{-1}).

Density and FFV of Polymer Membranes. Table 3 lists the van der Waals volume (v_w), density (ρ), and fractional free volume (FFV) of the polymer membranes (**1** and **2a**–**f**). All of the silylated derivatives (**2a**–**f**) exhibited lower membrane density as compared to ethyl cellulose (**1**); *e.g.*, the ρ value of **1** was observed to be 1.095 while those of **2a**–**f** were in the range of 1.034–1.091. It was observed that an increase in the length of the alkyl chain in the silyl group led to a decrease in the density of the polymer membranes. Although silylation of ethyl cellulose resulted in the decreased density of polymer membranes, this decrease was counterbalanced by the increased van der Waals volumes of the silylated derivatives and resulted in net decrease in the FFV of **2a**–**f** as compared to the starting polymer membrane (**1**). For instance, **2e** exhibited the lowest value of fractional free volume (FFV is 0.148) in spite of its lowest density among all the silylated derivatives of ethyl cellulose (ρ is

1.034), which is probably due to its highest van der Waals volume.

Table 3. Physical Properties of Polymers 1 and 2a–f

polymer	T_0[a] (°C)	v_w[b] (cm^3/mol)	ρ[c] (g/cm^3)	FFV[d]
1	338	135.8	1.095	0.185
2a	280	152.1	1.076	0.180
2b	283	162.1	1.065	0.177
2c	305	159.0	1.067	0.178
2d	298	162.1	1.083	0.163
2e	273	183.8	1.034	0.148
2f	338	162.6	1.091	0.173

[a] Onset temperature of weight loss observed from TGA measurement in air. [b] v_w: van der Waals volume. [c] ρ: density. Determined by hydrostatic weighing. [d] FFV: fractional free volume. Estimated from membrane density.

Gas Permeation Properties. The permeability coefficients of the membranes of polymers **1** and **2a–f** to various gases measured at 25 °C are listed in Table 4, and their plot versus kinetic diameter of gases is shown in Figure 4. The gas permeability of the silylated derivatives was higher than that of ethyl cellulose, and

Table 4. Gas Permeability Coefficients (*P*) of Polymer Membranes at 25 °C

polymer	*P* (barrer)[a]						P_{CO_2}/P_{N_2}	P_{CO_2}/P_{CH_4}
	He	H_2	O_2	N_2	CO_2	CH_4		
1	53	76	18	5.0	110	12	22	9.2
2a	98	160	45	14	250	35	18	7.1
2b	81	130	42	13	230	33	18	7.0
2c	82	130	40	13	230	31	18	7.4
2d	67	100	27	8.0	150	18	19	8.3
2e	65	98	31	10	150	25	15	6.0
2f	58	86	23	7.0	130	15	19	8.7

[a] 1 barrer = $1x10^{-10}$ cm^3 (STP) cm cm^{-2} s^{-1} $cmHg^{-1}$.

approximately obeys the following order: **2a** > **2b** ≈ **2c** > **2d** > **2e** > **2f** > **1**. The order of the gas permeability coefficients corresponds to the shape, size, and mobility of the silyl substituents. It has been reported that the increase in the bulk or the length of the alkyl group in the silyl moiety accompanies a decrease in the gas permeability; *e.g.*, the P_{O_2} of poly(TMSDPA) is 1500 barrers,[5a] while those of poly[1-phenyl-2-(*p*-triisopropylsilyl)-phenylacetylene] and

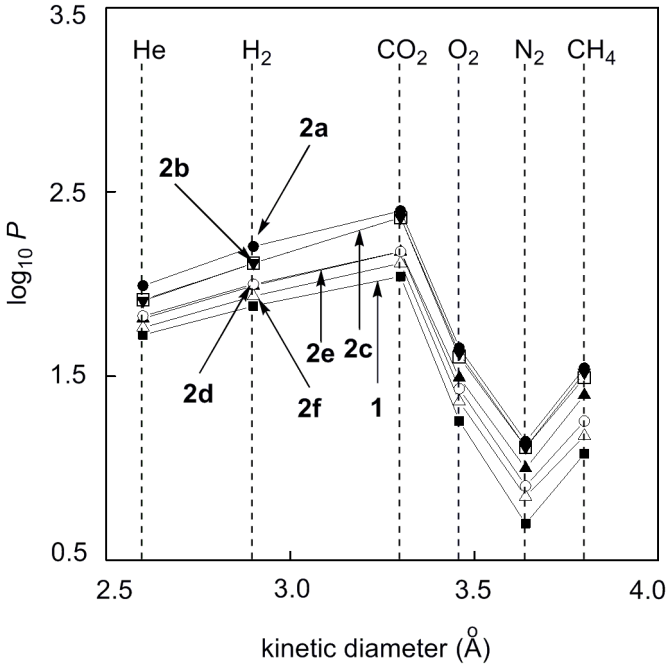

Figure 4. Gas permeability coefficients ($\log_{10}P$) of ethyl cellulose (**1**) and its silylated derivatives (**2a**–**f**) vs kinetic diameter of gases.

poly[1-phenyl-2-(*p*-triphenylsilyl)-phenylacetylene] are 20 and 3.8 barrers, respectively.[13]

Among all the silylated derivatives of ethyl cellulose (**2a**–**f**), **2a** exhibited the highest permeability to all the gases, and this trend bears a resemblance to that observed in the case of silylated polyacetylenes. This tendency has been explained in terms of the finding that the trimethylsilyl group effectively generates many molecular-scale voids and simultaneously exhibits large local mobility.[14] For instance, the P_{O_2} of poly(TMSP) is 10,000 barrers, while that of

poly(1-triethylsilyl-1-propyne) is not more than 640 barrers.[15] The lowest gas permeability has been observed for **2f** emanating from the planar and non-flexible nature of the aryl group present in the silyl moiety thus leading to the stacking and decreased local mobility of the substituent.

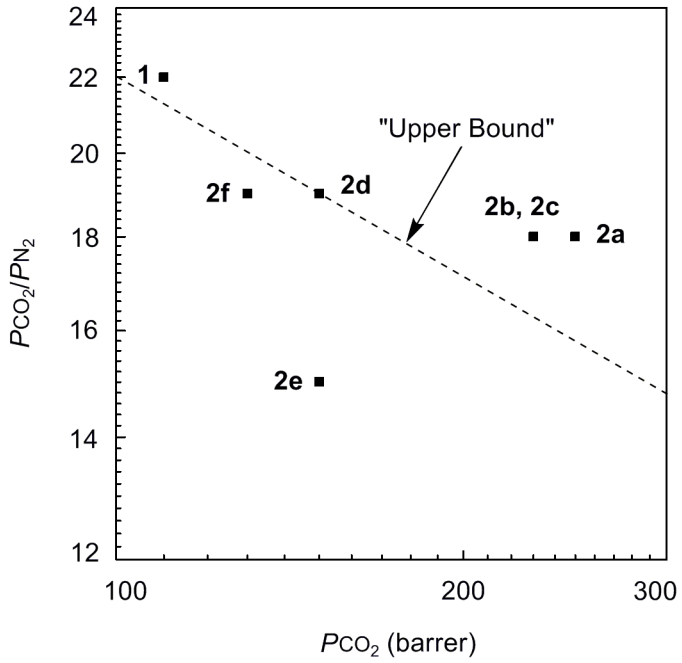

Figure 5. Plot of permselectivity vs permeability for the CO_2/N_2 gas pair.

The most important feature of the gas permeability data of ethyl cellulose and its silylated derivatives is relatively high P_{CO_2}/P_{N_2} selectivity (>15) of these polymers. Especially, **2a**–**c** displayed good performance for CO_2 separation, and their data were located above the upper bound,[16] in the plot of permselectivity versus permeability for CO_2/N_2 gas pair (Figure 5). However, as the gas permeability undergoes an increase, a decrease in the permselectivity is observed. These results imply that spherical substituents with appropriate size are required to achieve high gas permeability rather than planar and bulky groups, and those having long alkyl chains.

Gas Diffusivity and Solubility. Gas permeability can be expressed as the product of gas solubility in the upstream face of the membrane and effective average gas diffusion through the membrane, strictly in rubbery and approximately in glassy

polymers:[1a,17]

$$P = S \times D$$

.

In order to carry out a detailed investigation of the gas permeability of **1** and **2a**–**f**, gas diffusion coefficients (*D*) and gas solubility coefficients (*S*) were determined. The *D* and *S* values of polymers **1** and **2a**–**f** for O_2, N_2, CO_2, and CH_4 are given in Tables 5 and 6, respectively. In polymeric membranes, generally the *D* value undergoes a decrease with increasing critical volume of gases while the *S* value experiences an increase with increasing critical temperature of gases. Similar tendencies were observed in the *D* and *S* values of the polymer membranes of ethyl cellulose and its silylated derivatives; *e.g.*, in the case of **2a**, the diffusivity of CH_4 (5.0) was the lowest and that of O_2 (19) was the highest while CO_2 (33) displayed the highest solubility and N_2 (1.1) the lowest.

As shown in Table 5, the diffusion coefficients of all the gases increased upon silylation. For instance, **1** displayed the D_{O_2} value of 8.3 while those of **2a**–**f** were in

Table 5. Gas Diffusion Coefficients[a] (*D*) of the Polymer Membranes

	$10^7 D$ ($cm^2 s^{-1}$)			
	N_2	O_2	CH_4	CO_2
critical volume (cm^3/mol)	73.4	89.8	93.9	99.2
1	8.3	3.8	2.6	1.8
2a	19	13	7.6	5.0
2b	30	21	8.5	5.4
2c	27	18	7.3	4.5
2d	16	8.0	4.7	3.1
2e	38	18	10	7.0
2f	16	9.5	5.3	3.0

[a] Determined by the 'time lag' method at 25° C.

the range of 16–38. The increment of gas diffusivity can be accounted for by the increase in the local mobility of the substituents.[14]

As far as the gas solubility coefficients are concerned, a decrease in the *S* value was observed in almost all of the silylated derivatives as compared to ethyl cellulose itself, as shown in Table 6. The decrement in the solubility coefficients presumably ensued from the attenuated fractional free volume accompanied by silylation, as summarized in Table 3. Quite interestingly, the S_{CO_2} values underwent a relatively large decline in comparison with all the other gases under study; *e.g.*, the S_{CO_2} and S_{CH_4} of **1** were discerned to be 45 and 6.5 while those for **2a** were 33 and 6.1, respectively. Such behavior can be explained in terms of the strong interaction of CO_2 with the hydroxy groups present in ethyl cellulose prior to silylation. Similar effect has been observed in poly(diphenylacetylene) membranes bearing hydroxy groups in their side chain.[18]

Table 6. Gas Solubility Coefficients[a] (*S*) of the Polymer Membranes

	$10^3 S$ (cm^3 (STP) cm^{-3} $cmHg^{-1}$)			
	N_2	O_2	CH_4	CO_2
critical temperature (K)	126.2	154.8	191.0	304.1
1	1.4	2.2	6.5	45
2a	1.1	2.3	6.1	33
2b	0.64	1.4	6.2	27
2c	0.79	1.6	6.7	31
2d	0.96	1.6	5.7	33
2e	0.58	0.8	3.5	15
2f	0.68	1.4	4.7	24

[a] Calculated by using quotients, *P*/*D*.

Among **2a**–**f**, **2e** exhibited the highest *D* value for all the gases while its *S* value was the lowest, suggesting no increase in FFV but enhanced local mobility due to the presence of the silyl substituent with long alkyl chain, leading to the increased

diffusion coefficient. These findings are consistent with those observed in various substituted polyacetylenes.[12] It is noteworthy that the increase in the diffusion coefficients upon silylation was more pronounced than the decrease in the solubility coefficients, thus leading to the net effect of enhanced permeability. Furthermore, these results indicate the significance of silyl groups to enhance the gas permeability by increasing the gas diffusion coefficients of the polymer membranes.

Conclusions

The present study is concerned with the synthesis of novel silyl ethers of ethyl cellulose (**2a**–**f**). It was demonstrated that halosilanes served as excellent silylating agents, in the presence of imidazole, accomplishing the complete silylation of ethyl cellulose even at room temperature without any chain degradation of the starting material. All of the silylated polymers (**2a**–**f**) displayed good solubility in common organic solvents, fair thermal stability, and adequate membrane-forming ability. Membranes of **2a**–**f** exhibited higher gas permeability than that of **1** due to the increased diffusion coefficients resulting from the introduction of silyl moieties in ethyl cellulose. Although silylation could not affect a very large increase in gas flux, probably due to the very small extent of hydroxy groups (0.31 per anhydroglucose unit) available for derivatization yet good separation performance for CO_2/N_2 and CO_2/CH_4 was discerned.

References and Notes

1. (a) Pinnau, I.; Freeman, B. D. *Advanced Materials for Membrane Separations*; ACS Symposium Series 876; American Chemical Society: Washington, DC, 2004. (b) Nagai, K.; Masuda, T.; Nakagawa, T.; Freeman, B. D.; Pinnau, I. *Prog. Polym. Sci.* **2001**, *26*, 721–798. (c) Nunes, S. P.; Peinemann, K.-V. *Membrane Technology in the Chemical Industry*; Wiley: New York, 2001. (d) Koros, W. J.; Mahajan, R. *J. Membr. Sci.* **2000**, *175*, 181–196. (e) Aoki, T. *Prog. Polym. Sci.* **1999**, *24*, 951–993. (f) Maier, G. *Angew. Chem. Int. Ed.* **1998**, *37*, 2961–2974.
2. (a) Alentiev, A. Y.; Shantarovich, V. P.; Merkel, T. C.; Bondar, V. I.; Freeman, B.

D.; Yampolskii, Yu. P. *Macromolecules* **2002**, *35*, 9513–9522. (b) Freeman, B. D.; Pinnau, I. *Trends Polym. Sci.* **1997**, *5*, 167–173. (c) Langsam, M. *Plastics Engineering* **1996**, *36*, 697–741. (d) Chung, I. J.; Lee, K. R.; Hwang, S. T. *J. Membr. Sci.* **1995**, *105*, 177–185. (e) Henis, J. M. S. *Commercial and Practical Aspects of Gas Separation Membranes*; CRC Press: Boca Raton, FL, 1994. (f) Koros, W. J. In *Membrane Separation Systems: Recent Developments and Future Directions*, Baker, R. W., Cuasler, E. L., Eykamp, W., Koros, W. J., Riley, R. L., Strathmann, H., Eds.; Noyes Data Corporation: Park Ridge, NJ, 1991; pp 189–241. (g) Spillman, R. W. *Chem. Eng. Prog*. **1989**, *85*, 41–62.

3. (a) Sakaguchi, T.; Shiotsuki, M.; Masuda, T. *Macromolecules* **2004**, *37*, 4104–4108. (b) Sakaguchi, T.; Kwak, G.; Masuda, T. *Polymer* **2002**, *43*, 3937–3942. (c) Morisato, A.; Pinnau, I. *J. Membr. Sci.* **1996**, *121*, 243–250. (d) Tsuchihara, K.; Masuda, T.; Higashimura, T. *Macromolecules* **1992**, *25*, 5816–5820. (e) Hayakawa, Y.; Nishida, M.; Aoki, T.; Muramatsu, H. *J. Polym. Sci., Part A: Polym. Chem.* **1992**, *30*, 873–877.
4. (a) Nagai, K.; Kanehashi, S.; Tabei, S.; Nakagawa, T. *J. Membr. Sci.* **2005**, *251*, 101–110. (b) Starannikova, L.; Khodzhaeva, V.; Yampoľskii, Y. *J. Membr. Sci.* **2004**, *244*, 183–191. (c) Hill, A. J.; Pas, S. J.; Bastow, T. J.; Burgar, M. I.; Nagai, K.; Toy, L. G.; Freeman, B. D. *J. Membr. Sci.* **2004**, *243*, 37–44. (d) Bi, J. J.; Wang, C. L.; Kobayashi, Y.; Ogasawara, K.; Yamasaki, A. *J. Appl. Polym. Sci.* **2003**, *87*, 497–501. (e) Madkour, T. M. *Polymer* **2000**, *41*, 7489–7497.
5. (a) Sakaguchi, T.; Yumoto, K.; Shiotsuki, M.; Sanda, F.; Yoshikawa, M.; Masuda, T. *Macromolecules* **2005**, *38*, 2704–2709. (b) Raharjo, R. D.; Lee, H. J.; Freeman, B. D.; Sakaguchi, T.; Masuda, T. *Polymer* **2005**, *46*, 6316–6324. (c) Kouzai, H.; Masuda, T.; Higashimura, T. *J. Polym. Sci., Part A: Polym. Chem.* **1994**, *32*, 2523–2530. (d) Tsuchihara, K.; Masuda, T.; Higashimura, T. *J. Polym. Sci., Part A: Polym. Chem.* **1993**, *31*, 547–552.
6. (a) Crowley, M. M.; Schroeder, B.; Fredersdorf, A.; Obara, S.; Talarico, M.; Kucera, S.; McGinity, J. W. *Int. J. Pharm.* **2004**, *269*, 509–522. (b) Li, X.-G.; Kresse, I.; Xu, Z.-K.; Springer, J. *Polymer* **2001**, *42*, 6801–6810. (c) Klemm, D.; Philipp, B.; Heinze, T.; Heinze, U.; Wagenknecht, W. *Comprehensive Cellulose Chemistry*; Wiley-VCH: Weinheim, 1998; Vol. 2.
7. (a) Li, X.-G.; Huang, M.-R.; Hu, L.; Lin, G.; Yang, P.-C. *Eur. Polym. J.* **1999**, *35*, 157–166. (b) He, Y.; Yang, J.; Li, H.; Huang, P. *Polymer* **1998**, *39*, 3393–3397. (c) Li, X.-G.; Huang, M.-R. *J. Appl. Polym. Sci.* **1997**, *66*, 2139–2147. (d) Houde, A. Y.; Stern, S. A. *J. Membr. Sci.* **1997**, *127*, 171–183. (e) Suto, S.; Niimi, T.; Sugiura, T. *J. Appl. Polym. Sci.* **1996**, *61*, 1621–1630. (f) Houde, A. Y.; Stern, S. A. *J. Membr. Sci.* **1994**, *92*, 95–101.

8. (a) Li, X.-G.; Huang, M.-R.; Gu, G.-F.; Qiu, W.; Lu, J.-Y. *J. Appl. Polym. Sci.* **2000**, *75*, 458–463. (b) Bai, S.; Sridhar, S.; Khan, A. A. *J. Membr. Sci.* **2000**, *174*, 67–79. (c) Ravindra, R.; Sridhar, S.; Khan, A. A.; Rao, A. K. *Polymer* **2000**, *41*, 2795–2806. (d) Wang, Y.; Easteal, A. J. *J. Membr. Sci.* **1999**, *157*, 53–61. (e) Spencer, H. G.; Ibrahim, I. M. *J. Appl. Polym. Sci.* **1978**, *22*, 3607–3609.
9. Lin, H.; Freeman, B. D. *J. Membr. Sci.* **2004**, *239*, 105–117.
10. (a) Pixton, M. R.; Paul, D. R. In *Polymeric Gas Separation Membranes*; Paul, D. R., Yampolskii, Yu. P., Eds.; CRC Press: Boca Raton, FL, 1994; pp 83–153. (b) Lee, W. M. *Polym. Eng. Sci.* **1980**, *20*, 65–69. (c) Bondi, A. *Physical Properties of Molecular Crystals, Liquids, and Glasses*; John Wiley and Sons: New York, 1968; pp 25–97.
11. van Krevelen, D. W. *Properties of Polymers: Their Correlation with Chemical Structure; Their Numerical Estimation and Prediction from Additive Group Contributions*, 3rd ed.; Elsevier Science: Amsterdam, 1990; pp 71–107.
12. Masuda, T.; Iguchi, Y.; Tang, B.-Z.; Higashimura, T. *Polymer* **1988**, *29*, 2041–2049.
13. Teraguchi, M.; Masuda, T. *J. Polym. Sci., Part A: Polym. Chem.* **1998**, *36*, 2721–2725.
14. (a) Kanaya, T.; Tsukushi, I.; Kaji, K.; Sakaguchi, T.; Kwak, G.; Masuda, T. *Macromolecules* **2002**, *35*, 5559–5564. (b) Kanaya, T.; Teraguchi, M.; Masuda, T.; Kaji, K. *Polymer* **1999**, *40*, 7157–7161.
15. Robeson, L. M.; Burgoyne, W. F.; Langsam, M.; Savoca, A. C.; Tien, C. F. *Polymer* **1994**, *35*, 4970–4978.
16. (a) Dai, Y.; Guiver, M. D.; Roberson, G. P.; Kang, Y. Su.; Lee, K. J.; Jho, J. Y. *Macromolecules* **2004**, *37*, 1403–1410. (b) Park, J. Y.; Paul, D. R. *J. Membr. Sci.* **1997**, *125*, 23–39.
17. Graham, T. *Philos. Mag.* **1866**, *32*, 401–420.
18. (a) Shida, Y.; Sakaguchi, T.; Shiotsuki, M.; Sanda, F.; Freeman, B. D.; Masuda, T. *Macromolecules* **2006**, *39*, 569–574. (b) Shida, Y.; Sakaguchi, T.; Shiotsuki, M.; Sanda, F.; Freeman, B. D.; Masuda, T. *Macromolecules* **2005**, *38*, 4096–4102. (c) Shida, Y.; Sakaguchi, T.; Shiotsuki, M.; Wagener, K. B.; Masuda, T. *Polymer* **2005**, *46*, 1–4.

Chapter 2

Synthesis, Characterization, and Gas Permeation Properties of Perfluoroacylated Ethyl Cellulose

Abstract

Perfluoroacylated derivatives of ethyl cellulose [R = CF_3CO (**2a**), C_2F_5CO (**2b**), C_3F_7CO (**2c**), $C_7F_{15}CO$ (**2d**), C_6F_5CO (**2e**)] were synthesized in good yield by the reaction of various perfluoroacylating agents with residual hydroxy groups of ethyl cellulose (**1**; DS_{Et}, 2.69). FTIR spectra of the resulting polymers (**2a**–**d**) furnished the evidence for complete substitution of hydroxy protons by the perfluoroacyl groups. All the derivatives (**2a**–**e**) were soluble in common organic solvents and displayed enhanced solubility in moderately polar aprotic and nonpolar solvents. The onset temperatures of weight loss of **2a**–**d** in air were higher than 270 ºC, indicating fair thermal stability. Free-standing membranes of **1** and **2a**–**e** were fabricated, and **2a**–**d** exhibited large contact angle with water and enhanced gas permeability (*P*) as compared to **1**. An optimum increment in the size of the perfluoroacyl group led to the largest increment in the gas permeability of polymers; *i.e.*, **2c** exhibited the highest *P* values (*e.g.*, P_{CO_2} 284 barrers; cf. P_{CO_2} of **1**, 110 barrers). The P_{CO_2}/P_{N_2} and P_{CO_2}/P_{CH_4} selectivity values of the polymers (**2a**–**e**) were in the range of 14–22 and 8–11, respectively.

Introduction

Cellulose, an inexhaustible natural polymeric material, endowed with a polyfunctional macromolecular structure and an environmentally benign nature, suffers from the lack of solubility in most organic solvents emanating from its supramolecular architecture. However, ethyl cellulose, an organosoluble cellulosic, possesses the fascinating structure and properties such as extensive linearity, chain stiffness, excellent durability, good flexibility, chemical resistance, mechanical strength, hydrophobicity, non-toxicity, low cost, and above all remarkably good solubility in organic solvents, thus adequate membrane-forming ability and moderate gas permeation/pervaporation capability.[1]

Physical or chemical modification of polymers is as an attractive alternative to tailor the material properties as desired for specific applications. The incorporation of fluorine-containing groups is an apt way to alter the physical and chemical properties of polymers because of the highly electronegative nature of fluorine,[2] and is known to enhance polymer solubility (commonly referred to as the fluorine effect) and fractional free volume without forfeiture of thermal stability, and affords materials with low dielectric constants, low water absorption, excellent barrier properties, and extremely low critical surface tension.[3] Owing to their unique properties, partially fluorinated polymers have attracted considerable attention as a new class of materials, finding a variety of applications in organic thin film transistors (OTFT),[4] organic light-emitting diodes (OLED),[5] photonic devices,[6] low energy surfaces,[7] etc. Furthermore, gases dissolve well in fluorinated compounds,[8] and high gas permeability of some fluorine-containing polymer membranes including polysulfone,[9] polyacetylene,[10] polynorbornene,[11] polycarbonate,[12] and polyphosphazene[13] has been reported.

Derivatization of polysaccharides starting from the organosoluble polymer has undoubtedly broadened the diversity of products and reaction paths. Despite many aforementioned remarkable features and organosolubility of ethyl cellulose, studies concerning the systematic investigation of chemical derivatization of ethyl cellulose

are few and far between.[14] Esterification is one of the facile means to exploit the hydroxy groups present in ethyl cellulose, however, there have been a few reports regarding the synthesis of mixed esters of ethyl cellulose; and (acetyl)(ethyl) cellulose is probably the one whose properties have been studied in detail.[14j–m] Although the organo-fluorine compounds have engrossed substantial prominence as a new class of polymeric materials, trifluoroacetyl derivative is most likely the only fluorine-containing derivative of ethyl cellulose, reported so far.[15] Since, there have been a few reports concerning the incorporation of fluorinated substituents into ethyl cellulose and fluorine-containing groups often favor high gas permeability,[9–13] it is anticipated that the perfluoroacylated derivatives of ethyl cellulose will serve as interesting candidates for gas separation membranes.

Scheme 1. Perfluoroacylation of Ethyl Cellulose with Various Perfluoroacylating Agents

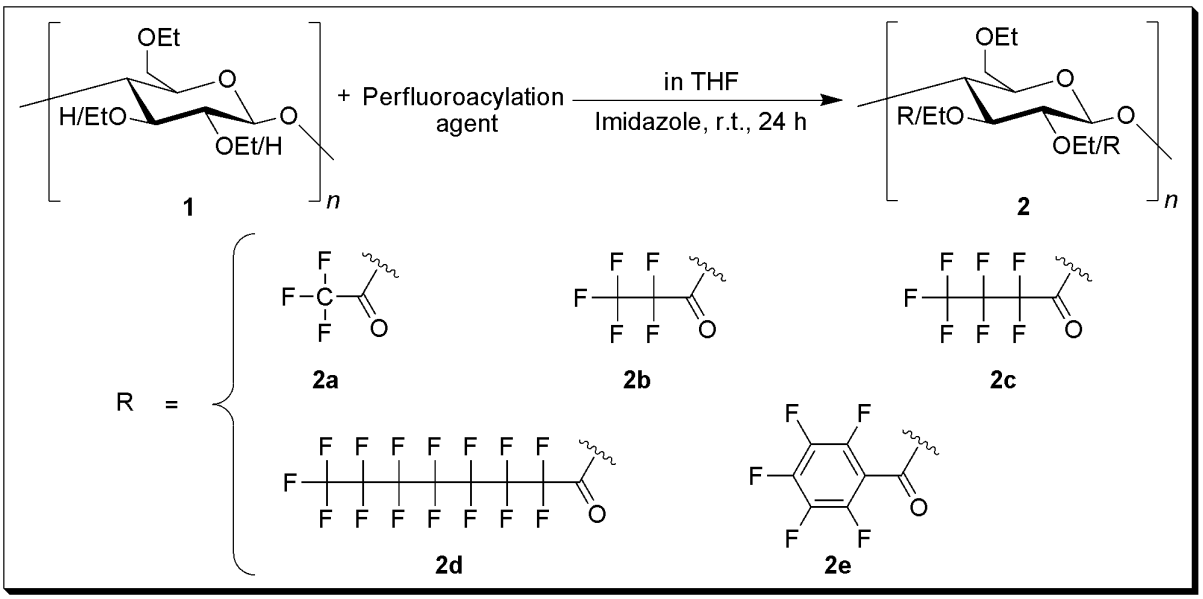

The present chapter deals with the synthesis of various perfluoroacyl derivatives (**2a**–**e**) of ethyl cellulose (**1**), their characterization, and elucidation of solubility and thermal properties (Scheme 1). Free-standing membranes of the perfluoroacylated polymers were fabricated and their contact angle with water, density, fractional free volume, and gas permeation parameters were determined. Moreover, the diffusion and solubility coefficients of polymer membranes for O_2, N_2, CO_2, and

CH_4 were also revealed.

Experimental Section

Measurements. Infrared spectra were recorded on a Jasco FTIR-4100 spectrophotometer. The number- and weight-average molecular weights (M_n and M_w, respectively) and polydispersity indices (M_w/M_n) of polymers were determined by size-exclusion chromatography (SEC) at 40 ºC with a Jasco PU-980/RI-930 and Viscotek UV/LS-T60A chromatograph (eluent THF, column TSK-GEL GMHXL (Tosoh), molecular weight range up to 4×10^8, flow rate 1 mL/min). Elemental analyses were performed at the Microanalytical Center of Kyoto University. Thermogravimetric analyses (TGA) were conducted in air with a Perkin-Elmer TGA7 thermal analyzer by heating the samples (3–5 mg) from 100–700 ºC at a scanning rate of 10 ºC min^{-1}. Differential scanning calorimetric (DSC) analyses were performed using a Seiko DSC6200/EXSTAR6000 apparatus and measurements were carried out by making use of 3–5 mg samples, under a nitrogen atmosphere, after calibration with an indium standard. The samples were first heated from ambient temperature (25 ºC) to +200 °C at a scanning rate of 20 ºC min^{-1} (first heating scan) and then immediately quenched to -50 °C at a rate of about 80 ºC min^{-1}. The second heating scans were run from -50 to +200 °C at a scanning rate of 20 ºC min^{-1} to record stable thermograms. The data for glass transition temperature (T_g), cold crystallization temperature (T_{cc}), and melting temperature (T_m), were all obtained from the second run and correspond to the midpoint of discontinuity in the heat flow. The static contact angle (CA) of water with polymer membranes was determined by the sessile-drop method using a Kyowa Interface Science CA-X contact angle meter at room temperature. A droplet of water (10 μL) was placed on a specimen for 30 s and then the contact angle was recorded. The measurement was repeated at ten different positions on the same specimen and the data were averaged. Membrane thickness was estimated by using a Mitutoyo micrometer. The gas permeability coefficients (P) were measured with a Rikaseiki K-315-N gas permeability apparatus using a

constant volume/variable-pressure system. All of the measurements were carried out at 25 ºC and a feed pressure of 0.1 MPa (1 atm) while the system was being evacuated on the downstream side of the membrane.

Materials. Ethyl cellulose (**1**; ethoxy content, 49 wt%) and imidazole were purchased from Aldrich and Wako (Japan), respectively, and used as received. Trifluoroacetic anhydride, heptafluorobutanoyl chloride, pentafluorobenzoyl chloride (Aldrich), pentafluoropropionic anhydride (Tokyo Kasei, Japan), and pentadecafluorooctanoyl chloride (Wako, Japan) were obtained commercially and used without further purification. Tetrahydrofuran (THF), used as reaction solvent, was purchased from Wako (Japan) and employed after distillation.

Perfluoroacylated derivatives of ethyl cellulose (**2a**–**e**) were synthesized according to Scheme 1. The details of the synthetic procedure and analytical data are as follows:

Trifluoroacetyl Derivative of Ethyl Cellulose (2a). A 200 mL one-necked flask was equipped with a dropping funnel, a three-way stopcock, and a magnetic stirring bar. Ethyl cellulose, **1**, (1.43 g, 6.10 mmol) and imidazole (0.83 g, 12.2 mmol) were placed in the flask, evacuated for half an hour, flushed with nitrogen, and dissolved in THF (50 mL) at room temperature. Then, trifluoroacetic anhydride (0.85 mL, 6.10 mmol) was added dropwise and stirring was continued for 24 h at room temperature. Product was isolated by precipitation in methanol (1000 mL), filtered with a membrane filter, washed repeatedly with methanol, and dried under vacuum to constant weight to afford the desired product (91%) as white solid. IR (ATR, cm^{-1}): 2974, 2870, 1794, 1375, 1220, 1090, 1050, 920, 880, 770, 736.

Pentafluoropropanoyl Derivative of Ethyl Cellulose (2b). This derivative was prepared by following the same procedure as for **2a** using pentafluoropropionic anhydride (1.21 mL) instead of trifluoroacetic anhydride. Yield 93%, white solid, IR (ATR, cm^{-1}): 2974, 2872, 1789, 1376, 1354, 1221, 1090, 1049, 1027, 920, 883, 839, 739.

Heptafluorobutanoyl Derivative of Ethyl Cellulose (2c). This derivative

was prepared by following the same procedure as for **2a** using heptafluorobutanoyl chloride (0.91 mL) instead of trifluoroacetic anhydride. Yield 92%, white solid, IR (ATR, cm^{-1}): 2975, 2872, 1789, 1377, 1299, 1233, 1088, 1050, 928, 827, 722.

Pentadecafluorooctanoyl Derivative of Ethyl Cellulose (2d). This derivative was prepared by following the same procedure as for **2a** using pentadecafluorooctanoyl chloride (1.51 mL) instead of trifluoroacetic anhydride. Yield 94%, white solid, IR (ATR, cm^{-1}): 2976, 2873, 1790, 1376, 1354, 1240, 1208, 1091, 1052, 920.

Pentafluorobenzoyl Derivative of Ethyl Cellulose (2e). This derivative was prepared by following the same procedure as for **2a** using pentafluorobenzoyl chloride (0.85 mL) instead of trifluoroacetic anhydride and precipitation was carried out in water rather than methanol, as **2e** was soluble in it. Yield 90%, white solid, IR (ATR, cm^{-1}): 2974, 2869, 1693, 1502, 1374, 1055, 917, 877, 797.

Determination of the Degree of Substitution. The degree of substitution with ethyl group (DS_{Et}) of the starting material, **1**, was determined by ^{1}H NMR and complete substitution of the residual hydroxy protons by the perfluoroacyl group in **2a**–**d** was confirmed by the complete disappearance of the peak characteristic of the hydroxy group (3600–3200 cm^{-1}) in the FTIR spectra of the polymers (Figure 1). The degree of substitution with pentafluorobenzoyl group in **2e** was estimated from the elemental analysis. The total degree of substitution (DS_{total}) of **2a**–**e** was calculated by the following equation:

$$DS_{total} = DS_{Et} + DS_{Ac}$$

Membrane Fabrication. Membranes (thickness ca. 40–80 μm) of polymers **1** and **2e** were fabricated by casting their toluene solution and those of **2a**–**d** from their 1,3-bis(trifluoromethyl)benzene solution (concentration ca. 0.50–1.0 wt%) onto a Petri dish. The dish was covered with a glass vessel to retard the rate of solvent evaporation (3–5 days).

Membrane Density. Membrane densities (ρ) were determined by hydrostatic weighing using a Mettler Toledo balance (model AG204, Switzerland) and a density determination kit.[16] This method makes use of a liquid with known density (ρ_0), and membrane density (ρ) is calculated by the following equation:

$$\rho = \rho_0 M_A/(M_A - M_L)$$

where M_A is the weight of membrane in air and M_L is that in the auxiliary liquid. Aqueous $NaNO_3$ solution was used as an auxiliary liquid to measure the density of the polymer membranes except for **2d**, whose density was determined by using aqueous NaI solution.

Fractional Free Volume (FFV) of Polymer Membranes. FFV (cm^3 of free volume/cm^3 of polymer) is commonly used to estimate the efficiency of chain packing and the amount of space (free volume) available for gas permeation in the polymer matrix. FFV is calculated by the following equation:[17]

$$FFV = (\upsilon_{sp} - \upsilon_0)/\upsilon_{sp} \approx (\upsilon_{sp} - 1.3\,\upsilon_w)/\upsilon_{sp}$$

where υ_{sp} and υ_0 are the specific volume and occupied volume (or zero-point volume at 0 K) of the polymer, respectively. Typically, occupied volume (υ_0) is estimated as 1.3 times the van der Waals volume (υ_w), which is calculated by the group contribution method.[18]

Measurement of Gas Permeation Parameters. The *P* values were calculated from the slopes of the time-pressure curves in the steady state where Fick's law holds.[19] The gas diffusion coefficients (*D*) were determined by the time lag method using the following equation:

$$D = l^2/6\theta$$

here, l is the membrane thickness and θ is the time lag, which is given by the intercept

of the asymptotic line of the time-pressure curve to the time axis. The membrane thickness was controlled so that the time lag would be in the range 10–300 s, preferably 30–150 s. When the time lag was < 10 s, the error of measurement became relatively large. If the time lag was, on the contrary, > 300 s, the error arising from the baseline drift became serious. The gas solubility coefficients (*S*) were calculated by using the equation, $S = P/D$.

Results and Discussion

Perfluoroacylation of Ethyl Cellulose. Perfluoroacylation of ethyl cellulose (**1**) was carried out by using various perfluorinated acid anhydrides/chlorides as perfluoroacylating agents, THF as a solvent, and imidazole as a base as shown in Scheme 1, and the results are summarized in Table 1. The DS_{Et} of **1** was estimated to be 2.69, by calculating the integration ratio of methyl protons to the rest of the protons in **1**, indicating the presence of 0.31 hydroxy groups per anhydroglucose unit.[14a] The

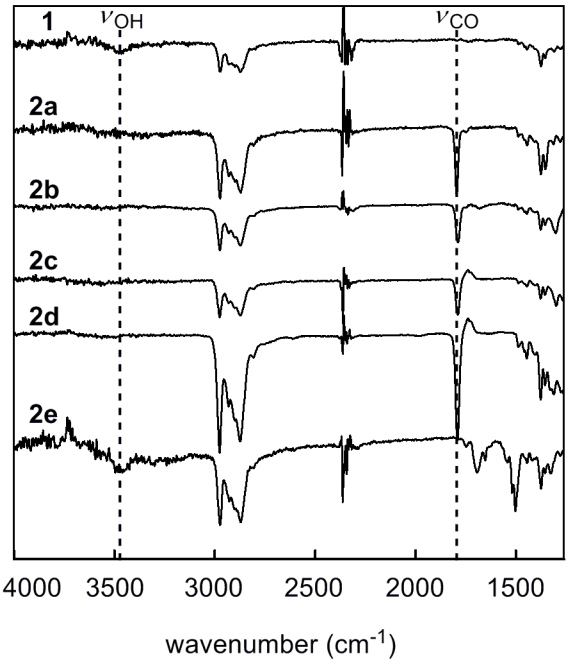

Figure 1. FTIR spectra of polymers **1** and **2a**–**e**.

IR spectrum of **1** (Figure 1) has a broad band characteristic of the residual hydroxy groups (3600–3200 cm^{-1}), which disappeared upon complete perfluoroacylation in polymers **2a**–**d**. Further evidence was furnished by the presence of the peaks characteristic of the carbonyl group (1695–1690 cm^{-1}) in the IR spectra of perfluoroalkanoyl derivatives (**2a**–**d**). On the other hand, complete substitution could not be achieved with pentafluorobenzoyl group, as is indicated by the presence of the broad band for the hydroxy group (3600–3200 cm^{-1}) in the IR spectrum of **2e**; its degree of acylation (DS_{Ac}) was determined by the elemental analysis and total degree

Table 1. Degree of Substitution and Molecular Weight of Polymers 1 and 2a–e

polymer	DS_{total} [a]	M_n [b]	M_w [b]	M_w/M_n [b]
1	2.69	47 000	106 000	2.3
2a	3.00	68 000	103 000	1.5
2b	3.00	93 000	117 000	1.3
2c	3.00	96 000	120 000	1.2
2d	3.00	132 000	147 000	1.1
2e	2.92[c]	49 000	124 000	2.5

[a] Determined by FTIR. [b] Determined by SEC/RALLS (size-exclusion chromatography/right-angle laser light scattering). [c] Determined by elemental analysis.

of substitution (DS_{total}) was 2.92. According to SEC data of the polymers (Table 1), the number-average molecular weight (M_n) of **1** was found to be 47 000 and a regular increase in the M_n values of perfluoroacylated polymers was observed with the increase in the bulk of perfluoroacyl group. Moreover, the polydispersity indices (M_w/M_n) of perfluoroacylated polymers (**2a**–**d**) were not quite different from those of **1**. For instance, the M_n and M_w/M_n of **1** were observed to be 47 000 and 2.3, respectively, while those of **2a** were 68 000 and 1.5. These facts rule out the possibility of polymer chain cleavage in the course of perfluoroacylation.

Solubility and Thermal Properties of Polymers. The solubility properties of ethyl cellulose (**1**) and **2a**–**e** are summarized in Table 2. **1** is soluble in highly

polar protic solvents such as methanol, while its perfluoroacylated derivatives (**2a**–**d**) were found to be insoluble (except **2e**), which is presumably due to the loss of hydrogen bonding because of the complete substitution of hydroxy groups by the perfluoroacyl moieties in **2a**–**d**. The solubility behavior of perfluoroacylated polymers in polar aprotic solvents exhibited several variations depending on the polarity of the solvent and an increased affinity towards relatively less polar solvents was discerned. For instance, **1** is soluble in DMF while its perfluoroalkanoylated

Table 2. Solubility[a] of Polymers 1 and 2a–e

polymer	**1**	**2a**	**2b**	**2c**	**2d**	**2e**
methanol	+	–	–	–	–	+
DMF	+	±	±	–	–	+
acetone	±	±	+	+	+	+
EtOAc	+	+	+	+	+	+
THF	+	+	+	+	+	+
CH_2Cl_2	+	+	+	+	+	+
$CHCl_3$	+	+	+	+	+	+
toluene	+	+	+	+	+	+
hexane	–	–	+	+	+	+
C_6F_6	–	+	+	+	+	–
1,3-$(CF_3)_2C_6H_4$	–	+	+	+	+	–

[a] Symbols: +, soluble; ±, partly soluble; –, insoluble.

derivatives exhibited a decrease in solubility with the increase in the length of the perfluoroalkanoyl chain; on the other hand, **1** is partly soluble in acetone while **2b**–**e** were completely soluble. Solubility characteristics of **1** in EtOAc, THF, $CHCl_3$, and toluene remain unchanged upon perfluoroacylation. Furthermore, **1** is insoluble in hexane, a nonpolar solvent, while its perfluoroacylated derivatives except **2a** were found to be soluble due to the presence of long perfluorocarbon chains in **2b**–**d** and an aromatic ring in **2e**. Moreover, the solubility of perfluoroacylated polymers in perfluorinated solvents such as hexafluorobenzene and

1,3-bis(trifluoromethyl)benzene was examined and it was observed that the completely perfluoroacylated derivatives of ethyl cellulose (**2a**–**d)** were soluble in these solvents. Thus it can be said that the perfluoroacylated ethyl cellulose derivatives (**2a**–**e)** display enhanced solubility in moderately polar aprotic solvents like acetone and nonpolar solvents like hexane.

The thermal stability of polymers **1** and **2a**–**e** was examined by thermogravimetric analysis (TGA) in air (Figure 2). The onset temperatures of weight loss (T_0) of **2a**–**d** were in the range of 270–300 ºC while that of **1** was 338 ºC, thus indicating a slight decrease in T_0 values resulting from the substitution of hydroxy groups by the perfluoroacyl moieties (Table 3). It was observed that the onset temperature of weight loss underwent a slight decrease with an increase in the length of the perfluoroalkanoyl group; for instance, T_0 of **2a** and **2b** were 293 and 288 ºC, respectively. The TGA thermogram of pentafluorobenzoyl derivative (**2e**) displayed two major points of weight loss at 145 and 293 ºC, respectively; the weight loss at 145 ºC corresponds to that of the pentafluorobenzoyl moiety (~ 8%) while that at 293 ºC to the rest of the polymer. The first T_0 value of perfluorobenzoyl derivative (**2e)** was

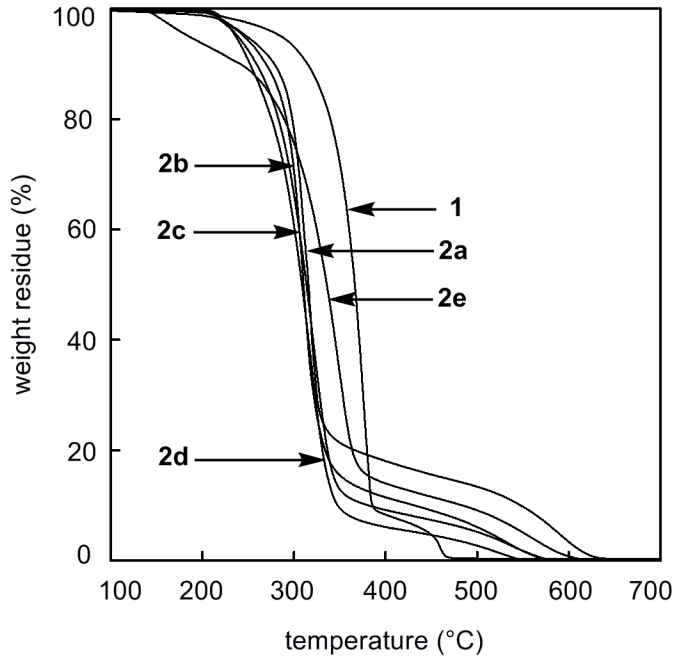

Figure 2. TGA curves of polymers **1** and **2a**–**e** (in air, heating rate 10 ºC min^{-1}).

considerably lower than those of the perfluoroalkanoyl derivatives (**2a**–**d**), which is presumably due to a weaker ester linkage than those in **2a**–**d** (as C_6F_5COOH is a considerably stronger acid than perfluoroalkanoic acids). These results imply that the thermal stability undergoes a slight decrease as the length of the alkyl chain in the perfluoroalkanoyl group increases while decreases considerably by the incorporation of relatively less stable perfluorobenzoyl moiety. Although the thermal stability of the perfluoroacylated derivatives of ethyl cellulose (**2a**–**d**) is slightly lower than that of the starting material (**1)**, it is still appreciably reasonable for practical applications as membrane-forming materials.

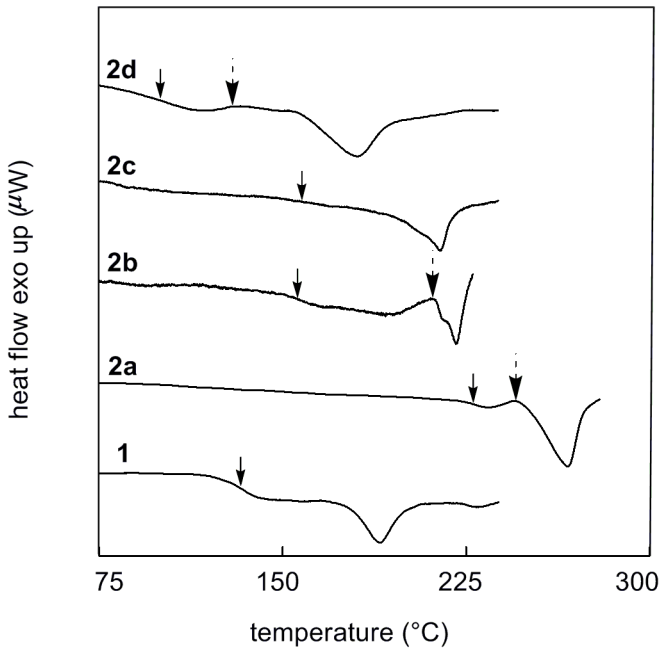

Figure 3. DSC thermograms of polymers **1** and **2a**–**d** (under N_2, second scan).

Other thermal properties such as glass transition temperature (T_g), cold crystallization temperature (T_{cc}), and melting temperature (T_m) of polymers **1** and **2a**–**e** were determined by the differential scanning calorimetric (DSC) analysis under nitrogen (Figure 3). It was observed that the glass transition temperature (T_g) of **1** (132 ºC) underwent a significant increase upon the substitution of trifluoroacetyl group (227 ºC), and then followed a decline as the length of the perfluoroalkanoyl group increased; *e.g.* T_g values for **2c** and **2d** were 159 and 101 ºC, respectively (Table 3).

The increase in the polymer chain stiffness due to the hindered rotation of the substituent, resulting from the substitution of hydroxy group by a relatively bulky, stiff, and polar trifluoroacetyl group, presumably led to the increased T_g in **2a**, which became offset due to the plasticization induced by the increased length of the perfluoroalkanoyl chain, thus leading to the decreased T_g values (**2b**–**d**). In general, the glass transition temperature (T_g) depends on the energy barriers that conformational transitions must overcome in such a way that the larger the barriers are, the fewer the conformational transitions that occur at a given temperature.[20] The substitution of relatively small hydroxy moieties by the stiff and polar trifluoroacetyl groups appeared to increase the energy barriers associated with the conformational transitions in the chains, and as a result the T_g of **1** underwent an increase upon perfluoroacylation/trifluoroacetylation.

Herein the term, cold crystallization temperature (T_{cc}), represents the temperature above the glass transition temperature (T_g) at which a small portion of the structurally irregular amorphous state of the polymer attains regularity and turns into crystalline state; the T_{cc} values were observed in the case of perfluoroalkanoyl

Table 3. Thermal Properties of Polymers 1 and 2a–e

polymer	T_0[a] (°C)	T_g[b] (°C)	T_{cc}[b] (°C)	T_m[b] (°C)	ΔH_{cc}[b] (mJ/mg)	ΔH_f[b] (mJ/mg)
1	338	132	–[c]	190	–[c]	4.2
2a	293	227	244	266	0.96	14.9
2b	288	158	211	221	1.21	7.8
2c	275	159	–[c]	215	–[c]	7.3
2d	273	101	131	180	0.50	6.2
2e	145, 293	–[c]	–[c]	–[c]	–[c]	–[c]

[a] T_0: Onset temperature of weight loss. Observed from TGA measurement in air. [b] T_g: Glass transition temperature. T_{cc}: Cold crystallization temperature. T_m: Melting temperature. ΔH_{cc}: Enthalpy of cold crystallization. ΔH_f: Enthalpy of fusion. Determined by DSC analysis in nitrogen. [c] Could not be determined.

derivatives of **1**, as shown in Table 3.

Similar tendencies were observed in T_m values of polymers as those in T_g, which can also be explained in terms of the increased rigidity of the polymer chains upon perfluoroacylation; and this effect was more pronounced in the case of trifluoroacetyl derivative (**2a**) in comparison with those having longer chain of carbon atoms. The increase in the melting temperature (T_m) of polymers suggests an increase in crystallinity as a result of perfluoroacylation; however, this effect has significantly been observed only in **2a**, displaying a T_m value of 266 ºC as compared to that of **1** (190 ºC) while those of **2b**–**d** were 221, 215, and 180 ºC, respectively.

Contact Angle of Water with Polymer Membranes. Static contact angles (θ) of water were measured for all the polymer films, under study, to determine the relative hydrophobicity of the surface. Table 4 lists the contact angles[21] of water with the surface of polymer membranes at 25 ºC, and their plot as a function of % F content of polymers (**1** and **2a**–**e**) is shown in Figure 4. The polymer membranes of perfluoroacylated derivatives (**2a**–**e**) displayed larger contact angle ($\theta > 90^o$) with water than that of **1** ($\theta = 83^o$). In other words, the introduction of fluorine-containing substituents led to an increase in the hydrophobicity or non-wettability of ethyl cellulose membranes; and this trend bears a resemblance to that observed in the case of

Table 4. Contact Angle of Water with the Surface of Polymers 1 and 2a–e

polymer	θ (º)[a]
1	83.4 ± 0.3
2a	92.1 ± 0.2
2b	94.2 ± 0.5
2c	95.6 ± 0.2
2d	97.0 ± 0.5
2e	93.1 ± 0.3

[a] Determined at 25 ºC.

other fluorinated polymeric materials.[22] Moreover, it was revealed that an increment in the F content of the perfluoroacylated polymers accompanied an increase in the contact angle of water with the surface of the membranes, and **2d** having the highest F content displayed the highest CA value. For instance, the % F content of **2a** and **2d** were 7.2 and 28.3 while the contact angle of water with their membranes were observed to be 92º and 97º, respectively.

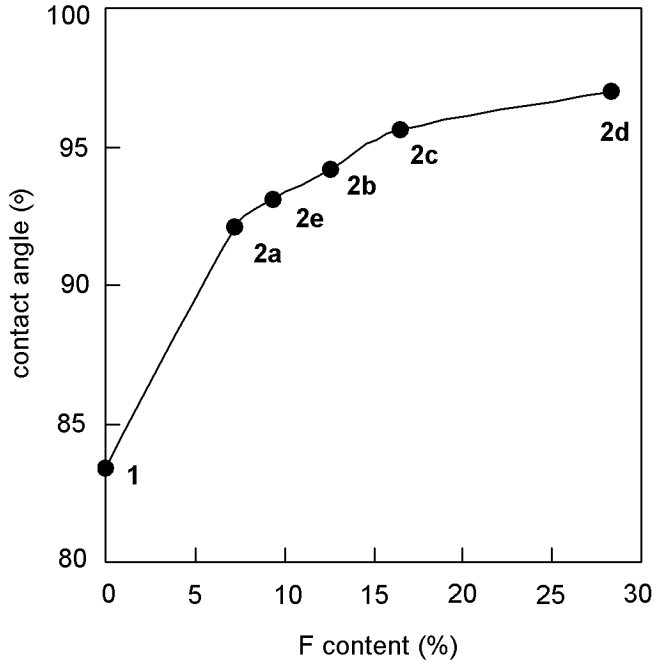

Figure 4. Contact angle of water with the surface of polymer membranes **1** and **2a**–**e** vs their % F content.

Density and FFV of Polymer Membranes. The van der Waals volume (v_w), density (ρ), and fractional free volume (FFV) of the polymer membranes (**1** and **2a**–**e**) are summarized in Table 5. All of the perfluoroacylated derivatives (**2a**–**e**) exhibited higher membrane density than that of ethyl cellulose (**1**); for instance, the ρ value of **1** was observed to be 1.099 while those of **2a**–**e** were in the range of 1.155–1.206. It was observed that an increase in the F content of the perfluoroacyl group accompanied an increase in the density of the polymer membranes. These findings are quite reasonable as fluorine-containing polymers generally possess larger densities than the

corresponding hydrocarbon polymers.[10b] It is worth mentioning that the perfluoroalkanoylation resulted in an enhancement in the FFV values of polymer membranes (**2a**–**d**) regardless of the simultaneous increase in their density as compared to the starting material (**1**). For instance, **2c** was observed to possess the highest fractional free volume (FFV is 0.197), in spite of its quite high density (ρ is 1.194) among all of the perfluoroacylated derivatives of **1**, which probably indicates the formation of relatively sparse structures due to the incorporation of fluorine-containing moieties. Similar tendencies have been reported in F-containing polycarbonates.[12] Furthermore, it is a general trend that the bulky substituents sterically obstruct intersegmental packing,[9] and in the case of F-containing polymers chain packing is further restrained by the intermolecular repulsive forces resulting from the presence of fluorine atoms having high electron density.

Table 5. Physical Properties of Polymers 1 and 2a–e

polymer	v_w[a] (cm^3/mol)	ρ[b] (g/cm^3)	FFV[c]
1	135.8	1.099	0.182
2a	145.0	1.155	0.185
2b	149.6	1.178	0.189
2c	154.2	1.194	0.197
2d	172.5	1.298	0.191
2e	150.9	1.206	0.161

[a] v_w: van der Waals volume. [b] ρ: density. Determined by hydrostatic weighing. [c] FFV: fractional free volume. Estimated from membrane density.

Gas Permeation Properties. The permeability coefficients of the membranes of polymers **1** and **2a**–**e** to various gases measured at 25 °C are listed in Table 6, and their plot versus kinetic diameter of gases is shown in Figure 5. The gas permeability coefficients (*P*) of the perfluoroacylated derivatives (except **2e**) were higher than that of **1**, and approximately obey the following order: **2c** > **2b** ≈ **2d** > **2a** > **1** > **2e**, which is in accordance with the FFV of the polymer membranes. The order

of the gas permeability coefficients depends upon the shape, size, and mobility of the perfluoroacyl substituents.

Table 6. Gas Permeability Coefficients (*P*) of Polymer Membranes at 25 °C

polymer	*P* (barrer)[a]						PCO_2/PN_2	PCO_2/PCH_4
	He	H_2	O_2	N_2	CO_2	CH_4		
1	53	76	18	5.0	110	12	22	9
2a	72	102	28	8.0	172	17	21	10
2b	100	140	44	16	250	30	16	9
2c	114	155	52	20	284	37	14	8
2d	110	130	48	16	251	29	16	9
2e	40	51	11	3.0	64	6.0	22	11

[a] 1 barrer = $1x10^{-10}$ cm^3 (STP) cm cm^{-2} s^{-1} $cmHg^{-1}$.

In this study, it has been revealed that an optimum increase in the bulk or the length of the perfluoroalkanoyl group accompanies an enhancement in the gas permeability whereas an excessive increase affects conversely. For instance, the

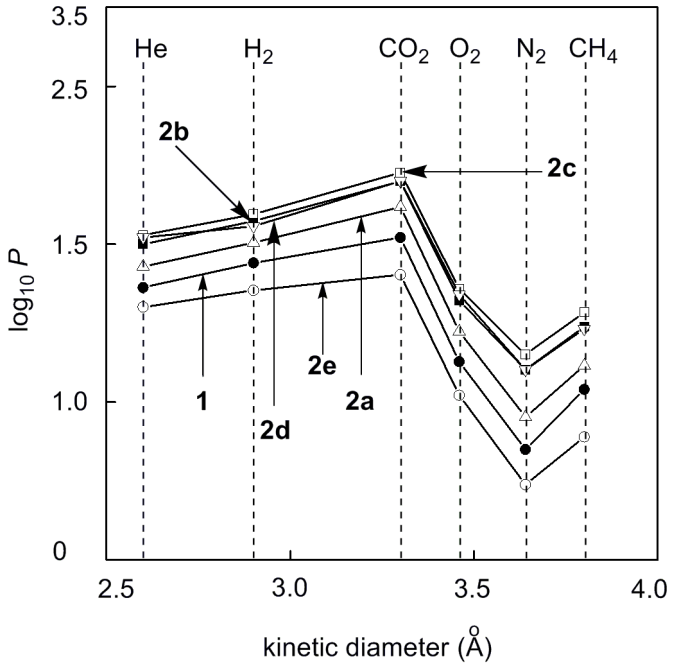

Figure 5. Gas permeability coefficients of ethyl cellulose (**1**) and its perfluoroacylated derivatives (**2a**–**e**) vs kinetic diameter of gases.

carbon dioxide permeability coefficients (P_{CO_2}) of **2a**–**d** were 172, 250, 284, and 251 barrers, respectively, where **2c** displayed the highest CO_2 permeability, and similar tendencies were observed for other gases in the present study. These trends in the gas permeability suggest that an optimum increase in the bulk and length of the perfluoroalkanoyl group results in a looser chain packing, leading to the increased free volume space inside the polymer matrix, and in turn enhanced gas permeability; these effects are counterbalanced to some extent by an excessive increase in the bulk/length of the substituent due to the hindered chain/segmental mobility. The lowest *P* values have been observed for **2e** ensuing from the planar and non-flexible nature of the aryl group present in the pentafluorobenzoyl moiety thus leading to the stacking (as indicated by the decreased FFV) and decrement in the local mobility of the substituent.

The most important feature of the gas permeability data of ethyl cellulose (**1**) and its perfluoroacylated derivatives (**2a**–**e**) is relatively high P_{CO_2}/P_{N_2} selectivity ($\geq$ 14) of these polymers, and notably **2a**–**c** displayed good perforamance for CO_2 separation. However, as the gas permeability undergoes an increase, a decrease in permselectivity is observed. Moreover, similar tendencies were displayed by the P_{CO_2}/P_{CH_4} selectivity data of the perfluoroacylated polymers. Enhanced gas permeability without loss of permselectivity in **2a** was probably due to the decreased chain packing (as indicated by the slight increase in FFV) and increased chain stiffness/hindered rotation of the pendant groups (as indicated by the increased T_g), following the trifluoroacetylation of **1**. These findings are consistent with the previous results that the structural alterations, which inhibit chain packing and simultaneously constrain the rotational motion about flexible linkages on the polymer backbone, for instance, the incorporation of fluorinated substituents, tend to increase permeability while maintaining or increasing permselectivity.[20a,23]

The present results imply that the gas transport properties of membrane-forming materials can be selectively improved through a controlled modification of subtle structural features such as interchain spacing and chain stiffness.

Gas Diffusivity and Solubility. Gas permeability (*P*) can be expressed as the product of gas solubility in the upstream face of the membrane and effective average gas diffusion through the membrane, strictly in rubbery and approximately in glassy polymers:[24]

$$P = S \times D$$

.

In order to carry out a detailed investigation of the gas permeability of **1** and **2a**–**e**, their gas diffusion coefficients (*D*) and gas solubility coefficients (*S*) were determined. The *D* and *S* values of polymers **1** and **2a**–**e** for O_2, N_2, CO_2, and CH_4 are given in Table 7 and 8, respectively. In polymeric membranes, generally the *D* value undergoes a decrease with increasing critical volume of gases while the *S* value experiences an increase with increasing critical temperature of gases. Similar tendencies were observed in the *D* and *S* values of the polymer membranes of **1** and its perfluoroacylated derivatives; *e.g.*, in **2a** the diffusivity of CH_4 (2.2) was the lowest and that of O_2 (9.6) was the highest while CO_2 (43.7) displayed the highest solubility and N_2 (1.5) the lowest.

Table 7. Gas Diffusion Coefficients[a] (*D*) of the Polymer Membranes

	$10^7 D$ ($cm^2 s^{-1}$)			
	O_2	N_2	CO_2	CH_4
critical volume (cm^3/mol)	73.4	89.8	93.9	99.2
1	8.3	3.8	2.6	1.8
2a	9.6	5.3	3.9	2.2
2b	14.2	8.9	5.3	3.8
2c	16.7	10.8	6.0	4.9
2d	14.6	8.3	5.3	3.8
2e	5.4	2.5	1.9	1.1

[a] Determined by the 'time lag' method at 25° C.

As shown in Table 7, the diffusion coefficients of all the gases increased upon perfluoroalkanoylation (**2a**–**d**), while underwent a considerable decline upon perfluorobenzoylation (**2e**). For instance, **1** displayed the D_{O_2} value of 8.3 and those of **2a**–**d** were in the range of 9.6–16.7 while that of **2e** was 5.4. The increment in gas diffusivity can be accounted for by the increase in the FFV of the polymer membranes (**2a**–**d**) as a result of perfluoroacylation; however, the enhanced local mobility of the substituents might also be anticipated to make a major contribution in the case of **2b**–**d**, having substituents with longer alkyl chain.[25]

As far as the gas solubility coefficients are concerned, a small increase in the *S* value was observed in almost all of the perfluoroalkanoyl derivatives as compared to **1**, as shown in Table 8. A small increment in the *S* values probably arises from the higher FFV of the perfluoroalkanoyl derivatives (**2a**–**d**) than that of **1**, as summarized in Table 5. It was observed that the *S* values underwent a subtle increase with the increase in the size of the perfluoroalkanoyl group (**2a**–**d**); *e.g.*, S_{CO_2} values of **2a**–**d** were 43.7, 46.9, 47.05, and 47.35, respectively.

Table 8. Gas Solubility Coefficients[a] (*S*) of the Polymer Membranes

10^3 *S* (cm^3 (STP) cm^{-3} $cmHg^{-1}$)				
	N_2	O_2	CH_4	CO_2
critical temperature (K)	126.2	154.8	191.0	304.1
1	1.4	2.2	6.5	45
2a	1.1	2.3	6.1	33
2b	0.64	1.4	6.2	27
2c	0.79	1.6	6.7	31
2d	0.96	1.6	5.7	33
2e	0.58	0.8	3.5	15

[a] Calculated by using quotients, *P*/*D*.

Among **2a**–**e**, **2c** exhibited the highest *D* value for all the gases, presumably emanating from its highest FFV (0.197) and also because of the enhanced local

mobility of the perfluoroacyl substituent due to the presence of the alkyl chain of optimum length. Similar tendencies have been observed in various substituted polyacetylenes.[19] It is noteworthy that the increase in the diffusion coefficients upon perfluoroacylation (**2a**–**d**) was more pronounced than that in the solubility coefficients, thus penetrant diffusivity playing the major role, leading to the net effect of enhanced gas permeability.[12a,23e] Furthermore, these results indicate the significance of perfluoroalkanoyl groups to enhance the gas permeability by mainly increasing the gas diffusion coefficients of the polymer membranes along with a slight increase in the gas solubility.

Conclusions

The present study is concerned with the synthesis of various perfluoroalkanoyl(benzoyl) esters of ethyl cellulose (**2a**–**e**). It was demonstrated that the perfluorinated acid anhydrides/chlorides served as excellent acylating agents, in the presence of imidazole, which accomplished the complete perfluoroalkanoylation of ethyl cellulose (**1)** even at room temperature without any chain degradation. All of the perfluoroalkanoyl derivatives of ethyl cellulose (**2a**–**d**) displayed good solubility in common organic and perfluorinated solvents, fair thermal stability, increased chain stiffness, enhanced hydrophobicity, and adequate membrane-forming ability. Membranes of **2a**–**d** exhibited higher gas permeability than that of **1**, primarily due to the increased diffusion coefficients resulting from the introduction of fluorine-containing acyl moieties. Although perfluoroacylation could not induce a very large increase in gas flux, probably due to a very small extent of hydroxy groups (0.31 per anhydroglucose unit) available for derivitization yet good separation performance for CO_2/N_2 and CO_2/CH_4 gas pairs was discerned.

References and Notes

1. (a) Klemm, D.; Heublein, B.; Fink, H.-P.; Bohn, A. *Angew. Chem. Int. ed.* **2005**,

44, 3358–3393. (b) Crowley, M. M.; Schroeder, B.; Fredersdorf, A.; Obara, S.; Talarico, M.; Kucera, S.; McGinity, J. W. *Int. J. Pharm.* **2004**, *269*, 509–522. (c) Li, X.-G.; Kresse, I.; Xu, Z.-K.; Springer, J. *Polymer* **2001**, *42*, 6801–6810. (d) Barton, D. H. R.; Nakanishi, K.; Meth-Cohn, O. *Comprehensive Natural Products Chemistry*; Elsevier Science: Oxford, 1999; Vol. 3. (e) Klemm, D.; Philipp, B.; Heinze, T.; Heinze, U.; Wagenknecht, W. *Comprehensive Cellulose Chemistry*; Wiley-VCH: Weinheim, 1998; Vol. 1, 2.

2. (a) Grob, U.; Rüdiger, S. T. In *Organo-Fluorine Compounds*; Baasner, B., Hagemann, H., Tatlow, J. C., Eds.; Georg Thieme Verlag Stuttgart: New York, 1999; Vol. E10a, pp 18–26. (b) Renak, M. L.; Bartholomew, G. P.; Wang, S.; Ricatto, P. J.; Lachicotte, R. J.; Bazan, G, C. *J. Am. Chem. Soc.* **1999**, *121*, 7787–7799.
3. (a) Delucchi, M.; Turri, S.; Barbucci, A.; Bassi, M.; Novelli, S.; Cerisola, G. *J. Polym. Sci., Part B: Polym. Phys.* **2002**, *40*, 52–64. (b) Banerjee, S.; Maier, G.; Burger, M. *Macromolecules* **1999**, *32*, 4279–4289. (c) Wang, J. G.; Mao, G. P.; Ober, C. K.; Kramer, E. J. *Macromolecules* **1997**, *30*, 1906–1914.
4. (a) Sakamoto, Y.; Suzuki, T.; Kobayashi, M.; Gao, Y.; Fukai, Y.; Inoue, Y.; Sato, F.; Tokito, S. *J. Am. Chem. Soc.* **2004**, *126*, 8138–8140. (b) Facchetti, A.; Mushrush, M.; Katz, H. E.; Marks, T. J. *Adv. Mater.* **2003**, *15*, 33–38. (c) Bao, Z.; Lovinger, A. J.; Brown, J. *J. Am. Chem. Soc.* **1998**, *120*, 207–208.
5. (a) Sakamoto, Y.; Suzuki, T.; Miura, A.; Fujikawa, H.; Tokito, S.; Taga, Y. *J. Am. Chem. Soc.* **2000**, *122*, 1832–1833. (b) Heidenhain, S. B.; Sakamoto, Y.; Suzuki, T.; Miura, A.; Fujikawa, H.; Mori, T.; Tokito, S.; Taga, Y. *J. Am. Chem. Soc.* **2000**, *122*, 10240–10241. (c) Jiang, X.; Liu, S.; Ma, H.; Jen, A. K.-Y. *Appl. Phys. Lett.* **2000**, *76*, 1813–1815.
6. (a) Ma, H.; Jen, A. K.-Y.; Dalton, L. R. *Adv. Mater.* **2002**, *14*, 1339–1365. (b) Tanio, N.; Koike, Y. *Polym. J.* **2000**, *32*, 43–50. (c) Eldada, L.; Shacklette, L. W. *IEEE J. Select. Top. Quantum Electron.* **2000**, *6*, 54–68. (d) Resnick, P. R.; Buck, W. H. In *Modern Fluoropolymers*; Scheirs, J., Ed.; John Wiley & Sons: Chichester, UK, 1997; pp 397. (e) Sugiyama, N. In *Modern Fluoropolymers*; Scheirs, J., Ed.; John Wiley & Sons: Chichester, UK, 1997; pp 541. (f) Kaino, T.; Fujiki, M.; Jinguji, K. *Rev. Electron. Commun. Lab.* **1984**, *32*, 478–488.
7. (a) Böker, A.; Herweg, T.; Reihs, K. *Macromolecules* **2002**, *35*, 4929–4937. (b) Böker, A.; Reihs, K.; Wang, J.; Stadler, R.; Ober, C. K. *Macromolecules* **2000**, *33*, 1310–1320. (c) Iyengar, D. R.; Perutz, S. M.; Dai, C. A.; Ober, C. K.; Kramer E. J. *Macromolecules* **1996**, *29*, 1229–1234. (d) Katano, Y.; Tomono, H.; Nakajima, T. *Macromolecules* **1994**, *27*, 2342–2344.
8. (a) Gomes, M. F. C.; Deschamps, J.; Menz, D.-H. *J. Fluorine Chem.* **2004**, *125*,

1325–1329. (b) Hamza, M. A.; Serratrice, G.; Stebe, M. J.; Delpuech, J. J. *J. Am. Chem. Soc.* **1981**, *103*, 3733–3738. (c) Wesseler, E. P.; Iltis, R.; Clark Jr., L. C. *J. Fluorine Chem.* **1977**, *9*, 137–146.

9. Dai, Y.; Guiver, M. D.; Robertson, G. P.; Kang, Y. S.; Lee, K. J.; Jho, J. Y. *Macromolecules* **2004**, *37*, 1403–1410.
10. (a) Shida, Y.; Sakaguchi, T.; Shiotsuki, M.; Sanda, F.; Freeman, B. D.; Masuda, T. *Macromolecules* **2006**, *39*, 569–574. (b) Sakaguchi, T.; Shiotsuki, M.; Sanda, F.; Freeman, B. D.; Masuda, T. *Macromolecules* **2005**, *38*, 8327–8332. (c) Seki, H.; Masuda, T. *J. Polym. Sci., Part A: Polym. Chem.* **1995**, *33*, 1907–1912. (d) Hayakawa, Y.; Nishida, M.; Aoki, T.; Muramatsu, H. *J. Polym. Sci., Part A: Polym. Chem.* **1992**, *30*, 873–877.
11. (a) Yampol'skii, Yu. P.; Bespalova, N. B.; Finkel'shtein, E. S.; Bondar, V. I.; Popov, A. V. *Macromolecules* **1994**, *27*, 2872–2878. (b) Teplyakov. V. V.; Paul, D. R.; Bespalova, N. B.; Finkel'shtein, E. S. *Macromolecules* **1992**, *25*, 4218–4219.
12. (a) Hellums, M. W.; Koros, W. J.; Husk, G. R.; Paul, D. R. *J. Appl. Polym. Sci.* **1991**, *43*, 1977–1986. (b) Hellums, M. W.; Koros, W. J.; Husk, G. R. *Polym. Mater. Sci. Eng.* **1989**, *61*, 378–382.
13. (a) Nagai, K.; Freeman, B. D.; Cannon, A.; Allcock, H. R. *J. Membr. Sci.* **2000**, *172*, 167–176.
14. (a) Khan, F. Z.; Sakaguchi, T.; Shiotsuki, M.; Nishio, Y.; Masuda, T. *Macromolecules* **2006**, *39*, 6025–6030. (b) Olatunji, G.; Oladoye, S. *Cellulose Chem. Tech.* **2004**, *38*, 3–9. (c) Wu, C.; Gu, Q.; Huang, Y.; Chen, S. *Liq. Crys.* **2003**, *30*, 733–737. (d) Thies, J. C.; Cowie, J. M. G. *Polymer* **2001**, *42*, 1297–1301. (e) Olatunji, G.; Huang, Y.; Dai, Q. *Cellulose Chem. Tech.* **1999**, *33*, 179–182. (f) Olatunji, G.; Huang, Y.; Dai, Q. *Cellulose Chem. Tech.* **1998**, *32*, 393–396. (g) Dai, Q.; Huang, Y. *Polymer* **1998**, *39*, 3405–3409. (h) Olatunji, G.; Huang, Y.; Dai, Q. *Cellulose* **1997**, *4*, 247–253. (i) Pernikis, R.; Lazdina, B. *Cellulose Chem. Tech.* **1996**, *30*, 187–196. (j) Guo, J.-X.; Gray, D. G. *J. Polym. Sci., Part A: Polym. Chem.* **1994**, *32*, 889–896. (k) Kesting, R. E.; Fritzsche, A. K. *Polymeric Gas Separation Membranes*; Wiley: New York, 1993. (l) Guo, J.-X.; Gray, D. G. *Macromolecules* **1989**, *22*, 2082–2086. (m) Guo, J.-X.; Gray, D. G. *Macromolecules* **1989**, *22*, 2086–2090.
15. (a) Yang, C. W.; Wu, K. H.; Chang, T. C.; Hong, Y. S.; Chiu, Y. S. *Polym. Degrad. Stab.* **2001**, *72*, 297–302. (b) Wang, Y.; Easteal, A. J. *J. Membr. Sci.* **1999**, *157*, 53–61.
16. Lin, H.; Freeman, B. D. *J. Membr. Sci.* **2004**, *239*, 105–117.
17. (a) Pixton, M. R.; Paul, D. R. In *Polymeric Gas Separation Membranes*; Paul, D. R., Yampol'skii, Yu. P., Eds.; CRC Press: Boca Raton, FL, 1994; pp 83–153. (b)

Lee, W. M. *Polym. Eng. Sci.* **1980**, *20*, 65–69. (c) Bondi, A. *Physical Properties of Molecular Crystals, Liquids, and Glasses*; John Wiley and Sons: New York, 1968; pp 25–97.

18. van Krevelen, D. W. *Properties of Polymers: Their Correlation with Chemical Structure; Their Numerical Estimation and Prediction from Additive Group Contributions*, 3rd ed.; Elsevier Science: Amsterdam, 1990; pp 71–107.
19. Masuda, T.; Iguchi, Y.; Tang, B.-Z.; Higashimura, T. *Polymer* **1988**, *29*, 2041–2049.
20. (a) Tiemblo, P.; Guzman, J.; Riande, E.; Mijangos, C.; Reinecke, H. *Macromolecules* **2002**, *35*, 420–424. (b) Banerjee, S.; Maier, G.; Burger, M. *Macromolecules* **1999**, *32*, 4279–4289.
21. Young's equation: Young, T. *Philos. Trans. R. Soc. London* **1805**, 65.
22. (a) Brantley, E. L.; Jennings, G. K. *Macromolecules* **2004**, *37*, 1476–1483. (b) Delucchi, M.; Turri, S.; Barbucci, A.; Bassi, M.; Novelli, S.; Cerisola, G. *J. Polym. Sci., Part B: Polym. Phys.* **2002**, *40*, 52–64. (c) Wang, J. G.; Mao, G. P.; Ober, C. K.; Kramer, E. J. *Macromolecules* **1997**, *30*, 1906–1914.
23. (a) Xiao, Y.; Dai, Y.; Chung, T.-S.; Guiver, M. D. *Macromolecules* **2005**, *38*, 10042–10049. (b) Liu, B.; Dai, Y.; Robertson, G. P.; Guiver, M. D.; Hu, W.; Jiang, Z. *Polymer* **2005**, *46*, 11279–11287. (c) Guiver, M. D.; Robertson, G. P.; Dai, Y.; Bilodeau, F.; Kang, Y. S.; Lee, K. J.; Jho, J. Y.; Won, J. *J. Polym. Sci., Part A: Polym. Chem.* **2002**, *40*, 4193–4204. (d) Tanaka, K.; Kita, H.; Okano, M.; Okamoto, K. *Polymer* **1992**, *33*, 585–592. (e) Coleman, M. R.; Koros, W. J. *J. Membr. Sci.* **1990**, *50*, 285–297.
24. (a) Pinnau, I.; Freeman, B. D. *Advanced Materials for Membrane Separations*; ACS Symposium Series 876; American Chemical Society: Washington, DC, 2004. (b) Graham, T. *Philos. Mag.* **1866**, *32*, 401–420.
25. Kanaya, T.; Tsukushi, I.; Kaji, K.; Sakaguchi, T.; Kwak, G.; Masuda, T. *Macromolecules* **2002**, *35*, 5559–5564. (b) Kanaya, T.; Teraguchi, M.; Masuda, T.; Kaji, K. *Polymer* **1999**, *40*, 7157–7161.

Chapter 3

Synthesis and Properties of Amide-Containing Dendrons and Dendronized Cellulose Derivatives

Abstract

First and second generation amide-containing dendrons (**G1-a-II**–**G1-c-II** and **G2-a-II**–**G2-c-II**) having branched alkyl periphery and focal carboxyl functionality were synthesized via a convergent pathway and incorporated into ethyl cellulose. Dendronized ethyl cellulose derivatives (**2a**–**c**, **3a**–**c**) were synthesized in good yield by the reaction of terminal carboxyl moiety of various dendrons with residual hydroxy groups of ethyl cellulose (**1**; DS_{Et}, 2.69). ^{1}H NMR spectra and elemental analysis were employed to determine the degree of esterification (DS_{Est}) of the resulting polymers. The presence of the peak characteristic of the C=O group in the FTIR spectra furnished further evidence for the incorporation of dendritic moieties into ethyl cellulose. All of the derivatives (**2a**–**c**, **3a**–**c**) were soluble in chloroform and methanol, and the solubility window narrowed in going from G1- to G2-derivatized polymers. The onset temperatures of weight loss of **2a**–**c** (295–325 C°) and **3a**–**c** (312–320 °C) in air were slightly higher than 294 ºC, indicating that the thermal stability was retained upon dendron functionalization. Free-standing membranes of **1** and **2a**–**c** were fabricated, and **2a**–**c** exhibited enhanced permselectivity for He/N_2, H_2/N_2, CO_2/N_2, and CO_2/CH_4 gas pairs as compared to **1**.

Introduction

Dendrimers, a class of precisely branched, highly symmetrical, tree-like macromolecules capable of furnishing the most exquisitely tailored forms and functions ever realized outside the realms of nature, have evolved from a little more than a curiosity into new horizons of macromolecular architecture finding potential applications in pharmaceutical, biotechnological and polymer sciences and are expected to reign as the flagship building blocks of nanotechnology.[1] Owing to the unique architectural and functional control achieved during their synthesis, dendrimers possess characteristic structural features and properties quite different from those of their linear counterparts, and have extensively been studied in the past three decades.[2] Despite such an enormous activity enriching the structural diversities of dendrimers, research has almost exclusively been focused on dendrimers with small cores, except for a US patent filed by Tomalia and Kirchhoff in 1987,[3] followed by a few reports[4] until a breakthrough in the synthesis of dendronized polymers was reported by Schlüter in the mid 90s,[5] recognizing the significance of dendron functionalization for the backbone conformation and the overall shape of the resulting macromolecules.

Dendronized polymers are characterized by the presence of dendritic fragments attached to a polymeric backbone and the past few years have witnessed a variety of dendritic substituents and polymeric backbones to which they are appended to.[6] Recently, there is an increasing interest to exploit the dendritic macromolecules or dendron appendages for the chemical and surface modification of silica,[7] agarose,[8] carbon,[9] chitosan,[10] and DNA;[11] however, the reports concerning the dendronization of cellulose or its organosoluble derivatives are few and far between.[12]

Cellulose, an inexhaustible natural polymeric material endowed with a polyfunctional macromolecular structure and an environmentally benign nature, suffers from the lack of solubility in most organic solvents emanating from its supramolecular architecture. However, ethyl cellulose, an organosoluble cellulosic, possesses the fascinating features of extensive linearity, chain stiffness, excellent durability, chemical resistance, mechanical strength, hydrophobicity, non-toxicity, low

cost, and above all appreciably good solubility in organic solvents, thus adequate membrane-forming ability, good film-flexibility, and moderate gas permeation/pervaporation capability.[13]

Keeping in view many aforementioned remarkable features of dendritic

Chart 1. Structure of G1 and G2 Amide-Containing Dendrons.

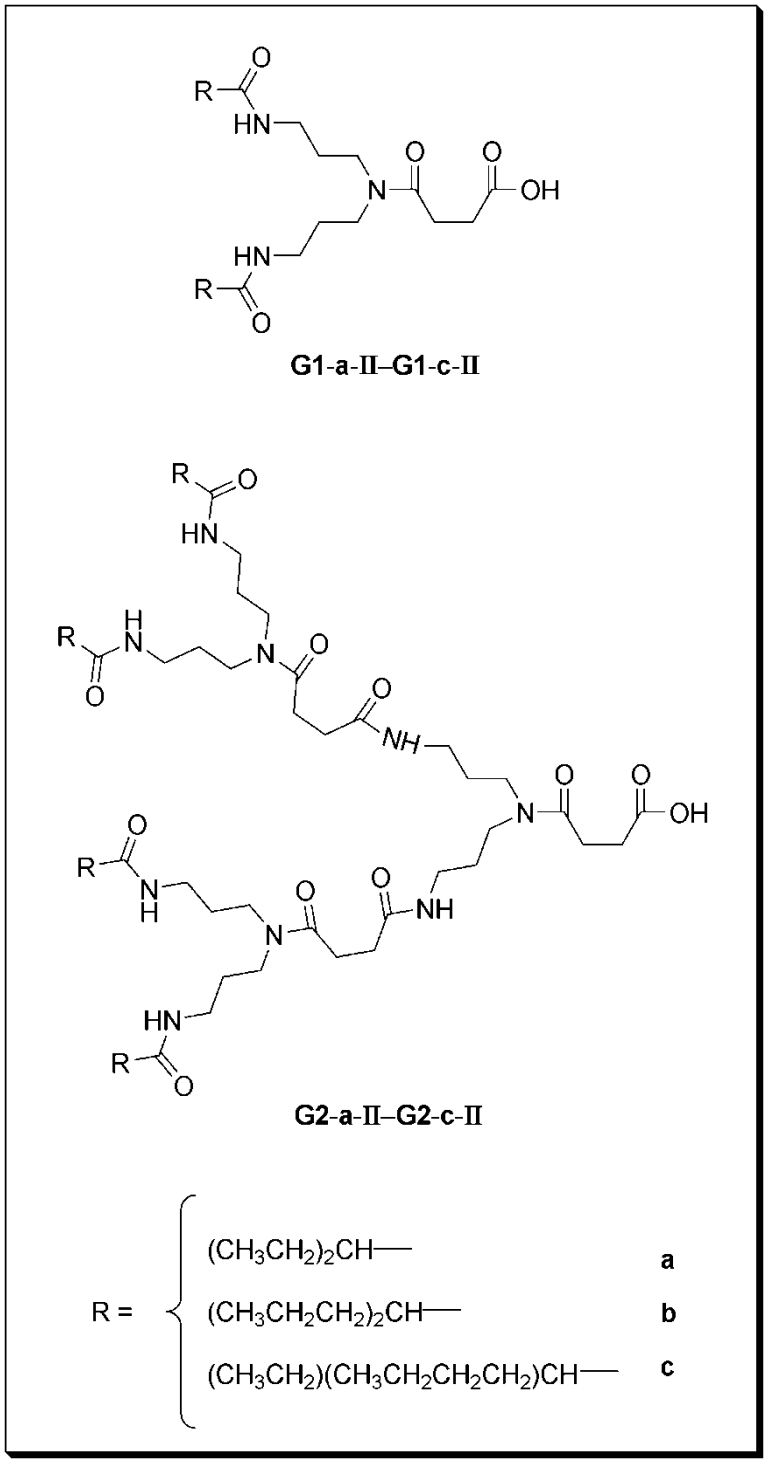

structures and organosolubility of ethyl cellulose carrying hydroxy (anchor) groups available for derivatization, it would be interesting to synthesize novel dendron-functionalized macromolecular architectures based on cellulose and to investigate the structural characteristics and functions of this new emerging class of 'hybrid architectures' derived from dendrimers and the most sustainable linear polymers.

The present episode narrates the synthesis and characterization of G1 and G2 of various amide-containing dendrons and dendronized derivatives (**2a**–**c**, **3a**–**c**) of ethyl cellulose (**1**) (Schemes 1 and 2). The solubility characteristics and thermal properties of the resulting polymers were elucidated. Free-standing membranes of the dendronized polymers (**2a**–**c**) were fabricated and their density, fractional free volume, and gas permeation parameters were determined. Moreover, the diffusion and solubility coefficients of polymer membranes for O_2, N_2, CO_2, and CH_4 were also revealed.

Experimental Section

Measurements. ^{1}H and ^{13}C NMR spectra were recorded on a JEOL EX-400 spectrometer and the residual proton or carbon signal of the deutrated solvent was used as internal standard. The samples for the NMR measurements were prepared at a concentration of approximately 10 mg/mL and chemical shifts are reported in parts per million (ppm). The ^{1}H NMR spectra of ethyl cellulose and dendronized polymers were recorded for 192 scans with a pulse delay of 37 s in order to obtain reliable integrations. Infrared spectra were recorded on a Jasco FTIR-4100 spectrophotometer and 68 spectra were accumulated at a resolution of 4 cm^{-1}, for each measurement. The FAB-MS analyses were conducted using the JEOL JMS-HX110A and JMS-SX102A spectrometers while 3-nitrobenzyl alcohol (MNBA) was used as a matrix. Melting points (mp) were determined with a Yanaco micro melting point apparatus and elemental analyses were conducted with a Yanaco-CHN corder at the Microanalytical Center of Kyoto University. The number- and weight-average

molecular weights (M_n and M_w, respectively) and polydispersity indices (M_w/M_n) of polymers were determined by gel permeation chromatography (GPC) on a JASCO Gulliver system (PU-980, CO-965, RI-930, and UV-2075). All of the measurements were carried out at 40 ºC using two TSK-Gel columns [α-M (bead size, 13 μm; molecular weight range > 1×10^7) and GMH_{XL} (bead size 9 μm; molecular weight range up to 4×10^8)] in series and LiBr solution (0.01 M) in *N*,*N*-dimethylformamide as an eluent at a flow rate of 1.0 mL/min. The elution times were converted into molecular weights using a calibration curve based on polystyrene standards in combination with the information obtained from the refractive index detector. Thermogravimetric analyses (TGA) were conducted in air with a Shimadzu TGA–50 thermal analyzer by heating the samples (3–5 mg) from 100–700 ºC at a scanning rate of 10 ºC min^{-1}. Differential scanning calorimetric (DSC) analyses were performed using a Seiko DSC6200/EXSTAR6000 apparatus and measurements were carried out by making use of 3–5 mg samples, under a nitrogen atmosphere, after calibration with an indium standard. The samples were first heated from ambient temperature (25 ºC) to 260 °C at a scanning rate of 20 ºC min^{-1} (first heating scan) and then immediately quenched to -100 °C at a rate of 100 ºC min^{-1}. The second heating scans were run from -100 to 260 °C at a scanning rate of 20 ºC min^{-1} to record stable thermograms. The data for glass transition temperature (T_g) were obtained from the second run and correspond to the midpoint of discontinuity in the heat flow. Membrane thickness was estimated by using a Mitutoyo micrometer. The gas permeability coefficients (P) were measured with a Rikaseiki K-315-N gas permeability apparatus using a constant volume/variable-pressure system.[14] All of the measurements were carried out at 25 ºC and a feed pressure of 0.1 MPa (1 atm) while the pressure difference across the membrane was ~107 kPa as the system was being evacuated on the downstream side of the membrane.

Materials. Ethyl cellulose (**1**; ethoxy content, 49 wt%) and *N*-(3-aminopropyl)propane-1,3-diamine (98%) were purchased from Aldrich and used as received. 1,1′-Carbonyldiimidazole (Sigma-Aldrich), 2-ethylbutanoic acid (97%,

Wako, Japan), 2-propylpentanoic acid (Sigma-Aldrich), 2-ethylhexanoic acid (Tokyo Kasei, Japan), succinic anhydride (≥ 99%, Tokyo Kasei, Japan), 4-(dimethylamino)pyridine (99%, Wako, Japan), *N*-(3-Dimethylaminopropyl)-*N*′-ethylcarbodiimide hydrochloride (EDC·HCl ; Eiweiss Chemical Corporation), and distilled water (Wako, Japan) were obtained commercially and used without further purification. Toluene and dichloromethane (CH_2Cl_2), used as reaction solvents, were purchased from Wako (Japan) and purified by distillation prior to use.

The first and second generation amide-containing dendrons (**G1-a-II**–**G1-c-II**, **G2-a-II**–**G2-c-II**) and dendronized ethyl cellulose derivatives (**2a**–**c**, **3a**–**c**) were synthesized according to Schemes 1 and 2, respectively. The details of the synthetic procedure and analytical data are as follows:

Dendron Synthesis.

***N*,*N*′-(3,3′-Azanediylbis(propane-3,1-diyl))bis(2-ethylbutanamide) (G1-a-I).** A 200 mL three-necked flask was equipped with a dropping funnel, a reflux condenser, a three-way stopcock, and a magnetic stirring bar, and evacuated and flushed with argon three times. 2-Ethylbutanoic acid (40.6 mL, 0.312 mol) was charged into the flask, toluene (100 mL) was added and the system was heated to 60 °C and stirred. 1,1′-Carbonyldiimidazole, CDI, (50.6 g, 0.312 mol) was added slowly along with constant stirring until CO_2 evolution had ceased. The solution was further heated for an hour at 80 °C and purged with argon. *N*-(3-aminopropyl)propane-1,3-diamine (22.5 mL, 0.156 mol) was added dropwise to the solution and stirring was continued for three hours at 80 °C. The reaction mixture was allowed to cool to room temperature, concentrated in vacuo, the remaining clear liquid was dissolved in CH_2Cl_2 and washed three times with water. The washed CH_2Cl_2 solution was dried with anhydrous $MgSO_4$, filtered, concentrated, and dried under vacuum to constant weight to afford the desired product as a white solid. Yield 67%, white solid, mp 95–96 °C, ^{1}H NMR ($CDCl_3$, 400 MHz, 25 °C, ppm): 0.97 (t, J = 7.2 Hz, 12H, CH_3CH$_2$), 1.51–1.72 (m, 8H, CH$_3$CH_2), 1.74–1.79 (m, 4H, C(=O)NHCH$_2$CH_2CH$_2$),

1.99–2.07 (m, 2H, $(CH_3CH_2)_2CH$)), 2.43 (brs, 1H, CH_2NHCH_2), 2.68–2.77 (m, 4H, $C(=O)NHCH_2CH_2CH_2$), 3.41–3.51 (m, 4H, $C(=O)NHCH_2CH_2CH_2$), 7.7 (brs, 2H, C(=O)NH); ^{13}C NMR ($CDCl_3$, 100 MHz, 25 °C, ppm): 11.8, 25.5, 29.2, 36.9, 46.8, 50.8, 175.8; HRMS(FAB): $[MH]^+$, calcd for $C_{18}H_{37}N_3O_2$ 328.2959, found 328.2931; anal. calcd for $C_{18}H_{37}N_3O_2$: C, 66.01; H, 11.39; N, 12.83; O, 9.77, found: C, 66.00; H, 11.09; N, 12.81; O, 10.10.

4-(bis(3-(2-Ethylbutanamido)propyl)amino)-4-oxobutanoic acid (G1-a-II). **G1-a-I** (25 g, 0.076 mol) and succinic anhydride (11.46 g, 0.1146 mol) were charged into a 200 mL three-necked flask equipped with a reflux condenser, a three-way stopcock, and a magnetic stirring bar, and argon exchange was carried out three times. Toluene (50 mL) was added and after stirring for three hours at 80 °C, the reaction mixture was allowed to cool to room temperature and concentrated in vacuo. After being concentrated in vacuo (in order to remove toluene), $CHCl_3$ (50 mL) was added to the reaction mixture and purification was carried out by washing three times with water followed by the drying under vacuum to constant weight. Yield 85%, white solid, mp 136 °C, ^1H NMR (CD_3OD, 400 MHz, 25 °C, ppm): 0.80 (t, J = 6.8 Hz, 12H, CH_3CH_2), 1.32–1.51 (m, 8H, CH_3CH_2), 1.60–1.78 (m, 4H, $C(=O)NHCH_2CH_2CH_2$), 1.89–1.94 (m, 2H, $(CH_3CH_2)_2CH$)), 2.51–2.58 (m, 4H, $CH_2CH_2C(=O)OH$), 3.07–3.18 (m, 4H, $C(=O)NHCH_2CH_2CH_2$), 3.22–3.28 (m, 4H, $C(=O)NHCH_2CH_2CH_2$), 7.81 (brs, 1H, C(=O)NH), 7.99 (brs, 1H, C(=O)NH), 12.18 (brs, 1H, C(=O)OH); ^{13}C NMR (CD_3OD, 100 MHz, 25 °C, ppm): 12.5, 26.8, 28.7, 29.9, 37.6, 44.6, 46.8, 52.0, 173.9, 176.4, 178.5, 178.8; HRMS(FAB): $[MH]^+$, calcd for $C_{22}H_{41}N_3O_5$ 428.3119, found 428.3130; anal. calcd for $C_{22}H_{41}N_3O_5$: C, 61.80; H, 9.67; N, 9.83; O, 18.71, found: C, 61.61; H, 9.78; N, 9.72; O, 18.89.

***N*,*N*′-(3,3′-Azanediylbis(propane-3,1-diyl))bis(2-propylpentanamide) (G1-b-I).** It was synthesized by using 2-propylpentanoic acid (44.9 mL, 0.312 mol) rather than 2-ethylbutanoic acid while rest of the conditions and procedure were the same as those for the synthesis of **G1-a-I**. Yield 84%, white solid, mp 92 °C, ^1H NMR ($CDCl_3$, 400 MHz, 25 °C, ppm): 0.84 (t, J = 7.2 Hz, 12H, CH_3CH_2), 1.18–1.34

(m, 8H, CH_3CH_2), 1.49–1.55 (m, 8H, $CH_3CH_2CH_2$), 1.62–1.68 (m, 4H, C(=O)NHCH$_2$CH_2CH$_2$), 1.99–2.06 (m, 2H, $(CH_3CH_2CH_2)_2CH$)), 2.15 (brs, 1H, CH_2NHCH_2), 2.56–2.64 (m, 4H, C(=O)NHCH$_2$CH$_2$CH_2), 3.29–3.34 (m, 4H, C(=O)NHCH_2CH$_2$CH$_2$), 6.63 (brs, 2H, C(=O)N*H*); ^{13}C NMR ($CDCl_3$, 100 MHz, 25 °C, ppm): 14.0, 20.8, 29.1, 35.2, 37.0, 46.7, 47.5, 176.4; HRMS(FAB): $[MH]^+$, calcd for $C_{22}H_{45}N_3O_2$ 384.3585, found 384.3588; anal. calcd for $C_{22}H_{45}N_3O_2$: C, 68.88; H, 11.82; N, 10.95; O,8.35, found: C, 68.69; H, 11.68; N, 10.98; O, 8.65.

4-(bis(3-(2-Propylpentanamido)propyl)amino)-4-oxobutanoic acid (G1-b-II). The reaction of **G1-b-I** (25 g, 0.065 mol) with succinic anhydride (9.79 g, 0.097 mol) and the purification of the product were carried out in the same way as that for the synthesis of **G1-a-II**. Yield 95%, white solid, mp 151 °C, ^{1}H NMR (CD_3OD, 400 MHz, 25 °C, ppm): 0.84 (t, *J* = 6.8 Hz, 12H, C*H*$_3$CH$_2$), 1.18–1.28 (m, 8H, CH_3CH_2), 1.42–1.53 (m, 8H, $CH_3CH_2CH_2$), 1.60–1.79 (m, 4H, C(=O)NHCH$_2$CH_2CH$_2$), 2.09–2.17 (m, 2H, $(CH_3CH_2CH_2)_2CH$)), 2.53–2.58 (m, 4H, CH_2CH_2C(=O)OH), 3.06–3.17 (m, 4H, C(=O)NHCH$_2$CH$_2$CH_2), 3.22–3.34/3.28 (m, 4H, C(=O)NHCH_2CH$_2$CH$_2$), 7.87 (brs, 1H, C(=O)N*H*), 8.05 (brs, 1H, C(=O)N*H*); ^{13}C NMR (CD_3OD, 100 MHz, 25 °C, ppm): 14.4, 21.8, 28.8, 30.1, 36.4, 37.6, 44.6, 46.8, 47.9, 173.9, 176.4, 178.7, 179.1; HRMS(FAB): $[MH]^+$, calcd for $C_{26}H_{49}N_3O_5$ 484.3745, found 484.3749; anal. calcd for $C_{26}H_{49}N_3O_5$: C, 64.56; H, 10.21; N, 8.69; O, 16.54, found: C, 64.59; H, 9.98; N, 8.62; O, 16.81.

***N*,*N*′-(3,3′-Azanediylbis(propane-3,1-diyl))bis(2-ethylhexanamide) (G1-c-I).** It was synthesized by using 2-ethylhexanoic acid (44.9 mL, 0.312 mol) rather than 2-ethylbutanoic acid whereas the rest of the conditions and procedure were the same as those for the synthesis of **G1-a-I**. Yield 89%, white solid, mp 50 °C, ^{1}H NMR ($CDCl_3$, 400 MHz, 25 °C, ppm): 0.81–0.85 (m, 12H, C*H*$_3$CH$_2$), 1.16–1.28 (m, 8H, $CH_3CH_2CH_2CH_2$), 1.31–1.44 (m, 4H, $CH_3CH_2CH_2CH_2$), 1.50–1.67 (m, 8H, CH_3CH_2, C(=O)NHCH$_2$CH_2CH$_2$), 1.85–1.94 (m, 2H, $(CH_3CH_2CH_2CH_2)(CH_3CH_2)CH$), 2.28 (brs, 1H, CH_2NHCH_2), 2.55–2.63 (m, 4H, C(=O)NHCH$_2$CH$_2$CH_2), 3.27–3.37 (m, 4H, C(=O)NHCH_2CH$_2$CH$_2$), 6.57 (brs, 2H, C(=O)N*H*); ^{13}C NMR ($CDCl_3$, 100 MHz,

25 °C, ppm): 11.9, 13.8, 22.6, 25.9, 29.1, 29.8, 32.4, 37.0, 46.8, 49.4, 176.1; HRMS(FAB): $[MH]^+$, calcd for $C_{22}H_{45}N_3O_2$ 384.3585, found 384.3593; anal. calcd for $C_{22}H_{45}N_3O_2$: C, 68.88; H, 11.82; N, 10.95; O, 8.35, found: C, 68.66; H, 11.91; N, 10.71; O, 8.72.

4-(bis(3-(2-Ethylhexanamido)propyl)amino)-4-oxobutanoic acid (G1-c-II). The reaction of **G1-c-I** (25 g, 0.065 mol) with succinic anhydride (9.79 g, 0.097 mol) and the purification of the product were carried out in the same way as that for the synthesis of **G1-a-II**. Yield 96%, white solid, mp 115 °C,-^{1}H NMR (CD_3OD, 400 MHz, 25 °C, ppm): 0.85–0.90 (m, 12H, C*H*$_3$CH$_2$), 1.22–1.47 (m, 8H, CH$_3$C*H*$_2$C*H*$_2$CH$_2$), 1.51–1.59 (m, 4H, CH$_3$CH$_2$CH$_2$C*H*$_2$), 1.68–1.75 (m, 4H, CH$_3$C*H*$_2$), 1.79–1.87 (m, 4H, C(=O)NHCH$_2$C*H*$_2$CH$_2$), 2.03–2.12 (m, 2H, (CH$_3$CH$_2$CH$_2$CH$_2$)(CH$_3$CH$_2$)C*H*), 2.59–2.65 (m, 4H, C*H*$_2$C*H*$_2$C(=O)OH), 3.14–3.25 (m, 4H, C(=O)NHCH$_2$CH$_2$C*H*$_2$), 3.36–3.41 (m, 4H, C(=O)NHC*H*$_2$CH$_2$CH$_2$), 7.89 (brs, 1H, C(=O)N*H*), 8.10 (brs, 1H, C(=O)N*H*); ^{13}C NMR (CD_3OD, 100 MHz, 25 °C, ppm): 12.4, 14.4, 23.7, 27.2, 28.9, 29.7, 30.1, 33.6, 37.6, 44.7, 46.9, 50.2, 174.0, 176.5, 178.7, 179.0; HRMS(FAB): $[MH]^+$, calcd for $C_{26}H_{49}N_3O_5$ 484.3745, found 484.3750; anal. calcd for $C_{26}H_{49}N_3O_5$: C, 64.56; H, 10.21; N, 8.69; O, 16.54, found: C, 64.58; H, 10.23; N, 8.62; O, 16.57.

***N*^{1},*N*$^{1\prime}$-(3,3′-Azanediylbis(propane-3,1-diyl))bis(*N*^{4},*N*^{4}-bis(3-(2-ethylbutana mido)propyl)succinamide) (G2-a-I).** The synthesis of **G2-a-I** was accomplished in the same way as that of **G1-a-I** by making use of **G1-a-II** instead of 2-ethylbutanoic acid and the product was purified by washing with water. Yield 55%, white solid, mp 148–149 °C, ^{1}H NMR (CD_3OD, 400 MHz, 25 °C, ppm): 0.85–0.90 (m, 24H, C*H*$_3$CH$_2$), 1.43–1.58 (m, 16H, CH$_3$C*H*$_2$), 1.66–1.72 (m, 4H, C(=O)NHCH$_2$C*H*$_2$CH$_2$NH), 1.79–1.86 (m, 8H, C(=O)NHCH$_2$C*H*$_2$CH$_2$), 1.95–2.05 (m, 4H, (CH$_3$CH$_2$)$_2$C*H*)), 2.21 (brs, 1H, CH$_2$N*H*CH$_2$), 2.47–2.67 (m, 12H, C(=O)NHCH$_2$CH$_2$C*H*$_2$NH, C(=O)C*H*$_2$C*H*$_2$C(=O)), 3.14–3.25 (m, 12H, C(=O)NHCH$_2$CH$_2$C*H*$_2$NC(=O), C(=O)NHC*H*$_2$CH$_2$CH$_2$NH), 3.34–3.40 (m, 8H, C(=O)NHC*H*$_2$CH$_2$CH$_2$), 7.94 (brs, 2H, C(=O)N*H*), 8.15 (brs, 4H, C(=O)N*H*); ^{13}C NMR (CD_3OD, 100 MHz, 25 °C, ppm):

12.5, 26.8, 28.6, 29.2, 30.1, 31.8, 37.7, 38.3, 44.7, 46.8, 52.0, 174.0, 174.8, 178.5, 178.8; HRMS(FAB): $[MH]^+$, calcd for $C_{50}H_{95}N_9O_8$ 950.7376, found 950.7383; anal. calcd for $C_{50}H_{95}N_9O_8$: C, 63.19; H, 10.08; N, 13.26; O, 13.47, found: C, 62.94; H, 10.13; N, 13.18; O, 13.75.

G2-a-II. It was synthesized by the reaction of **G2-a-I** (10 g, 0.010 mol) with succinic anhydride (1.58 g, 0.016 mol) under the same conditions as those for the synthesis of **G1-a-II** and the product was purified by washing with water. Yield 68%, white solid, mp 156 °C, ^{1}H NMR (CD_3OD, 400 MHz, 25 °C, ppm): 0.78–0.83 (m, 24H, C*H*$_3$CH$_2$), 1.35–1.51 (m, 16H, CH$_3$C*H*$_2$), 1.62–1.81 (m, 12H, C(=O)NHCH$_2$C*H*$_2$CH$_2$), 1.90–1.96 (m, 4H, (CH$_3$CH$_2$)$_2$C*H*)), 2.41–2.63 (m, 12H, C(=O)C*H*$_2$C*H*$_2$C(=O)), 3.07–3.24 (m, 16H, C(=O)NHCH$_2$CH$_2$C*H*$_2$, C(=O)NHC*H*$_2$CH$_2$CH$_2$), 3.32–3.36 (m, 8H, C(=O)NHC*H*$_2$CH$_2$CH$_2$), 7.89 (brs, 2H, C(=O)N*H*), 8.07 (brs, 4H, C(=O)N*H*); ^{13}C NMR (CD_3OD, 100 MHz, 25 °C, ppm): 12.5, 26.8, 28.4, 28.7, 29.1, 29.7, 31.8, 37.8, 44.7, 46.7, 51.9, 173.9, 174.2, 174.3, 178.5, 178.8; HRMS(FAB): $[MH]^+$, calcd for $C_{54}H_{99}N_9O_{11}$ 1050.7537, found 1050.7543; anal. calcd for $C_{54}H_{99}N_9O_{11}$: C, 61.74; H, 9.50; N, 12.00; O, 16.76, found: C, 61.90; H, 9.51; N, 11.95; O, 16.64.

***N*^{1},*N*$^{1\prime}$-(3,3′-Azanediylbis(propane-3,1-diyl))bis(*N*^{4},*N*^{4}-bis(3-(2-propylpenta namido)propyl)succinamide) (G2-b-I).** The synthesis of **G2-b-I** was carried out in the same way as that of **G1-a-I** by making use of **G1-b-II** instead of 2-ethylbutanoic acid and the product was isolated by washing with water. Yield 73%, white solid, mp 146–147 °C, ^{1}H NMR (CD_3OD, 400 MHz, 25 °C, ppm): 0.90 (t, J = 7.0 Hz, 24H, C*H*$_3$CH$_2$), 1.24–1.37 (m, 16H, CH$_3$C*H*$_2$), 1.51–1.58 (m, 16H, CH$_3$CH$_2$C*H*$_2$), 1.67–1.73 (m, 4H, C(=O)NHCH$_2$C*H*$_2$CH$_2$NH), 1.78–1.85 (m, 8H, (C(=O)NHCH$_2$C*H*$_2$CH$_2$), 2.03 (brs, 1H, CH$_2$N*H*CH$_2$), 2.15–2.25 (m, 4H, (CH$_3$CH$_2$CH$_2$)$_2$C*H*), 2.47–2.51 (m, 4H, C(=O)NHCH$_2$CH$_2$C*H*$_2$NH), 2.62–2.67 (m, 8H, C(=O)C*H*$_2$C*H*$_2$C(=O)), 3.12–3.24 (m, 12H, C(=O)NHCH$_2$CH$_2$C*H*$_2$NC(=O), C(=O)NHC*H*$_2$CH$_2$CH$_2$NH), 3.33–3.39 (m, 8H, C(=O)NHC*H*$_2$CH$_2$CH$_2$), 7.95 (brs, 2H, C(=O)N*H*), 8.11 (brs, 4H, C(=O)N*H*); ^{13}C NMR (CD_3OD, 100 MHz, 25 °C, ppm): 14.4, 21.8, 28.6, 29.2, 29.8, 31.8, 36.4, 37.7,

38.1, 44.7, 46.8, 47.9, 174.0, 174.9, 178.7, 179.0; HRMS(FAB): $[MH]^+$, calcd for $C_{58}H_{111}N_9O_8$ 1062.8628, found 1062.8636; anal. calcd for $C_{58}H_{111}N_9O_8$: C, 65.56; H, 10.53; N, 11.86; O, 12.05, found: C, 65.49; H, 10.67; N, 11.99; O, 11.85.

G2-b-II. It was synthesized by the reaction of **G2-b-I** (10 g, 0.009 mol) with succinic anhydride (1.41 g, 0.014 mol) under the same conditions as those for the synthesis of **G1-a-II** and the product was purified by washing with water. Yield 88%, white solid, mp 141 °C, ^{1}H NMR (CD_3OD, 400 MHz, 25 °C, ppm): 0.89 (t, J = 6.8 Hz, 24H, CH_3CH$_2$), 1.22–1.39 (m, 16H, CH$_3$CH_2), 1.49–1.59 (m, 16H, CH$_3$CH$_2$CH_2), 1.66–1.86 (m, 12H, C(=O)NHCH$_2$CH_2CH$_2$), 2.16–2.23 (m, 4H, (CH$_3$CH$_2$CH$_2$)$_2$CH), 2.49–2.68 (m, 12H, C(=O)CH_2CH_2C(=O)), 3.12–3.23 (m, 12H, C(=O)NHCH$_2$CH$_2$CH_2), 3.33–3.41 (m, 12H, C(=O)NHCH_2CH$_2$CH$_2$), 7.96 (brs, 2H, C(=O)NH), 8.12 (brs, 4H, C(=O)NH); ^{13}C NMR (CD_3OD, 100 MHz, 25 °C, ppm): 14.4, 21.9, 28.4, 28.6, 28.9, 29.1, 29.2, 29.6, 31.7, 36.4, 37.8, 44.7, 46.7, 48.0, 174.0, 174.7, 174.9, 178.8, 179.1; HRMS(FAB): $[MH]^+$, calcd for $C_{62}H_{115}N_9O_{11}$ 1162.8789, found 1162.8795; anal. calcd for $C_{62}H_{115}N_9O_{11}$: C, 64.05; H, 9.97; N, 10.84; O, 15.14, found: C, 63.88; H, 9.75; N, 11.08; O, 15.29.

***N*^{1},*N*$^{1\prime}$-(3,3′-Azanediylbis(propane-3,1-diyl))bis(*N*^{4},*N*^{4}-bis(3-(2-ethylhexanamido)propyl)succinamide) (G2-c-I).** The synthesis of **G2-c-I** was carried out in the same way as that of **G1-a-I** by making use of **G1-c-II** instead of 2-ethylbutanoic acid and the product was isolated by washing with water. Yield 91%, white solid, mp 99 °C, ^{1}H NMR (CD_3OD, 400 MHz, 25 °C, ppm): 0.85–0.90 (m, 24H, CH_3CH$_2$), 1.21–1.45 (m, 24H, CH$_3$CH_2CH_2CH_2), 1.50–1.59 (m, 8H, CH$_3$CH_2), 1.64–1.74 (m, 4H, C(=O)NHCH$_2$CH_2CH$_2$NH), 1.79–1.84 (m, 8H, (C(=O)NHCH$_2$CH_2CH$_2$), 2.04–2.11 (m, 4H, (CH$_3$CH$_2$CH$_2$CH$_2$)(CH$_3$ CH$_2$)CH), 2.23 (brs, 1H, CH$_2$NHCH$_2$), 2.47–2.67 (m, 12H, C(=O)NHCH$_2$CH$_2$CH_2NH, C(=O)CH_2CH_2C(=O)), 3.13–3.24 (m, 12H, C(=O)NHCH$_2$CH$_2$CH_2NC(=O), C(=O)NHCH_2CH$_2$CH$_2$NH), 3.34–3.41 (m, 8H, C(=O)NHCH_2CH$_2$CH$_2$), 7.91 (brs, 2H, C(=O)NH), 8.08 (brs, 4H, C(=O)NH); ^{13}C NMR (CD_3OD, 100 MHz, 25 °C, ppm): 12.5, 14.4, 23.7, 27.2, 28.6, 29.2, 29.7, 30.1, 30.9, 31.8, 33.6, 37.7, 38.2, 44.7, 46.8, 174.0, 174.8, 178.7, 179.0; HRMS(FAB):

$[MH]^+$, calcd for $C_{58}H_{111}N_9O_8$ 1062.8628, found 1062.8620; anal. calcd for $C_{58}H_{111}N_9O_8$: C, 65.56; H, 10.53; N, 11.86; O, 12.05, found: C, 65.61; H, 10.50; N, 11.77; O, 12.12.

G2-c-II. It was synthesized by the reaction of **G2-c-I** (10 g, 0.009 mol) with succinic anhydride (1.41 g, 0.014 mol) under the same conditions as those for the synthesis of **G1-a-II** and the product was purified by washing with water. Yield 94%, white solid, mp 118–119 °C, ^{1}H NMR (CD_3OD, 400 MHz, 25 °C, ppm): 0.85–0.90 (m, 24H, C*H*$_3$CH$_2$), 1.21–1.45 (m, 24H, CH$_3$C*H*$_2$C*H*$_2$C*H*$_2$), 1.51–1.57 (m, 8H, CH$_3$C*H*$_2$), 1.69–1.85 (m, 12H, C(=O)NHCH$_2$C*H*$_2$CH$_2$), 2.01–2.10 (m, 4H, (CH$_3$CH$_2$CH$_2$CH$_2$)(CH$_3$CH$_2$)C*H*), 2.48–2.67 (m, 12H, C(=O)C*H*$_2$C*H*$_2$C(=O)), 3.13–3.25 (m, 12H, C(=O)NHCH$_2$CH$_2$C*H*$_2$), 3.34–3.41 (m, 12H, C(=O)NHC*H*$_2$CH$_2$CH$_2$), 7.93 (brs, 2H, C(=O)N*H*), 8.10 (brs, 4H, C(=O)N*H*); ^{13}C NMR (CD_3OD, 100 MHz, 25 °C, ppm): 12.5, 14.4, 23.7, 27.2, 28.7, 29.2, 29.7, 30.3, 31.0, 31.7, 31.9, 33.6, 37.7, 37.8, 44.7, 46.9, 50.2, 173.9, 174.7, 174.9, 178.7, 178.9; HRMS(FAB): $[MH]^+$, calcd for $C_{62}H_{115}N_9O_{11}$ 1162.8789, found 1162.8779; anal. calcd for $C_{62}H_{115}N_9O_{11}$: C, 64.05; H, 9.97; N, 10.84; O, 15.14, found: C, 63.76; H, 9.85; N, 11.03; O, 15.36.

Synthesis of Dendronized Ethyl Cellulose. 2a. A 200 mL one-necked flask was equipped with a stopper and a magnetic stirring bar. Ethyl cellulose, **1**, (1.43 g, 6.10 mmol) and 4-(dimethylamino)pyridine (0.75 g, 6.10 mmol) were added to the flask and dissolved in CH_2Cl_2 (50 mL) at room temperature, followed by the addition of **G1-a-II** (2.61 g, 6.10 mmol) and EDC·HCl (1.17 g, 6.10 mmol), respectively, and stirring was continued for 48 h at room temperature. The product was isolated by the precipitation in aqueous $NaHCO_3$ solution (1000 mL), filtered with a membrane filter, washed with water several times to ensure the complete removal of $NaHCO_3$, and dried under vacuum to constant weight to afford the desired product as a beige solid. Yield 95%, ^{1}H NMR (400 MHz, $CDCl_3$, 25 ºC, ppm): 0.85 (brs, 3.72H, C*H*$_3$CH$_2$), 1.13 (brs, 8.07H, OCH$_2$C*H*$_3$), 1.44 (brs, 2.48H, CH$_3$C*H*$_2$), 1.57 (brs, 1.24H, C(=O)NHCH$_2$C*H*$_2$CH$_2$), 1.86 (brs, 0.62H, (CH$_3$CH$_2$)$_2$C*H*), 2.07 (brs, 1.86H,

CH_2CH_2C(=O)O), 2.50–4.51 (m, (12.4H, OCH_2CH$_3$, OCH, OCH$_2$) and (2.48H, C(=O)NHCH_2CH$_2$CH_2)), 6.26 (brs, 0.31H, C(=O)N*H*), 6.68 (brs, 0.31H, C(=O)N*H*); IR (ATR, cm^{-1}): 3310 (*v*NH), 2970, 2873, 1746 (*v*CO), 1645, 1539, 1443, 1375, 1277, 1228, 1088, 1052, 921, 883, 798, 674; anal. calcd for $(C_{18.2}H_{32.85}N_{0.93}O_{6.24})_n$ $(364.57)_n$: C, 59.96; H, 9.08; N, 3.57; O, 27.39, found: C, 59.36; H, 8.56; N, 3.99; O, 28.09.

2b. This derivative was prepared by following the same procedure as for **2a** using **G1-b-II** (2.95 g, 6.10 mmol) instead of **G1-a-II**. Yield 93%, peach-colored solid, ^{1}H NMR (400 MHz, CDCl$_3$, 25 ºC, ppm): 0.86 (brs, 3.72H, CH_3CH$_2$), 1.13 (brs, 8.07H, OCH$_2$CH_3), 1.24 (brs, 4.96H, CH$_3$CH_2CH_2), 1.55 (brs, 1.24H, C(=O)NHCH$_2$CH_2CH$_2$), 1.82 (brs, 0.62H, (CH$_3$CH$_2$CH$_2$)$_2$C*H*), 2.04 (brs, 1.24H, CH_2CH_2C(=O)O), 2.51–4.60 (m, (12.4H, OCH_2CH$_3$, OCH, OCH$_2$) and (2.48H, C(=O)NHCH_2CH$_2$CH_2)), 6.03 (brs, 0.31H, C(=O)N*H*), 6.64 (brs, 0.31H, C(=O)N*H*); IR (ATR, cm^{-1}): 3308 (*v*NH), 2973, 2930, 2872, 1743 (*v*CO), 1646, 1539, 1443, 1375, 1309, 1265, 1091, 1053, 920, 882, 794, 656; anal. calcd for $(C_{19.4}H_{35.3}N_{0.93}O_{6.24})_n$ $(381.96)_n$: C, 61.13; H, 9.32; N, 3.41; O, 26.14, found: C, 60.56; H, 9.26; N, 3.49; O, 26.69.

2c. This derivative was prepared by following the same procedure as for **2a** using **G1-c-II** (2.95 g, 6.10 mmol) instead of **G1-a-II**. Yield 98%, off-white solid, ^{1}H NMR (400 MHz, CDCl$_3$, 25 ºC, ppm): 0.84 (brs, 3.72H, CH_3CH$_2$), 1.13 (brs, 8.07H, OCH$_2$CH_3), 1.23 (brs, 2.48H, CH$_3$CH_2CH_2CH$_2$), 1.39 (brs, 1.24H, CH$_3$CH$_2$CH$_2$CH_2), 1.56 (brs, 1.24H, CH$_3$CH_2), 1.82 (brs, 1.24H, C(=O)NHCH$_2$CH_2CH$_2$), 1.92 (brs, 0.62H (CH$_3$CH$_2$CH$_2$CH$_2$)(CH$_3$CH$_2$)C*H*), 2.11 (brs, 1.24H, CH_2CH_2C(=O)O), 2.49–4.45 (m, (12.4H, OCH_2CH$_3$, OCH, OCH$_2$) and (2.48H, C(=O)NHCH_2CH$_2$CH_2)), 6.14 (brs, 0.31H, C(=O)N*H*), 6.63 (brs, 0.31H, C(=O)N*H*); IR (ATR, cm^{-1}): 3299 (*v*NH), 2970, 2930, 2871, 1744 (*v*CO), 1645, 1541, 1458, 1376, 1300, 1272, 1232, 1091, 1053, 920, 855, 798; anal. calcd for $(C_{19.4}H_{35.3}N_{0.93}O_{6.24})_n$ $(381.96)_n$: C, 61.13; H, 9.32; N, 3.41; O, 26.14, found: C, 60.74; H, 9.37; N, 3.88; O, 26.01.

3a. This derivative was prepared by following the same procedure as for **2a** using **G2-a-II** (6.41 g, 6.10 mmol) instead of **G1-a-II**. Yield 92%, peach-colored

solid, ^{1}H NMR (400 MHz, $CDCl_3$, 25 ºC, ppm): 0.845 (brs, 7.44H, C*H*$_3$CH$_2$), 1.12 (brs, 8.07H, OCH$_2$C*H*$_3$), 1.43 (brs, 4.96H, CH$_3$C*H*$_2$), 1.55–1.64 (m, 3.72H, C(=O)NHCH$_2$C*H*$_2$CH$_2$), 1.86 (brs, 1.24H, (CH$_3$CH$_2$)$_2$C*H*), 2.15 (brs, 1.24H, C(=O)C*H*$_2$C*H*$_2$C(=O)), 2.47–4.59 (m, (12.4H, OC*H*$_2$CH$_3$, OCH, OCH$_2$) and (9.92H, C(=O)C*H*$_2$C*H*$_2$C(=O), C(=O)NHC*H*$_2$CH$_2$C*H*$_2$)), 6.55 (brs, 0.62H, C(=O)N*H*), 6.65 (brs, 1.24H, C(=O)N*H*); IR (ATR, cm^{-1}): 3300 (*v*NH), 3090, 2960, 2928, 2873, 1744 (*v*CO), 1638, 1540, 1455, 1378, 1276, 1231, 1091, 1058, 920, 856, 804; anal. calcd for $(C_{28.12}H_{50.8}N_{2.8}O_{8.1})_n$ $(557.65)_n$: C, 60.57; H, 9.19; N, 7.01; O, 23.23, found: C, 60.02; H, 9.28; N, 7.59; O, 23.11.

3b. This derivative was prepared by following the same procedure as for **2a** using **G2-b-II** (7.1 g, 6.10 mmol) instead of **G1-a-II**. Yield 96%, light peach-colored solid, ^{1}H NMR (400 MHz, $CDCl_3$, 25 ºC, ppm): 0.85 (brs, 7.44H, C*H*$_3$CH$_2$), 1.11–1.36 (m, (8.07H, OCH$_2$C*H*$_3$) and (9.92H, CH$_3$C*H*$_2$C*H*$_2$)), 1.51–1.65 (m, 3.72H, C(=O)NHCH$_2$C*H*$_2$CH$_2$), 1.82 (brs, 1.24H, (CH$_3$CH$_2$CH$_2$)$_2$C*H*), 2.07 (brs, 1.24H, C(=O)C*H*$_2$C*H*$_2$C(=O)), 2.47–4.59 (m, (12.4H, OC*H*$_2$CH$_3$, OCH, OCH$_2$) and (9.92H, C(=O)C*H*$_2$C*H*$_2$C(=Om), C(=O)NHC*H*$_2$CH$_2$C*H*$_2$)), 6.73 (brs, 0.62H, C(=O)N*H*), 6.99 (brs, 1.24H, C(=O)N*H*); IR (ATR, cm^{-1}): 3292 (*v*NH), 3075, 2972, 2929, 2871, 1739 (*v*CO), 1635, 1542, 1441, 1378, 1257, 1221, 1091, 1053, 879, 802, 710; anal. calcd for $(C_{30.6}H_{55.8}N_{2.8}O_{8.1})_n$ $(592.43)_n$: C, 62.04; H, 9.49; N, 6.60; O, 21.87, found: C, 62.58; H, 9.11; N, 7.09; O, 21.22.

3c. This derivative was prepared by following the same procedure as for **2a** using **G2-c-II** (7.1 g, 6.10 mmol) instead of **G1-a-II**. Yield 90%, light yellow solid, ^{1}H NMR (400 MHz, $CDCl_3$, 25 ºC, ppm): 0.83 (brs, 7.44H, C*H*$_3$CH$_2$), 1.12 (brs, 8.07H, OCH$_2$C*H*$_3$), 1.22 (brs, 4.96H, CH$_3$C*H*$_2$C*H*$_2$CH$_2$), 1.38 (brs, 2.48H, CH$_3$CH$_2$CH$_2$C*H*$_2$), 1.55 (brs, 2.48H, CH$_3$C*H*$_2$), 1.63 (brs, 3.72H, C(=O)NHCH$_2$C*H*$_2$CH$_2$), 1.83 (brs, 1.24H, (CH$_3$CH$_2$CH$_2$CH$_2$)(CH$_3$CH$_2$)C*H*), 1.95 (brs, 1.24H, C(=O)C*H*$_2$C*H*$_2$C(=O)), 2.44–4.61 (m, (12.4H, OC*H*$_2$CH$_3$, OCH, OCH$_2$) and (9.92H, C(=O)NHC*H*$_2$CH$_2$C*H*$_2$)), 6.60 (brs, 0.62H, C(=O)N*H*), 6.95 (brs, 1.24H, C(=O)N*H*); IR (ATR, cm^{-1}): 3294 (*v*NH), 3080, 2958, 2929, 2872, 1732 (*v*CO), 1636, 1545, 1456, 1379, 1232, 1123,

1091, 1053, 853, 806, 707; anal. calcd for $(C_{30.6}H_{55.8}N_{2.8}O_{8.1})_n$ $(592.43)_n$: C, 62.04; H, 9.49; N, 6.60; O, 21.87, found: C, 61.45; H, 9.16; N, 7.13; O, 22.26.

Determination of the Degree of Substitution. The degree of substitution with ethyl group (DS_{Et}) of the starting material, **1**, was determined by ^{1}H NMR measurement, which also provided a clear indication of the incorporation of the dendritic moieties into ethyl cellulose. However, the overlapping of the peaks arising due to the methyl protons of the dendritic moiety and those of ethyl cellulose did not allow the exact estimation of the degree of esterification (DS_{Est}) which was determined by the elemental analysis (%N content) of the polymers (**2a**–**c**, **3a**–**c**). The total degree of substitution (DS_{total}) of **2a**–**c** and **3a**–**c** was calculated by the following equation:

$$DS_{total} = DS_{Et} + DS_{Est}$$

Membrane Fabrication. Membranes (thickness ca. 40–80 μm) of polymers **1** and **2a**–**c** were fabricated by casting their chloroform solution (concentration ca. 0.50–1.0 wt%) onto a Petri dish. The dish was covered with a glass vessel to retard the rate of solvent evaporation (3–5 days).

Membrane Density. Membrane densities (ρ) were determined by hydrostatic weighing using a Mettler Toledo balance (model AG204, Switzerland) and a density determination kit.[15] This method makes use of a liquid with known density (ρ_0), and membrane density (ρ) is calculated by the following equation:

$$\rho = \rho_0 M_A/(M_A - M_L)$$

where M_A is the weight of membrane in air and M_L is that in the auxiliary liquid. Aqueous $NaNO_3$ solution was used as an auxiliary liquid to measure the density of the polymer membranes.

Fractional Free Volume (FFV) of Polymer Membranes. FFV (cm^3 of free

volume/cm^3 of polymer) is commonly used to estimate the efficiency of chain packing and thus the amount of space (free volume) available for gas permeation in the polymer matrix. FFV is calculated by the following equation:[16]

$$\text{FFV} = (v_{sp} - v_0)/ v_{sp} \approx (v_{sp} - 1.3\, v_w)/ v_{sp}$$

where v_{sp} and v_0 are the specific volume and occupied volume (or zero-point volume at 0 K) of the polymer, respectively. Typically, occupied volume (v_0) is estimated as 1.3 times the van der Waals volume (v_w), which is calculated by the group contribution method.[17]

Measurement of Gas Permeation Parameters. The *P* values were calculated from the slopes of the time-pressure curves in the steady state where Fick's law holds.[18] The gas diffusion coefficients (*D*) were determined by the time lag method using the following equation:

$$D = l^2/6\theta$$

here, *l* is the membrane thickness and θ is the time lag, which is given by the intercept of the asymptotic line of the time-pressure curve to the time axis. The membrane thickness was controlled so that the time lag would be in the range of 10–300 s, preferably 30–150 s. When the time lag was < 10 s, the error of measurement became relatively large. If the time lag was, on the contrary, > 300 s, the error arising from the baseline drift became serious. The gas solubility coefficients (*S*) were calculated by using the equation, $S = P/D$.

Results and Discussion

Dendron Synthesis. A series of G1 and G2 amide-containing dendrons with branched alkyl periphery and focal carboxyl moiety (Chart 1) were prepared via a convergent pathway[19] as shown in Scheme 1. The first generation amide-containing

dendrons (**G1-a-II**–**G1-c-II**) were prepared by the reaction of branched aliphatic acids with 1,1′-carbonyldiimidazole, and subsequently with *N*-(3-aminopropyl)propane-1,3-diamine generating a secondary amine at the focal point (**G1-a-I**–**G1-c-I**), which upon further treatment with succinic anhydride afforded a carboxyl moiety at the dendron termini. The second generation dendrons (**G2-a-II**–**G2-c-II**) were prepared by the iteration of the same three-step reaction sequence.[20] The presence of the branched alkyl periphery helps prevent the dendrons from being insoluble in common organic solvents thus making the otherwise cumbersome purification quite practicable, and the presence of carboxyl functionality at the dendron termini renders them capable to be engineered for various applications.

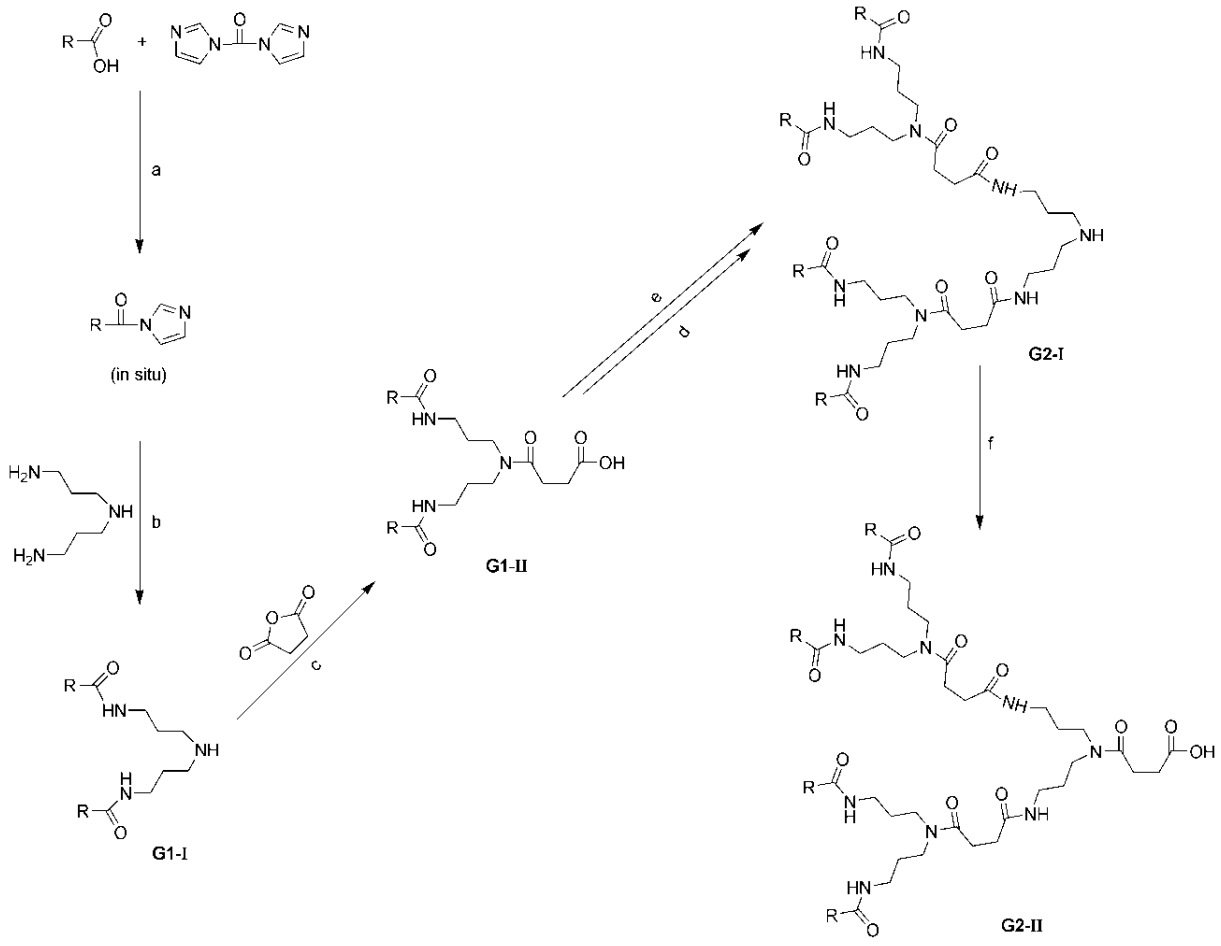

Scheme 1. Synthesis of G1 and G2 Amide-Containing Dendrons.[a]

[a] Conditions: (a) toluene, 80 °C, 1 h; (b) toluene, 80 °C, 3 h; (c) toluene, 80 °C, 3 h; (d) 1,1′-Carbonyldiimidazole, as in (a); (e) *N*-(3-Aminopropyl)propane -1,3-diamine, as in (b); (f) Succinic anhydride, as in (c).

All of the synthetic procedures were carried out several times and can be considered optimized. The characterization of the first and second generation amide-containing dendrons was accomplished by ^{1}H and ^{13}C NMR spectroscopy, mass spectrometry, and elemental analysis.

Synthesis of Dendronized Ethyl Cellulose. The incorporation of dendritic moieties (**G1-a- II**–**G1-c-II** and **G2-a-II**–**G2-c-II**) into ethyl cellulose (**1**) was carried out by coupling the carboxyl termini of dendrons to the hydroxy functionalities of ethyl cellulose; *N*-(3-dimethylaminopropyl)-*N*′-ethylcarbodiimide hydrochloride (EDC·HCl) was employed as a condensating agent and 4-(dimethylamino)pyridine

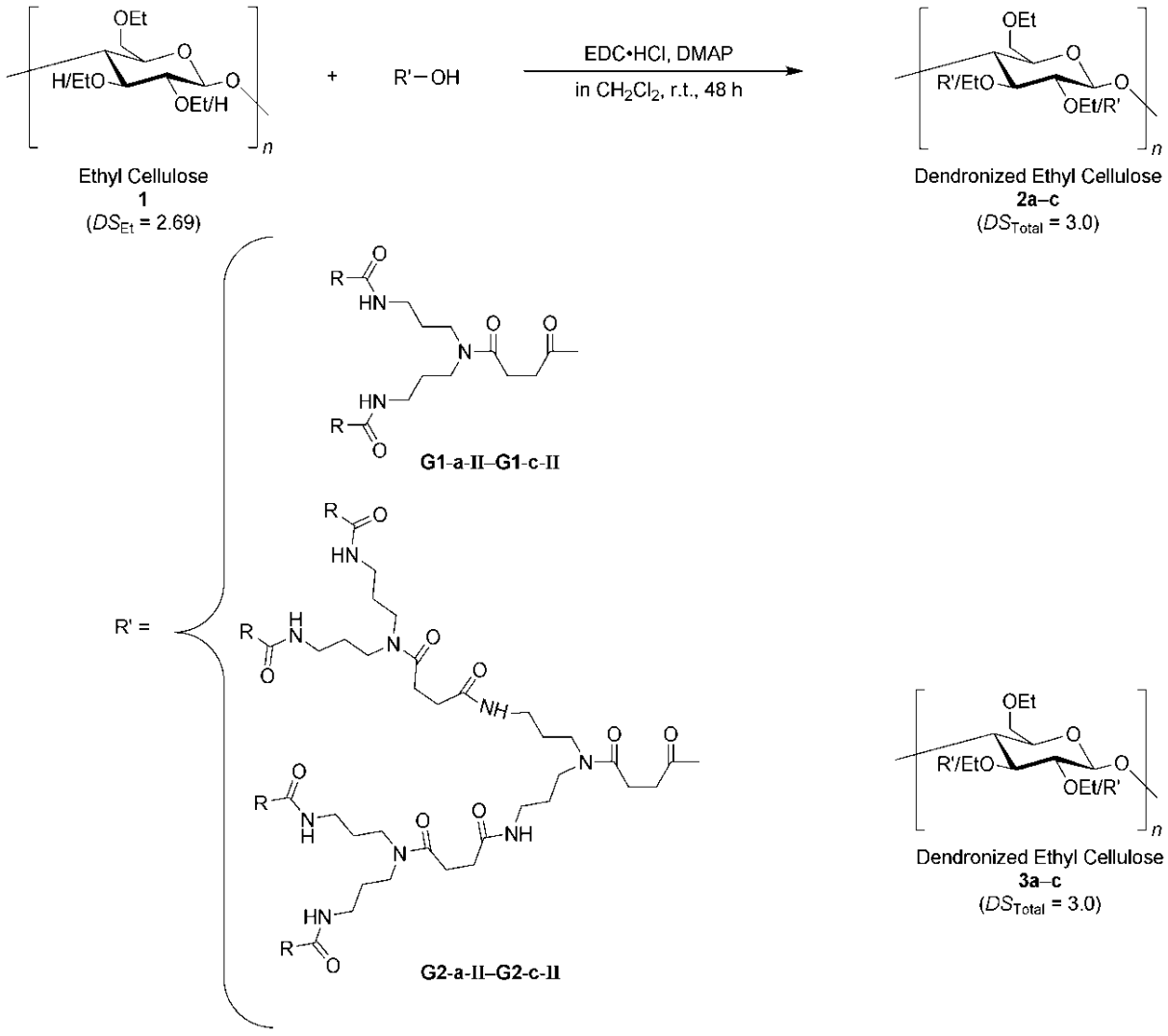

Scheme 2. Esterification of ethyl cellulose with G1 and G2 dendrons.[a]

[a] Abbreviations: EDC·HCl, *N*-(3-Dimethylaminopropyl)-*N*′-ethylcarbodiimide Hydrochloride; DMAP, 4-(Dimethylamino)pyridine.

(DMAP) as a base, as shown in Scheme 2, and the results are summarized in Table 1. The dendronized ethyl cellulose derivatives (**2a**–**c** and **3a**–**c**) were characterized by the ^{1}H NMR and IR spectroscopy and elemental analysis. The DS_{Et} of **1** was estimated to be 2.69, by calculating the integration ratio of methyl protons to the rest of the protons in **1**, indicating the presence of 0.31 hydroxy groups per anhydroglucose unit.[21] The ^{1}H NMR spectra of one of the G1 dendrons (**G1-c-II**), ethyl cellulose (**1**), and the corresponding dendronized ethyl cellulose (**2c**) are shown in Figure 1 and a similar information for a G2-derivatized ethyl cellulose (**3c**) is depicted in Figure 2. Although the ^{1}H NMR spectra of the dendronized polymers provide a clear indication of the substitution of hydroxy protons by the dendritic moieties, the calculation of the exact degree of esterification could not be carried out due to the overlapping of the peaks arising from the methyl protons of the ethyl group of ethyl cellulose and those of the dendrons' periphery. Further evidence was furnished by the presence of the peaks characteristic of the carbonyl group of an ester (1746–1732 cm^{-1}) in the IR spectra of the dendronized derivatives (**2a**–**c** and **3a**–**c**). The IR spectrum of **1** (Figure 3) has a broad band due to the residual hydroxy groups (3600–3200 cm^{-1}), which did not disappear completely upon dendronization as the NH groups of the dendritic moiety also absorb IR radiation in the same wavenumber region.

Despite the fact that the starting as well as the dendronized polymers are soluble in chloroform, the attempts to carry out molecular weight determination by GPC, using chloroform as an eluent, were unsuccessful to yield satisfactory and reproducible results probably due to the aggregation of the polymers. Therefore, molecular weights of the polymers were determined by making use of the LiBr solution in DMF (10 mM) and reproducible results were obtained for G1-derivatized ethyl cellulose (**2a**–**c**). According to GPC data of the polymers (Table 1), the number-average molecular weight (M_n) of **1** was found to be 71 000 and a significant increase in the M_n values ($\geq$ 222 000) was observed as a consequence of the substitution of small hydroxy groups with fairly bulky G1 dendritic moieties. Meanwhile, the polydispersity indices (M_w/M_n) of the dendronized polymers (**2a**–**c**)

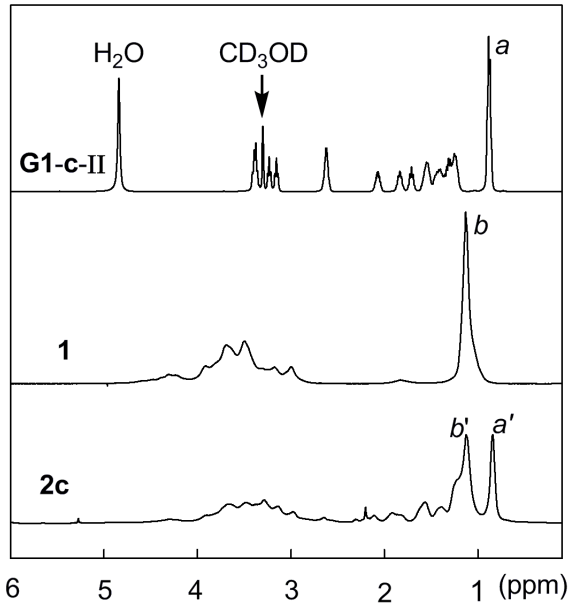

Figure 1. ^{1}H NMR spectra of **G1-c-II**, **1**, and **2c**

Labels: *a*, terminal methyl protons of dendron; *b*, terminal methyl protons of ethyl cellulose; *a′*, terminal methyl protons derived from the dendron; *b′*, terminal methyl protons derived from eth

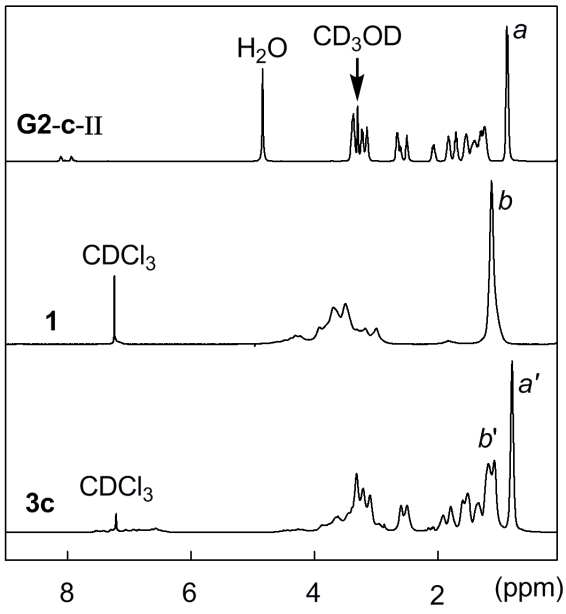

Figure 2. ^{1}H NMR spectra of **G2-c-II**, **1**, and **3c**

Labels: *a*, terminal methyl protons of dendron; *b*, terminal methyl protons of ethyl cellulose; *a′*, terminal methyl protons derived from the dendron; *b′*, terminal methyl protons derived from ethyl cellulose.

were not quite different from those of **1**. For instance, the M_n and M_w/M_n of **1** were

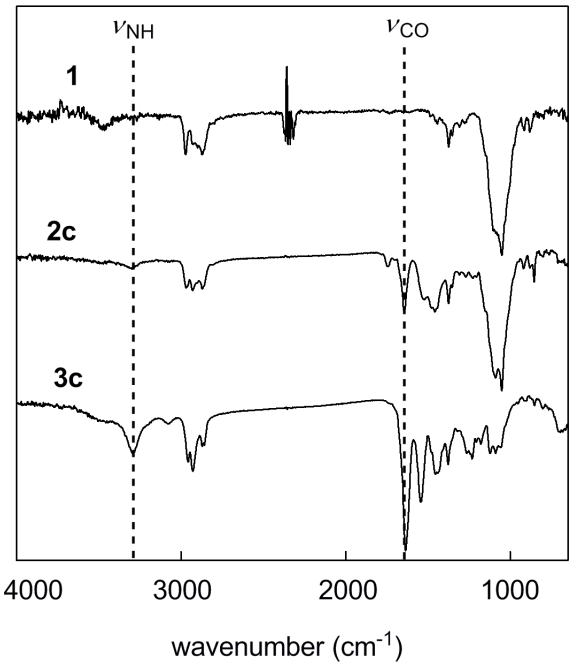

Figure 3. FTIR spectra of **1**, **2c**, and **3c**.

Table 1. Degree of Substitution and Molecular Weight of Polymers 1, 2a–c, and 3a–c

polymer	DS_{total}	M_n [c]	M_w [c]	M_w/M_n [c]
1	2.69[a]	71 000	237 000	3.3
2a	≈ 3.00[b]	222 000	750 000	3.4
2b	≈ 3.00[b]	225 000	677 000	3.0
2c	≈ 3.00[b]	226 000	739 000	3.3
3a	≈ 3.00[b]	–[d]	–[d]	–[d]
3b	≈ 3.00[b]	–[d]	–[d]	–[d]
3c	≈ 3.00[b]	–[d]	–[d]	–[d]

[a] Determined by ^{1}H NMR. [b] Determined by elemental analysis. [c] Determined by GPC (0.01 M LiBr in DMF as eluent). [d] Could not be determined.

observed to be 71 000 and 3.3, respectively, while those of **2a** were 222 000 and 3.4.

These facts rule out the possibility of polymer chain cleavage in the course of esterification. However, observed M_n values were twice those of the theoretical ones for G1-functionalized polymers (**2a**–**c**) which might have resulted either due to the aggregation of dendronized polymers in DMF or relatively nonpolar and quite different morphological nature of the polystyrene standards which have been used to construct the calibration curve employed for the estimation of the molecular weight. With G2-derivatized polymers (**3a**–**c**), very broad GPC elution curves and irreproducibility of the results did not allow the correct molecular weight determination. This might be due to the low solubility (Table 2) and/or anomalous elution, which is known to occur in very large polymers or aggregated systems.[22]

Solubility and Thermal Properties of Polymers. The solubility properties of ethyl cellulose (**1**) and its G1- and G2-functionalized (**2a**–**c** and **3a**–**c**) derivatives are summarized in Table 2. **1** is soluble in polar protic solvents such as methanol and the same tendency was retained after dendronization. The solubility behavior of dendronized polymers in polar aprotic solvents exhibited several variations depending on the polarity of the solvent and the length of the peripheral alkyl groups of dendritic moieties. For instance, **1**, **2a**–**c**, and **3a** were soluble in DMF whereas **3b** and **3c** were almost soluble (can not be described as completely soluble); on the other hand, **1** is soluble in DMSO but all of the dendronized derivatives were insoluble except **2a**

Table 2. Solubility[a] of Polymers 1, 2a–c, and 3a–c

polymer	**1**	**2a**	**2b**	**2c**	**3a**	**3b**	**3c**
methanol	+	+	+	+	+	+	+
DMF	+	+	+	+	+	±	±
DMSO	+	±	–	–	+	–	–
acetone	±	+	+	+	–	–	–
THF	+	+	+	+	–	–	±
$CHCl_3$	+	+	+	+	+	+	+
toluene	+	±	+	+	–	–	–
hexane	–	–	–	–	–	–	–

[a] Symbols: +, soluble; ±, partly soluble; –, insoluble.

(partly soluble) and **3a** (soluble). Ethyl cellulose is partly soluble in acetone and switched to being soluble (**2a**–**c**) when derivatized with first generation amide-containing dendrons and turned insoluble (**3a**–**c**) upon the incorporation of second generation dendritic moieties. **1** and **2a**–**c** were soluble in the moderately polar cyclic ether, THF, while **3a**–**c** were insoluble. The solubility characteristics of **1** in $CHCl_3$ were unchanged upon dendronization, and all of the dendronized derivatives of ethyl cellulose were soluble in $CHCl_3$. The appreciably good solubility of G1-derivatized polymers (**2a**–**c**) in $CHCl_3$ was exploited for membrane fabrication. Furthermore, **1** and **2a**–**c** are soluble (**2a** is almost soluble) in toluene, a less polar solvent, while the higher polarity of **3a**–**c** due to the presence of nine amide linkages renders them insoluble. Thus it can be inferred that the dendronized ethyl cellulose derivatives tend to be soluble in polar protic solvents like methanol, highly polar aprotic solvents like DMF, and moderately polar halogenated solvents like $CHCl_3$. Moreover, the solubility window narrows in going from the G1- to G2-derivatized polymers.

The thermal stability of polymers **1**, **2a**–**c**, and **3a**–**c** was examined by thermogravimetric analysis (TGA) in air (Figure 4). The onset temperatures of weight loss (T_0) of **2a**–**c** and **3a**–**c** were in the ranges of 295–325 ºC and 312–320 ºC, respectively, while that of **1** was 297 ºC (Table 3) thus indicating no decrement in

Table 3. Thermal Properties of Polymers 1, 2a–c, and 3a–c

polymer	T_0[a] (°C)	T_g[b] (°C)
1	297	132
2a	295	69
2b	317	57
2c	325	53
3a	320	52
3b	312	40
3c	313	28

[a] T_0: Onset temperature of weight loss. Determined from TGA measurement in air.

[b] T_g: Glass transition temperature. Determined by DSC analysis under nitrogen.

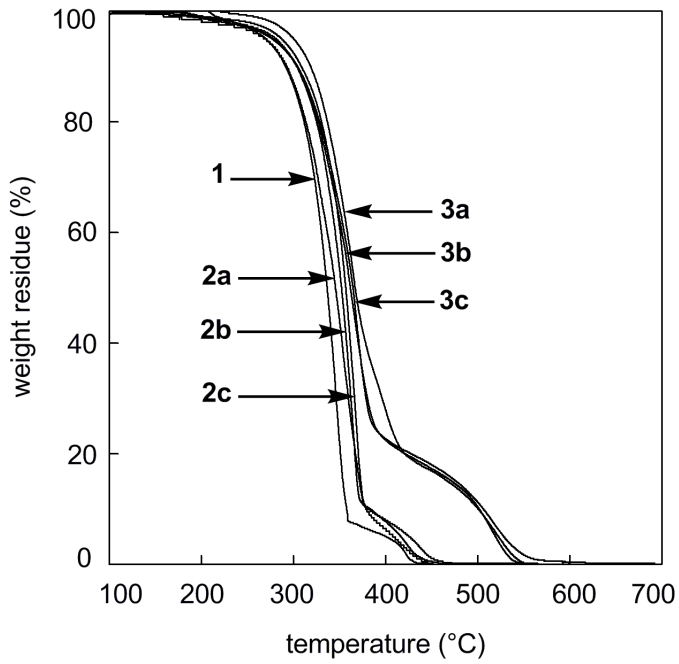

Figure 4. TGA curves of polymers **1**, **2a**–**c**, and **3a**–**c** (in air, heating rate 10 ºC min^{-1}).

thermal stability. The retained thermal stability, despite the substitution of small hydroxy groups by the bulky dendritic moieties, is most likely to arise from the polarity of the dendritic substituents and the conjunctional ester linkage. The incorporated dendritic structures are also capable of hydrogen bond formation as the parent polymeric material (**1**) is; but it is probably the retainment of the individual bond strengths in the polymer structure which is responsible for the retained thermal stability upon dendron functionalization.

The glass transition temperature (T_g) of polymers **1**, **2a**–**c**, and **3a**–**c** were determined by the differential scanning calorimetric (DSC) analysis under nitrogen (Figure 5). It was observed that the glass transition temperature (T_g) of **1** (132 ºC) underwent a significant decrease as a result of the substitution by dendritic appendages; for instance, the T_g of **2a**–**c** and **3a**–**c** were 53–69 ºC and 28–52 ºC, respectively (Table 3). The variation in the glass transition temperature of the dendritic macromolecules is dramatically affected by the nature of chain ends and the

increased polarity of the peripheral groups (convergent pathway) entails enhanced T_g values and vice versa.[23] The amide-containing dendritic moieties have fairly bulky nonpolar peripheral alkyl groups which are responsible for such a significant decrease in the glass transition temperature when incorporated into the ethyl cellulose.

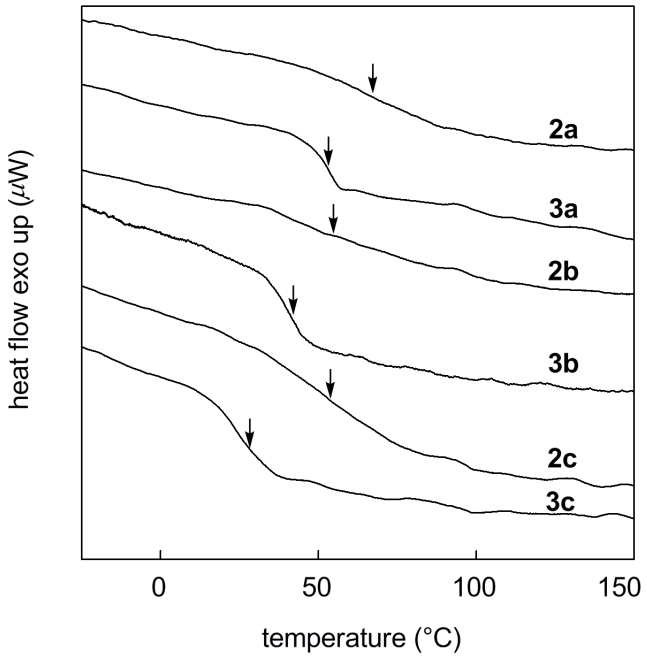

Figure 5. DSC thermograms of polymers **1**, **2a**–**c**, and **3a**–**c** (under N_2, second scan).

Furthermore, the T_g of dendron-functionalized ethyl cellulosics underwent a decrement in going from the G1- to G2-derivatized ones perhaps due to the increment in the number of the peripheral alkyl groups.

Density and FFV of Polymer Membranes. An appreciably good solubility of the G1-functionalized polymers (**2a**–**c**) in $CHCl_3$ rendered the fabrication of free-standing membranes attainable. The van der Waals volume (υ_w), density (ρ), and fractional free volume (FFV) of the polymer membranes (**1** and **2a**–**c**) are summarized in Table 4. All of the dendronized derivatives (**2a**–**c**) exhibited higher values of membrane density than that of ethyl cellulose (**1**); thus, the ρ value of **1** was observed to be 1.099 while those of **2a**–**c** were in the range of 1.104–1.133. The increased density can be ascribed to the increased mass of the substituents and enhanced

interactions inside the polymer matrix due to the presence of polar amide linkages. These findings are quite reasonable as polymers bearing polar functionalities generally possess higher densities than those of the corresponding hydrocarbon polymers.[24] It is worth mentioning that the incorporation of dendritic moieties led to the reduction in the FFV of the polymer membranes (**1**, 0.182; **2a**–**c**, 0.148–0.159). For instance, **2a** was observed to possess the lowest fractional free volume (FFV is 0.148), which

Table 4. Physical Properties of Polymers 1 and 2a–c

polymer	v_w[a] (cm^3/mol)	ρ[b] (g/cm^3)	FFV[c]
1	135.8	1.099	0.182
2a	210.6	1.133	0.148
2b	223.3	1.104	0.159
2c	223.3	1.105	0.159

[a] v_w: van der Waals volume. [b] ρ: density. Determined by hydrostatic weighing. [c] FFV: fractional free volume. Estimated from membrane density.

indicates the reduction in the size of free volume cavities due to the introduction of polar dendritic substituents. However, it is a general trend that the presence of the polar substituents favors the intersegmental packing as has been reported in amino- and hydroxy-functionalized polymers.[24,25] Hence, the polarity of the dendron appendages, inducing the favorable interactions inside the polymer network, contributes to enhance the intersegmental packing which might have led to the decrease in the size of free volume elements in the polymer matrix. As another possible explanation, it can be assumed that the introduction of dendritic substituents with bulky alkyl periphery into ethyl cellulose has resulted in the more flexible polymeric structures (as indicated by the lowering of T_g) which often pack more tightly in the non-crystalline regions than their semi-rigid parent polymers with longer persistence length, thus exhibiting reduction in the fractional free volume.

Gas Permeation Properties. The permeability coefficients of the membranes of **1** and **2a**–**c** to various gases measured at 25 °C are listed in Table 5. The gas permeability coefficients (*P*) of the dendronized polymers were lower than

that of **1**, and approximately obey the following order: **1** > **2b** > **2a** ≈ **2c**. Although the *P* values of the dendron-functionalized polymers show a little disparity from each other, the general order of the gas permeability coefficients seems to be determined by the shape, size, chemical nature, and mobility of the dendritic substituents.

Table 5. Gas Permeability Coefficients (*P*) of Polymer Membranes at 25 °C

polymer	*P* (barrer)[a]						P_{He}/P_{N_2}	P_{H_2}/P_{N_2}	P_{CO_2}/P_{N_2}	P_{CO_2}/P_{CH_4}
	He	H_2	O_2	N_2	CO_2	CH_4				
1	47	68	15	4.5	91	9.2	10.4	15.1	20.2	9.9
2a	26	33	5.2	1.2	27	2.4	21.7	27.5	22.5	11
2b	28	37	7.0	1.7	38	3.8	16.5	21.8	22.2	10
2c	27	31	5.6	1.3	29	2.8	20.8	23.8	22.3	10

[a] 1 barrer = $1x10^{-10}$ cm^3 (STP) cm cm^{-2} s^{-1} $cmHg^{-1}$.

The present study reveals the effect of the incorporation of amide-containing dendritic appendages on the gas permeation characteristics of ethyl cellulose. There have been no systematic reports concerning the dendron functionalization of ethyl cellulose and outcomes of this successful conjunction as a membrane-forming material, till today. It has been discerned that the substitution of small hydroxy groups of ethyl cellulose with bulky and polar dendritic substituents resulted in the decreased permeability coefficients for all the gases. For instance, the P_{O_2} and P_{N_2} of **1** are 15 and 4.5 barrers and those observed for **2a**–**c** were 5.2–7.0 and 1.2–1.7 barrers, respectively. The gas permeability did not vary significantly with the change in the dendritic substituents as they possess great similarity in the composition and shape; however subtle variations in the gas permeability emanating from the slight structural modification did not go unnoticed. For instance, the carbon dioxide permeability coefficients (P_{CO_2}) for **2a**–**c** were 27, 38, and 29 barrers, respectively, where **2b** displayed the highest CO_2 permeability; and similar tendencies were observed for other gases in the present study. The *P* values for **2b** were higher than those for **2a** which stem probably from the relatively bulky alkyl periphery slightly overruling the effect of the polarity of amide linkages. In the case of **2c** the number of carbon atoms

is the same as that for **2b** but the shape/size might have played its role as the branching of alkyl groups at the peripheral amide linkages does not exhibit the same uniformity as that in **2b**. These results are quite in compliance with the previous ones describing the effect of the shape and the length of the alkyl groups, present in the side chains, on the gas permeability of polymeric membranes.[21,26] These trends in the gas permeability of dendronized polymers can reasonably be attributed to the presence of polar (amide and ester) groups resulting in a denser chain packing, leading to the reduced free volume space inside the polymer matrix, and in turn lower gas permeability; moreover, the bulk of the dendritic substituents might have influenced in the same way due to the hindered local mobility.

The most worth mentioning of the gas permeation characteristics of ethyl cellulose (**1**) and its dendronized derivatives (**2a**–**c**) is the increased permselectivity for various gas pairs (Table 5). The P_{CO_2}/P_{N_2} selectivity of ethyl cellulose (**1**) is 20.2 which increased upto 22.5 (**2a**) after the substitution of dendron appendages. Similarly, the P_{He}/P_{N_2}, P_{H_2}/P_{N_2}, P_{CO_2}/P_{CH_4} selectivity values of **1** (10.4, 15.1, and 9.9, respectively) experienced an increase upon derivatization and **2a** displayed the highest permselectivity (21.7, 27.5, and 11) for the corresponding gas pairs. The decrease in the gas permeability with a concomitant increase in the permselectivity for various gas pairs is in accordance with the well known '*tradeoff*' relation.[27] Furthermore, the decrease in gas permeability became more pronounced as the molecular size of the penetrant gases increased as is evident from the augmented selectivity of small gases such as He and H_2 over N_2 with larger kinetic diameter. These findings are consistent with the previous results that the structural alterations, which enhance chain packing and simultaneously hinder the segmental motion in the polymer matrix, tend to decrease permeability while increasing permselectivity.[24] The permselectivity enhancement in the present series of polymers might not appear quite significant at first glance; however, these results should be dealt with great care keeping in mind the two plausible reasons: (i) the dendronization across the polymer chain could not be effected at each monomer unit as there was one hydroxy group available for

derivatization per three anhydroglucose units, (ii) the polar amide and ester groups are not peripheral (due to the presence of bulky alkyl moieties) and might not be exposed enough to get involved in effective interactions with CO_2 molecules. The present results imply the sensitivity of the gas transport properties of membrane-forming materials towards the modification of subtle structural features such as interchain spacing and segmental mobility.

Gas Diffusivity and Solubility. Gas permeability (*P*), which is the steady-state, pressure- and thickness-normalized gas flux through a membrane, can be expressed as the product of gas solubility (*S*) in the upstream face of the membrane and effective average gas diffusion (*D*) through the membrane, strictly in rubbery and approximately in glassy polymers:[28]

$$P = S \times D$$

A detailed investigation of the gas permeation characteristics was carried out by determining the gas diffusion coefficients (*D*) and gas solubility coefficients (*S*) of the polymers. The plots of *D* and *S* values of polymers **1** and **2a**–**c** for CO_2 and CH_4 are illustrated in Figures 6 and 7, respectively. A distinct lowering of the gas permeability of ethyl cellulose as a consequence of the incorporation of fairly bulky and polar dendritic moieties has been revealed to stem from the subsidence of both the gas diffusion and gas solubility coefficients.

The *D* values of all the gases were observed to follow a decline upon dendronization (**2a**–**c**); for instance, **1** displayed the D_{O_2} value of 9.1, and those of **2a**–**c** were in the range of 4.8–5.9, in the units of 10^7 cm^2 s^{-1}. The gas diffusion coefficients, delineated as a complex interplay between fractional free volume and local/torsional mobility, tend to decrease if accompanied by a loss in either of these factors. The decrement in the gas diffusion coefficients finds its explanation in the reduced FFV and hindered segmental mobility of the dendronized ethyl cellulose derivatives.[24–26]

On the other hand, the dendron functionalization of ethyl cellulose

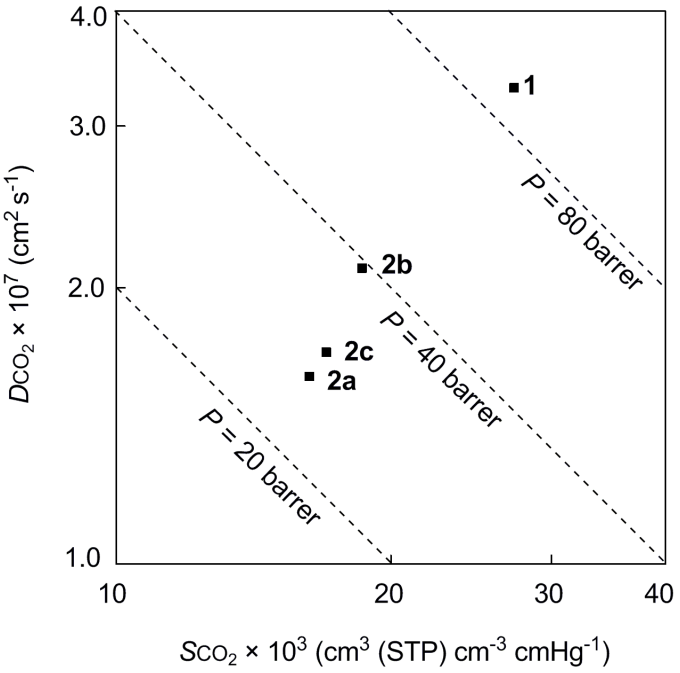

Figure 6. Plot of SCO_2 vs DCO_2 of ethyl cellulose (**1**) and its dendronized derivatives (**2a**–**c**).

accompanied a decrease in the gas solubility coefficients as well; *e.g.*, the S_{CO_2} of **1** and **2a**–**c** were 27.3 and 16.3–18.6 while the S_{N_2} values being 1.1 and 0.5–0.6, respectively, in the units of 10^3 cm^3 (STP) cm^{-3} $cmHg^{-1}$. The reduction in the *S* values can be accounted for by the attenuated fractional free volume of the dendronized polymers (**2a**–**c**), as summarized in Table 4.

In the glassy polymeric membranes, generally the *D* value undergoes a decrease with increasing critical volume of gases, whereas the *S* value experiences an increase with increasing critical temperature of gases.[28a] Similar tendencies were observed in the *D* and *S* values of the polymer membranes of **1** and its dendronized derivatives; *e.g.*, in the case of **2a**, the diffusivity of CH_4 was the lowest and that of O_2 was the highest (1.0 and 4.8 10^7 cm^2 s^{-1}, respectively) while CO_2 displayed the highest solubility and N_2 the lowest (16.3 and 0.5 10^3 cm^3 (STP) cm^{-3} $cmHg^{-1}$, respectively). The diffusion coefficients of this new family of dendron-functionalized cellulosics

(**2a**–**c**) were in the order $DO_2 > DN_2 > DCO_2 > DCH_4$, the same as for the starting polymer, ethyl cellulose. Similarly, the *S* values of **1** and **2a**–**c** were observed to follow the same trend ($SCO_2 > SCH_4 > SO_2 > SN_2$).

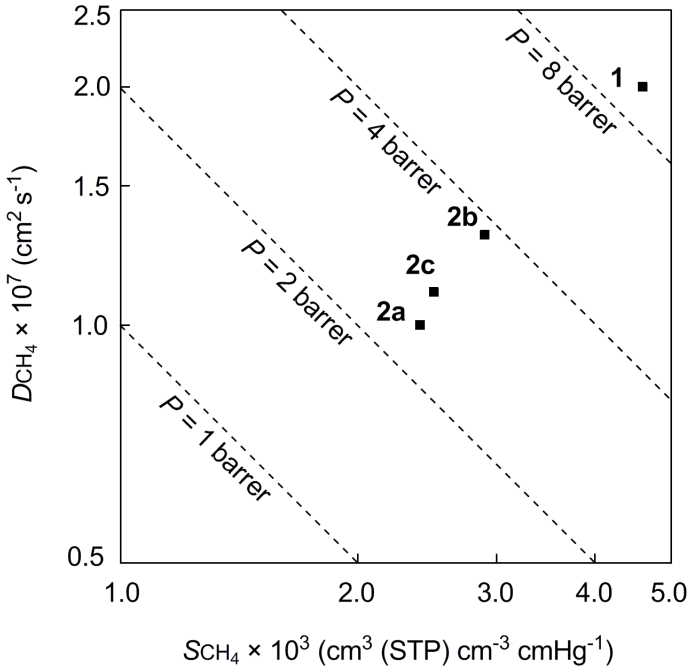

Figure 7. Plot of SCH_4 vs DCH_4 of ethyl cellulose (**1**) and its dendronized derivatives (**2a**–**c**).

It has already been mentioned that the dendronized polymers displayed better separation performance for various gas pairs, and as far as the CO_2/N_2 separation is concerned the increase in solubility selectivity is responsible for the enhanced PCO_2/PN_2 selectivity. Despite the DCO_2/DN_2 of **1** being almost unaffected by the dendron incorporation, the SCO_2/SN_2 experienced an augmentation probably due to the interaction of quadrupolar CO_2 molecules with the polar dendron appendages.

Conclusions

The present study is concerned with the synthesis of a series of first and second generation novel amide-containing dendrons (**G1-a-II**–**G1-c-II** and **G2-a-II**–**G2-c-II**) and describes an approach to design new dendritic macromolecules

based on ethyl cellulose. The complete substitution of the residual hydroxy protons of ethyl cellulose (**1**; DS_{Et}, 2.69) by the dendritic moieties has been demonstrated by ^{1}H NMR and is evidenced by the elemental analysis. The G1-derivatized polymers (**2a**–**c**) displayed better organosolubility than that of G2-derivatized ones (**3a**–**c**), however, all of the dendron-functionalized polymers were soluble in chloroform and methanol. The dendronization of ethyl cellulose accompanied the retention of thermal stability and the lowering of glass transition temperature. G1-appended polymers (**2a**–**c**) afforded free-standing membranes, exhibiting decrement in density and FFV, hence low gas permeability as compared to **1**. The decrease in the gas permeability was investigated to arise from the attenuation in the gas diffusion and solubility coefficients, presumably ensuing from the decreased FFV and hindered local mobility in the polymer matrix. The improved separation performance was discerned for He/N_2, H_2/N_2, CO_2/N_2 and CO_2/CH_4 gas pairs.

References and Notes

1. (a) Boas, U.; Christensen, J. B.; Heegaard, P. M. H. *Dendrimers in Medicine and Biotechnology: New Molecular Tools*; Royal Society of Chemistry: Cambridge, 2006. (b) Lee, C. C.; MacKay, J. A.; Fréchet, J. M. J. Szoka, F. C. *Nat. Biotech.* **2005**, *23*, 1517–1526. (c) Tomalia, D. A.; Fréchet, J. M. J. *Prog. Polym. Sci.* **2005**, *30*, 217–219. (d) Tomalia, D. A. *Prog. Polym. Sci.* **2005**, *30*, 294–324. (e) Liang, C.; Fréchet, J. M. J. *Prog. Polym. Sci.* **2005**, *30*, 385–402. (f) Jiang, D.-L.; Aida, T. *Prog. Polym. Sci.* **2005**, *30*, 403–422. (g) Fréchet, J. M. J. *Macromol. Symp.* **2003**, *201*, 11–22. (h) Newkome, G. R.; Moorefield, C. N.; Vögtle, F. *Dendrimers*, 2nd ed.; Wiley: Chichester, 2001. (i) Gestermann, S.; Hesse, R.; Windisch, B.; Vögtle, F. In *Stimulating Concepts in Chemistry*; Vögtle, F., Stoddart, J. F., Shibasaki, M. Eds.; Wiley-VCH: Weinheim, 2000; pp 187–198. (j) Archut, A.; Vögtle, F. In *Handbook of Nanostructured Materials and Nanotechnology*; Nalwa, H. S. Eds.; Academic Press: San Diego, 2000; pp 333–374. (k) Janssen, H. M.; Meijer, E. W. In *Materials Science and Technology*; Schlüter, A. D. Eds.; Wiley-VCH: Weinheim, 1999; pp 403–458. (l) Tomalia, D. A.; Esfand, R. *Chem. & Ind.* **1997**, 416–420.
2. (a) Percec, V. *Philos. Trans. Series A: Math. Phys. Eng. Sci.* **2006**, *364*,

2709–2719. (b) Schenning, A. P. H. J.; Meijer, E. W. *Chem. Commun.* **2005**, 3245–3258. (c) Tomalia, D. A. *Aldrichimica Acta* **2004**, *37*, 39–57. (d) Stiriba, S.-E.; Frey, H.; Haag, R. *Angew. Chem. Int. ed.* **2002**, *41*, 1329–1334. (e) Tomalia, D. A.; Fréchet, J. M. J. *J. Polym. Sci., Part A: Polym. Chem.* **2002**, *40*, 2719–2728. (f) Tully, D. C.; Fréchet, J. M. J. *Chem. Commun.* **2001**, 1229–1239. (g) Grayson, S. M.; Fréchet, J. M. J. *Chem. Rev.* **2001**, *101*, 3819–3867. (h) Andronov, A.; Fréchet, J. M. J. *Chem. Commun.* **2000**, 1701–1710. (i) Vögtle, F.; Gestermann, S.; Hesse, R.; Schwiers, H.; Windisch, B. *Prog. Polym. Sci.* **2000**, *25*, 987–1041. (j) Frey, H.; Schlenk, C. *Top. Curr. Chem.* **2000**, *210*, 69–129. (k) Fischer, M.; Vögtle, F. *Angew. Chem. Int. ed.* **1999**, *38*, 885–905. (l) Bosman, A. W.; Janssen, H. M.; Meijer, E. W. *Chem. Rev.* **1999**, *99*, 1665–1688. (m) Frey, H.; Lach, C.; Lorenz, K. *Adv. Mat.* **1998**, *10*, 279–293. (n) Archut, A.; Vögtle, F. *Chem. Soc. Rev.* **1998**, *27*, 233–240. (o) Narayanan, V. V.; Newkome, G. R. *Top. Curr. Chem.* **1998**, *197*, 19–77. (p) Newkome, G. R. *Pure and Appl. Chem.* **1998**, *70*, 2337–2343.

3. (a) Tomalia, D. A.; Kirchhoff, P. M. US Patent 4694064, 1987. (b) Yin, R.; Zhu, Y.; Tomalia, D. A.; Ibuki, H. *J. Am. Chem. Soc.* **1998**, *120*, 2678–2679.
4. (a) Percec, V.; Heck, J.; Tomazos, D.; Falkenberg, F.; Blackwell, H.; Ungar, G. *J. Chem. Soc. Perkin Trans.* **1993**, 2799–2811. (b) Percec, V.; Lee, M.; Heck, J.; Blackwell, H.; Ungar, G. Alveraz-Castillo, A. *J. Mater. Chem.* **1992**, *2*, 931–938. (c) Percec, V.; Heck, J.; Lee, M.; Ungar, G. Alveraz-Castillo, A. *J. Mater. Chem.* **1992**, *2*, 1033–1039. (d) Hawker, C. J.; Fréchet, J. M. J. *Polymer* **1992**, *33*, 1507–1511. (e) Percec, V.; Heck, J.; Ungar, G. *Macromolecules* **1991**, *24*, 4957–4962.
5. Freudenberger, R.; Claussen, W.; Schlüter, A. D.; Wallmeier, H. *Polymer* **1994**, *35*, 4496–4501.
6. (a) Rajaram, S.; Choi, T.-L.; Rolandi, M.; Fréchet, J. M. J. *J. Am. Chem. Soc.* **2007**, *129*, 9619–9621. (b) Frampton, M. J.; Anderson, H. L. *Angew. Chem. Int. ed.* **2007**, *46*, 1028–1064. (c) Canilho, N.; Kaseemi, E.; Mezzenga, R.; Schlüter, A. D. *J. Am. Chem. Soc.* **2006**, *128*, 13998–13999. (d) Leung, K. C.-F.; Mendes, P. M.; Magonov, S. N.; Northrop, B. H.; Kim, S.; Patel, K.; Flood, A. H.; Tseng, H.-R.; Stoddart, J. F. *J. Am. Chem. Soc.* **2006**, *128*, 10707–10715. (e) Park, C.; Choi, K. S.; Song, Y.; Jeon, H.-J.; Song, H. H.; Chang, J. Y.; Kim, C. *Langmuir* **2006**, *22*, 3812–3817. (f) Lee, C. C.; Fréchet, J. M. J. *Macromolecules* **2006**, *39*, 476–481. (g) Nyström, A.; Malkoch, M. Furó, I.; Nyström, D.; Unal, K.; Antoni, P.; Vamvounis, G.; Hawker, C. J.; Wooley, K. L.; Malmström, E.; Hult, A. *Macromolecules* **2006**, *39*, 7241–7249. (h) Schlüter, A. D. *Top. Curr. Chem.* **2005**, *245*, 151–191. (i) Frauenrath, H. *Prog. Polym. Sci.* **2005**, *30*, 325–384. (j) Zhang, A.; Okrasa, L.; Pakula, T.; Schlüter, A. D. *J. Am. Chem. Soc.* **2004**, *126*,

6658–6666. (k) Schlüter, A. D.; Rabe, J. P. *Angew. Chem. Int. ed.* **2000**, *39*, 864–883. (l) Frey, H. *Angew. Chem. Int. ed.* **1998**, *37*, 2193–2197. (m) Schlüter, A. D. *Top. Curr. Chem.* **1998**, *197*, 165–191.

7. (a) Kabir, A.; Hamlet, C.; Yoo, K.-S.; Newkome, G. R.; Malik, A. *J. Chromatogr. A.* **2004**, *1034*, 1–11. (b) Wu, X. Z.; Liu, P.; Pu, Q. S.; Sun, Q. Y.; Su, X. Z. *Talanta* **2004**, *62*, 918–923. (c) Newkome, G. R.; Yoo, K.-S.; Moorefield, C. N. *Des. Monom. Polym.* **2002**, *5*, 67–77. (d) Newkome, G. R.; Yoo, K.-S.; Kabir, A.; Malik, A. *Tetrahedron Lett.* **2001**, *42*, 7537–7541. (e) Kijak, A. M.; Moller, J. C.; Cox, J. A. *J. Sol-Gel Sci. Technol.* **2001**, *21*, 213–219. (f) Tsubokawa, N.; Ichioka, H.; Satoh, T.; Hayashi, S.; Fujiki, K. *React. Funct. Polym.* **1998**, *37*, 75–82.
8. Strumia, M. C.; Halabi, A.; Pucci. P. A.; Newkome, G. R.; Moorefield, C. N.; Epperson, J. D. *J. Polym. Sci., Part A: Polym. Chem.* **2000**, *38*, 2779–2786.
9. Gao, T.; Tillman, E. S.; Lewis, N. S. *Chem. Mater.* **2005**, *17*, 2904–2911.
10. (a) Sashiwa, H.; Shigemasa, Y.; Roy, R. *Carbohydr. Polym.* **2002**, *47*, 191–199. (b) Tsubokawa, N.; Takayama, T. *React. Funct. Polym.* **2000**, *43*, 341–350.
11. Goessl, I.; Shu, L.; Schlüter, A. D. Rabe, J. P. *J. Am. Chem. Soc.* **2002**, *124*, 6860–6865.
12. (a) Zhang, C.; Price, L. M.; Daly, W. H. *Biomacromolecules* **2006**, *7*, 139–145. (b) Hassan, M. L.; Moorefield, C. N.; Kotta, K. K.; Newkome, G. R. *Polymer* **2005**, *46*, 8947–8955.
13. (a) Klemm, D.; Heublein, B.; Fink, H.-P.; Bohn, A. *Angew. Chem. Int. ed.* **2005**, *44*, 3358–3393. (b) Crowley, M. M.; Schroeder, B.; Fredersdorf, A.; Obara, S.; Talarico, M.; Kucera, S.; McGinity, J. W. *Int. J. Pharm.* **2004**, *269*, 509–522. (c) Li, X.-G.; Kresse, I.; Xu, Z.-K.; Springer, J. *Polymer* **2001**, *42*, 6801–6810. (d) Barton, D. H. R.; Nakanishi, K.; Meth-Cohn, O. *Comprehensive Natural Products Chemistry*; Elsevier Science: Oxford, 1999; Vol. 3. (e) Klemm, D.; Philipp, B.; Heinze, T.; Heinze, U.; Wagenknecht, W. *Comprehensive Cellulose Chemistry*; Wiley-VCH: Weinheim, 1998; Vol. 1, 2.
14. Bondar, V. I.; Freeman, B. D.; Pinnau, I. *J. Polym. Sci., Part B: Polym. Phys.* **2000**, *38*, 2051–2062.
15. Lin, H.; Freeman, B. D. *J. Membr. Sci.* **2004**, *239*, 105–117.
16. (a) Pixton, M. R.; Paul, D. R. In *Polymeric Gas Separation Membranes*; Paul, D. R., Yampol'skii, Y. P., Eds.; CRC Press: Boca Raton, FL, 1994; pp 83–153. (b) Lee, W. M. *Polym. Eng. Sci.* **1980**, *20*, 65–69. (c) Bondi, A. *Physical Properties of Molecular Crystals, Liquids, and Glasses*; John Wiley and Sons: New York, 1968; pp 25–97.

17. van Krevelen, D. W. *Properties of Polymers: Their Correlation with Chemical Structure; Their Numerical Estimation and Prediction from Additive Group Contributions*, 3rd ed.; Elsevier Science: Amsterdam, 1990; pp 71–107.
18. Masuda, T.; Iguchi, Y.; Tang, B.-Z.; Higashimura, T. *Polymer* **1988**, *29*, 2041–2049.
19. Hawker, C. J.; Fréchet, J. M. J. *J. Am. Chem. Soc.* **1990**, *112*, 7638–7647.
20. (a) Kim, C.; Kim, K. T.; Chang, Y.; Song, H. H.; Cho, T.-Y.; Jeon, H.-J. *J. Am. Chem. Soc.* **2001**, *123*, 5586–5587. (b) Rannard, S. P.; Davis, N. J. *Org. Lett.* **2000**, *2*, 2117–2120. (c) Rannard, S. P.; Davis, N. J. *Org. Lett.* **1999**, *1*, 933–936. (d) Rannard, S. P.; Davis, N. J. *Polym. Mater. Sci. Eng.* **1997**, *77*, 160–161. (e) Llinares, M.; Roy, R. *Chem. Commun.* **1997**, 2119–2120.
21. (a) Khan, F. Z.; Sakaguchi, T.; Shiotsuki, M.; Nishio, Y.; Masuda, T. *Macromolecules* **2006**, *39*, 9208–9214. (b) Khan, F. Z.; Sakaguchi, T.; Shiotsuki, M.; Nishio, Y.; Masuda, T. *Macromolecules* **2006**, *39*, 6025–6030.
22. (a) Zhang, A.; Zhang, B.; Wächtersbach, E.; Schmidt, M.; Schlüter, A. D. *Chem. Eur. J.* **2003**, *9*, 6083–6092. (b) Gerle, M.; Fischer, K.; Müller, A. H. E.; Schmidt, M.; Sheiko, S. S.; Prokhorova, S.; Möller, M. *Macromolecules* **1999**, *32*, 2629–2637.
23. (a) Wooley, K. L.; Hawker, C. J.; Pochan, J. M.; Fréchet, J. M. J. *Macromolecules* **1993**, *26*, 1514–1519. (b) Hawker, C. J.; Fréchet, J. M. J. *J. Chem. Soc. Perkin Trans. 1* **1992**, 2459–2469.
24. (a) Senthilkumar, U.; Reddy, B. S. R. *J. Membr. Sci.* **2007**, *292*, 72–79. (b) Ghosal, K.; Chern, R. T.; Freeman, B. D.; Daly, W. H. Negulescu, I. I. *Macromolecules* **1996**, *29*, 4360–4369.
25. (a) Kono, T.; Sakaguchi, T.; Hu, Y.; Shiotsuki, M.; Sanda, F.; Masuda, T. *J. Polym. Sci., Part A: Polym. Chem.* **2006**, *44*, 5943–5953. (b) Shida, Y.; Sakaguchi, T.; Shiotsuki, M.; Sanda, F.; Freeman, B. D.; Masuda, T. *Macromolecules* **2005**, *38*, 4096–4102. (c) Lin, H.; Freeman, B. D. *J. Mol. Struct.* **2005**, *739*, 57–74. (d) Simril, V. L.; Hershberger, A. *Mod. Plast.* **1950**, *27*, 95–102.
26. (a) Kanaya, T.; Tsukushi, I.; Kaji, K.; Sakaguchi, T.; Kwak, G.; Masuda, T. *Macromolecules* **2002**, *35*, 5559–5564. (b) Kanaya, T.; Tsukushi, I.; Kaji, K.; Teraguchi, M.; Kwak, G.; Masuda, T. *J. Phys. Soc., Suppl. A* **2000**, *70*, 332–334. (c) Kanaya, T.; Teraguchi, M.; Masuda, T.; Kaji, K. *Polymer* **1999**, *40*, 7157–7161.
27. (a) Freeman, B. D. *Macromolecules* **1999**, *32*, 375–380. (b) Koros, W. J.; Fleming, G. K. *J. Membr. Sci.* **1993**, *83*, 1–80. (c) Robeson, L. M. *J. Membr. Sci.* **1991**, *62*, 165–185.

28. (a) Yampolskii, Yu.; Pinnau, I.; Freeman, B. D. *Materials Science of Membranes for Gas and Vapor Separation*; Wiley: Chichester, 2006. (b) Pinnau, I.; Freeman, B. D. *Advanced Materials for Membrane Separations*; ACS Symposium Series 876; American Chemical Society: Washington, DC, 2004. (c) Baker, R. W. *Membrane Technology and Applications*, 2nd ed.; Wiley: New York, 2004. (d) Graham, T. *Philos. Mag.* **1866**, *32*, 401–420.
29. Ghosal, K.; Freeman, B. D. *Polym. Adv. Technol.* **1994**, *5*, 673–697.

Chapter 4

Synthesis, Characterization, and Gas Permeation Properties of *t*-Butylcarbamates of Cellulose Derivatives

Abstract

t-Butylcarbamates of ethyl cellulose (**1**; DS_{Et}, 2.69 and **2**; DS_{Et}, 2.50) and cellulose acetate (**3**; DS_{Ac}, 2.46 and **4**; DS_{Ac}, 1.80) were synthesized by the reaction of residual hydroxy groups of cellulose derivatives with *t*-butylisocyanate. The ^{1}H NMR spectra and elemental analysis were employed to determine the degree of incorporation of carbamoyl moiety (DS_{Carb}) and almost complete substitution of the residual hydroxy protons was observed. The presence of the peaks characteristic of the carbamate linkage in the FTIR spectra furnished further evidence for the successful carbamoylation of ethyl cellulose and cellulose acetate. The resulting polymers (**1a**–**4a**) were soluble in common organic solvents. The onset temperatures of weight loss of **1a**–**4a** were 177–204 °C, indicating fair thermal stability. The free-standing membranes of **1**–**4** and **1a**–**4a** were fabricated, and derivatized polymers exhibited enhanced gas permeability, especially the gas permeability of cellulose acetate (**3**; DS_{Ac}, 2.46 and **4**; DS_{Ac}, 1.80) underwent a significant increment. **4a** exhibited a remarkable increase in CO_2 permeability, *i.e.*, 22 times higher than that of **4** (P_{CO_2} 38 barrers; cf. P_{CO_2} of **4**, 1.7 barrers). Quite interestingly, a more or less retainment of CO_2/N_2 permselectivity was revealed.

Introduction

Polymeric gas separation membranes, owing to the lower energy requirements, smaller footprints, and more chemical robustness than the conventional separation methodologies, have engrossed substantial prominence contributing to the sustainable chemical processing in the past two decades and are being exploited in a wide array of commercial applications.[1] At present, a variety of gas mixtures of industrial interest are being separated by the selective permeation of the components through non-porous membranes made of glassy polymers such as polyacetylenes, polyimides, and polysulfones.[2]

Ethyl cellulose and cellulose acetate are organosoluble derivatives of cellulose, an inexhaustible natural polymeric material, and along with the many inherited fascinating features of extensive linearity, chain stiffness, excellent durability, chemical resistance, mechanical strength, non-toxicity, and low cost, these cellulose derivatives enjoy remarkably good solubility in organic solvents, thus adequate membrane-forming ability and moderate gas permeation/pervaporation capability.[3]

There have been several reports concerning the gas permeation characteristics of ethyl cellulose and cellulose acetate,[4] and carbon dioxide selectivity of these materials is quite high, for instance, the CO_2/N_2 and CO_2/CH_4 selectivity of cellulose acetate is known to be higher than 38 and 30, respectively. The presence of the residual hydroxy groups in ethyl cellulose and cellulose acetate renders these polymeric materials capable of being engineered for desired applications. Moreover, the chemical derivatization is an apt way to tailor the gas permeation characteristics of these membrane-forming materials and carbamate formation serves as an attractive pathway due to the facile synthesis, fair chemical stability and good solubility of the resulting polymers. The past few decades have witnessed an extensive investigation concerning the synthesis and characterization of various carbamate derivatives of cellulose which on account of their solubility in organic solvents find a variety of applications as in the molecular weight determination of cellulose, lyotropic liquid-crystal formation,[5] and chiral stationary phases for enantiomer separation.[6]

Since, no significant research activity is known to be carried out regarding the carbamate synthesis of ethyl cellulose or cellulose acetate, it would be interesting to synthesize these novel polymeric materials and to reveal the effect of the carbamate linkage on the gas permeability and permselectivity of these cellulose derivatives.

This chapter describes the synthesis and characterization of *t*-butylcarbamates of ethyl cellulose (**1a** and **2a**) and cellulose acetate (**3a** and **4a**) (Scheme 1). The solubility characteristics and thermal properties of the derivatized polymers were elucidated. Free-standing membranes of the starting as well as resulting polymers (**1**–**4** and **1a**–**4a**) were fabricated and their gas permeation parameters were determined. Moreover, the diffusion and solubility coefficients of polymer membranes for O_2, N_2, CO_2, and CH_4 were also revealed.

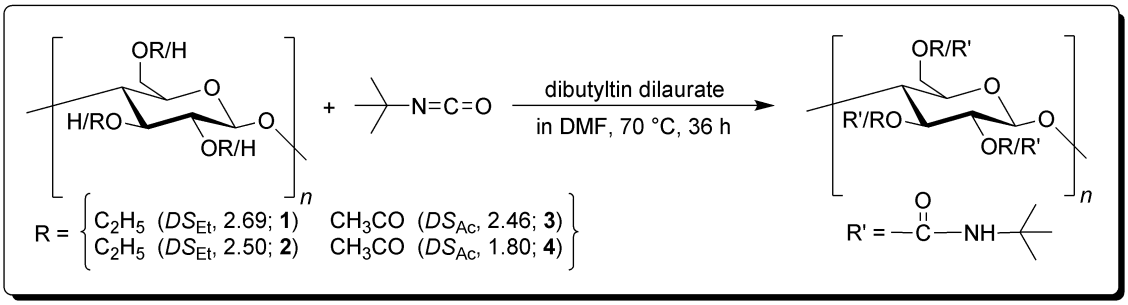

Scheme 1. Synthesis of *t*-Butylcarbamates of Cellulose Derivatives.

Experimental Section

Measurements. ^{1}H NMR spectra were recorded on a JEOL EX-400 spectrometer and the residual proton signal of the deutrated solvent ($CDCl_3$) was used as internal standard. The samples for the NMR measurements were prepared at a concentration of approximately 10 mg/mL and chemical shifts are reported in parts per million (ppm). All of the spectra were recorded for 192 scans with a pulse delay of 37 s in order to obtain reliable integrations. Infrared spectra were recorded on a Jasco FTIR-4100 spectrophotometer and 200 spectra were accumulated at a resolution of 4 cm^{-1}, for each measurement. The elemental analyses were conducted at the Microanalytical Center of Kyoto University. The number- and weight-average

molecular weights (M_n and M_w, respectively) and polydispersity indices (M_w/M_n) of polymers were determined by gel permeation chromatography (GPC) on a JASCO Gulliver system (PU-980, CO-965, RI-930, and UV-1570), except for 4 and 4a; all the measurements were carried out at 40 ºC using polystyrene gel columns (Shodex columns KF-805L × 3), and tetrahydrofuran (THF) as an eluent at a flow rate of 1.0 mL/min. For 4 and 4a, the molecular weight determination was carried out on a JASCO Gulliver system (PU-980, CO-965, RI-930, and UV-2075) at 40 ºC using two TSK-Gel columns (α-M and GMH_{XL}) in series and LiBr solution (10 mM) in *N*,*N*-dimethylformamide as an eluent at a flow rate of 1.0 mL/min. The elution times were converted into molecular weights using a calibration curve based on polystyrene standards (molecular weight range up to 4×10^6 for the system using THF and up to 4×10^8 for that using LiBr in DMF) in combination with the information obtained from the refractive index detector. Thermogravimetric analyses (TGA) were conducted in air with a Shimadzu TGA–50 thermal analyzer by heating the samples (3–5 mg) from 100–700 ºC at a scanning rate of 10 ºC min^{-1}. Differential scanning calorimetric (DSC) analyses were performed using a Seiko DSC6200/EXSTAR6000 apparatus and measurements were carried out by making use of 3–5 mg samples, under a nitrogen atmosphere, after calibration with an indium standard. The samples were first heated from ambient temperature (25 ºC) to +250 °C at a scanning rate of 20 ºC min^{-1} (first heating scan) and then immediately quenched to -100 °C at a rate of 100 ºC min^{-1}. The second heating scans were run from -100 to +250 °C at a scanning rate of 20 ºC min^{-1} to record stable thermograms. The data for glass transition temperature (T_g) were obtained from the second run and correspond to the midpoint of discontinuity in the heat flow. Membrane thickness was estimated by using a Mitutoyo micrometer. The gas permeability coefficients (*P*) were measured with a Rikaseiki K-315-N gas permeability apparatus using a constant volume/variable-pressure system.[7] All of the measurements were carried out at 25 ºC and a feed pressure of 0.1 MPa (1 atm) while the pressure difference across the membrane was ~107 kPa as the system was being evacuated on the downstream side of the membrane.

Materials. Ethyl cellulose (**1**; ethoxy content, 49 wt%), cellulose acetate (**3**; acetyl content, 36.7 wt%), *t*-butylisocyanate and dibutyltin dilaurate were purchased from Aldrich and used as received. Ethyl cellulose (**2**; ethoxy content, 45.6 wt%) was obtained commercially from Fluka and cellulose acetate (**4**; acetyl content, 26.9 wt%) was donated by Daicel Chemical Industries, Ltd. *N*,*N*-Dimethylformamide (DMF) used as the reaction solvent, was purchased from Wako (Japan) and purified by distillation prior to use while distilled water (Wako, Japan) was used without further purification.

The *t*-butylcarbamates of ethyl cellulose (**1a**, **2a**) and cellulose acetate (**3a**, **4a**) were synthesized according to Scheme 1. The details of the synthetic procedure and analytical data are as follows:

***t*-Butylcarbamate of Ethyl Cellulose (1a).** A 200 mL three-necked flask was equipped with a dropping funnel, a reflux condenser, a three-way stopcock, a stopper and a magnetic stirring bar. Ethyl cellulose, **1**, (1.43 g, 6.10 mmol) was placed in the flask, evacuated for half an hour, flushed with nitrogen, and dissolved in DMF (50 mL) at room temperature. Then, dibutyltin dilaurate (0.1 mL, 0.16 mmol) was added followed by the dropwise addition of *t*-butylisocyanate (2.9 mL, 24.4 mmol) along with constant stirring. The temperature was raised to 70 °C and stirring was continued for 36 h. Product was isolated by precipitation in a 1:3 methanol/water mixture (1000 mL), filtered with a membrane filter, washed repeatedly with water, and dried under vacuum. The product was stirred vigorously with hexane for 24 hours, washed thoroughly and dried to constant weight to afford the desired product (88%) as white solid. ^{1}H NMR (400 MHz, $CDCl_3$, 25 ºC, ppm): 1.13 (brs, 8.07H, OCH_2CH_3), 1.27 (s, 2.79H, $C(CH_3)_3$), 2.99–4.74 (m, 12.4H, OCH_2CH_3, OCH, OCH_2); IR (ATR, cm^{-1}): 3348, 2972, 2871, 1733, 1499, 1443, 1374, 1354, 1264, 1090, 1054, 942, 918, 869, 768; anal. calcd for $(C_{12.93}H_{23.55}N_{0.31}O_{5.31})_n$ $(268.33)_n$: C, 57.87; H, 8.85; N, 1.62; O, 31.66, found: C, 57.54; H, 8.66; N, 1.58; O, 32.22.

***t*-Butylcarbamate of Ethyl Cellulose (2a).** This derivative was prepared by following the same procedure as for **1a** using ethyl cellulose, **2**, (1.41 g, 6.10 mmol)

instead of **1**. Yield 92%, white solid, ^{1}H NMR (400 MHz, $CDCl_3$, 25 ºC, ppm): 1.11 (brs, 7.5H, OCH_2CH_3), 1.26 (s, 4.5H, $C(CH_3)_3$), 2.98–4.75 (m, 12H, OCH_2CH_3, OCH, OCH_2); IR (ATR, cm^{-1}): 3308, 2973, 2871, 1734, 1501, 1455, 1393, 1366, 1264, 1208, 1091, 1056, 923, 879, 814, 768; anal. calcd for $(C_{13.5}H_{24.5}N_{0.5}O_{5.5})_n$ $(281.84)_n$: C, 57.53; H, 8.76; N, 2.48; O, 31.22, found: C, 57.14; H, 8.65; N, 2.57; O, 31.64.

***t*-Butylcarbamate of Cellulose Acetate (3a).** This derivative was prepared by using cellulose acetate, **3**, (1.62 g, 6.10 mmol) as the starting polymer rather than **1** while the synthetic procedure was the same as for **1a**. Yield 89%, white solid, ^{1}H NMR (400 MHz, $CDCl_3$, 25 ºC, ppm): 1.21−1.31 (m, 4.86H, $C(CH_3)_3$), 1.89−2.12 (m, 7.38H, $OCOCH_3$), 3.40−5.11 (m, 7H, OCH, OCH_2); IR (ATR, cm^{-1}): 3299, 2965, 2873, 1742, 1638, 1524, 1456, 1430, 1366, 1227, 1164, 1041, 904, 846, 776; anal. calcd for $(C_{13.62}H_{19.78}N_{0.54}O_{8.0})_n$ $(319.08)_n$: C, 51.27; H, 6.25; N, 2.37; O, 40.11, found: C, 50.84; H, 6.21; N, 2.31; O, 40.64.

***t*-Butylcarbamate of Cellulose Acetate (4a).** This derivative was prepared by adopting the same procedure as for **1a** using cellulose acetate, **4**, (1.45 g, 6.10 mmol) instead of **1**. Yield 91%, white solid, ^{1}H NMR (400 MHz, $CDCl_3$, 25 ºC, ppm): 1.22−1.31 (m, 10.8H, $C(CH_3)_3$), 1.88−2.14 (m, 5.4H, $OCOCH_3$), 3.25−5.19 (m, 7H, OCH, OCH_2); IR (ATR, cm^{-1}): 3300, 2966, 2874, 1736, 1638, 1518, 1458, 1394, 1366, 1264, 1224, 1167, 1044, 923, 838, 773, 679; anal. calcd for $(C_{15.6}H_{24.4}N_{1.2}O_{8.0})_n$ $(356.76)_n$: C, 52.52; H, 6.89; N, 4.71; O, 35.88, found: C, 52.72; H, 6.65; N, 4.64; O, 35.99.

Determination of the Degree of Substitution. The degree of substitution with ethyl group (DS_{Et}) in ethyl cellulose (**1**, **2**) and that with acetyl group in cellulose acetate (**3**) was determined by ^{1}H NMR, which also provided a clear indication of the carbamate formation. However, the overlapping of the peaks arising due to the methyl protons of *t*-butyl and those of ethyl groups (in **1a** and **2a**) did not allow an exact estimation of the degree of carbamate formation (DS_{Carb}) which was confirmed by the elemental analysis (%N content) of the polymers. The total degree of substitution (DS_{total}) of the resulting polymers was calculated as below:

$$DS_{total} = DS_{Et} + DS_{Carb} \quad \text{(for } \mathbf{1a} \text{ and } \mathbf{2a}\text{)}$$

$$DS_{total} = DS_{Ac} + DS_{Carb} \quad \text{(for } \mathbf{3a} \text{ and } \mathbf{4a}\text{)}$$

Membrane Fabrication. Membranes (thickness ca. 40–80 μm) of polymers **1**, **2**, and **1a**–**4a** were fabricated by casting their chloroform solution (concentration ca. 0.50–1.0 wt%) onto a Petri dish whereas THF and DMF solutions were employed for **3** and **4**, respectively, due to the lack of solubility in $CHCl_3$. The dish was covered with a glass vessel to retard the rate of solvent evaporation (3–5 days).

Measurement of Gas Permeation Parameters. The *P* values were calculated from the slopes of the time-pressure curves in the steady state where Fick's law holds.[8] The gas diffusion coefficients (*D*) were determined by the time lag method using the following equation:

$$D = l^2/6\theta$$

here, l is the membrane thickness and θ is the time lag, which is given by the intercept of the asymptotic line of the time-pressure curve to the time axis. The membrane thickness was controlled so that the time lag would be in the range of 10–300 s, preferably 30–150 s. When the time lag was < 10 s, the error of measurement became relatively large. If the time lag was, on the contrary, > 300 s, the error arising from the baseline drift became serious. The gas solubility coefficients (*S*) were calculated by using the equation, $S = P/D$.

Results and Discussion

Carbamate Synthesis. The carbamoylation was accomplished by coupling the residual hydroxy functionalities of ethyl cellulose (**1** and **2**) and cellulose acetate (**3** and **4**) with *t*-butylisocyanate in the presence of dibutyltin dilaurate as a catalyst as shown in Scheme 1, and the results are listed in Table 1. The carbamate derivatives (**1a**–**4a**) were characterized by the ^{1}H NMR and IR spectroscopy and elemental

Table 1. Degree of Substitution (*DS*) and Molecular Weight of Polymers 1–4 and 1a–4a

polymer	DS_{Carb} [a]	DS_{Carb} [b]	DS_{total} [a]	M_n [c]	M_w/M_n [c]
1	–	–	2.69	57 000	2.6
1a	≈ 0.31	≈ 0.30	≈ 3.00	63 000	2.3
2	–	–	2.50	50 000	2.6
2a	≈ 0.50	≈ 0.52	≈ 3.00	57 000	2.4
3	–	–	2.46	64 000	2.3
3a	≈ 0.54	≈ 0.53	≈ 3.00	70 000	2.2
4	–	–	1.80	89 000	2.0
4a	≈ 1.20	≈ 1.18	≈ 3.00	93 000	2.0

[a] Determined by ^{1}H NMR. [b] Determined by elemental analysis. [c] Determined by GPC (THF as eluent). [d] Determined by GPC (0.01 M LiBr in DMF as eluent).

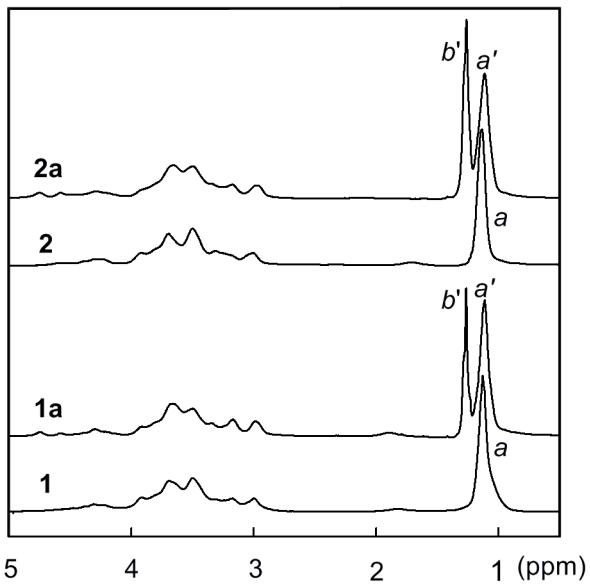

Figure 1. ^{1}H NMR spectra of **1**, **2**, **1a**, and **2a**.
Labels: *a*, terminal methyl protons of ethyl cellulose; *a′*, terminal methyl protons derived from ethyl cellulose; *b′*, terminal methyl protons of the carbamoyl moiety.

analysis. The DS_{Et} of **1** and **2** was estimated to be 2.69 and 2.50, by calculating the integration ratio of methyl protons to the rest of the protons in **1** and **2**, respectively,

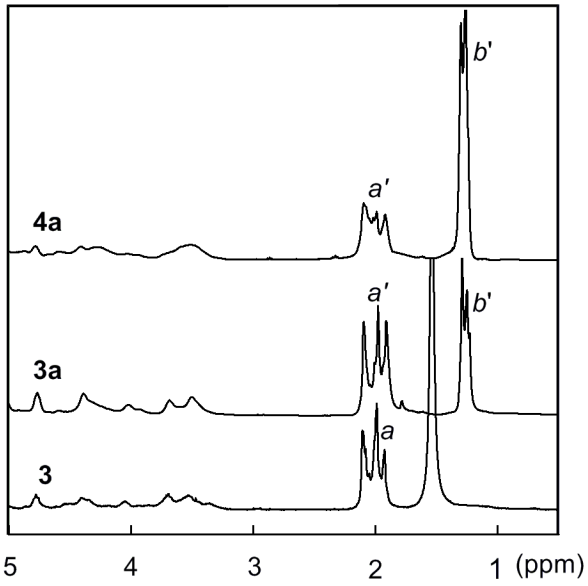

Figure 2. ^{1}H NMR spectra of **3**, **3a**, and **4a**.
Labels: *a*, terminal methyl protons of cellulose acetate; *a′*, terminal methyl protons derived from cellulose acetate; *b′*, terminal methyl protons of the carbamoyl moiety.

indicating the presence of 0.31 and 0.50 hydroxy groups per anhydroglucose unit. The DS_{Ac} of **3** was determined in a similar way whereas that for **4** was provided by the manufacturer. The ^{1}H NMR spectra of the starting polymers (**1**–**3**) and their carbamate derivatives (**1a**–**4a**) are shown in Figures 1 and 2. Although the ^{1}H NMR spectra of the derivatized polymers provided a clear indication of the incorporation of *t*-buytlcarbamoyl group, the calculation of the exact degree of carbamoylation (DS_{Carb}) for **1a** and **2a** could not be carried out due to the overlapping of the peaks arising from the methyl protons of the ethyl group of ethyl cellulose and those of the carbamate moiety. Further evidence was furnished by the presence of the peaks characteristic of the C=O stretching (1742–1733 cm^{-1}) and NH-bending (1524–1499 cm^{-1}) of the carbamate, in the IR spectra of the resulting polymers (**1a**–**4a**). The IR spectra of **1**–**4** (Figures 3 and 4) displayed a broad band attributable to the residual hydroxy groups (3600–3200 cm^{-1}), which did not disappear completely upon carbamate formation as the NH bond of the carbamoyl moiety also absorbs IR radiation in the same

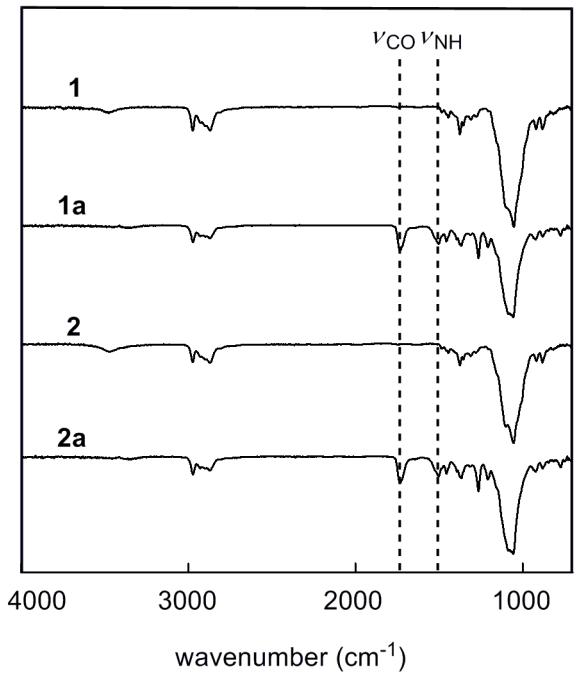

Figure 3. FTIR spectra of **1**, **2**, **1a**, and **2a**.

wavenumber range. Moreover, the absence of the peak around 2270–2100 cm^{-1}, assignable to the isocyanate group of the starting material, provided a clear evidence of the product purification.

The molecular weights of the starting as well as the derivatized polymers were determined by the gel permeation chromatography and the data are summarized in Table 1. The molecular weight determination of ethyl cellulose (**1**; DS_{Et}, 2.69 and **2**; DS_{Et}, 2.50), cellulose acetate (**3**; DS_{Ac}, 2.46), and their carbamate derivatives (**1a**–**3a**) was carried out by making use of THF as eluent while for **4** and **4a**, elution was effected with LiBr solution (10 mM) in DMF because of the insolubility of cellulose acetate (**4**; DS_{Ac}, 1.80) in THF. The carbamoylation of cellulose derivatives accompanied an increase in the molecular weight of the polymers, *e.g.*, the M_n of **3** and **4** were observed to be 64 000 and 89 000 while those for **3a** and **4a** were 70 000 and 93 000, respectively. Moreover, the polydispersity indices (M_w/M_n) of the carbamate derivatives (**1a**–**4a**) were not quite different from those of **1**–**4**, for instance, the M_w/M_n of **2** and **2a** were 2.6 and 2.4 and for **3** and **3a** were 2.3 and 2.2, respectively, thus

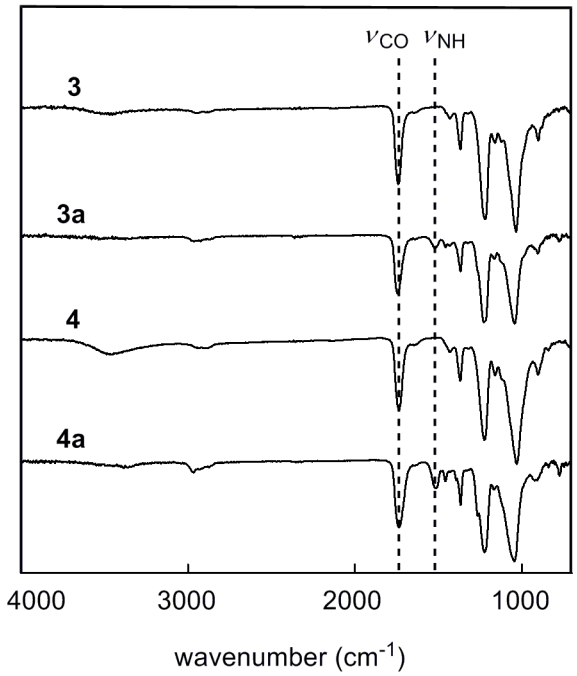

Figure 4. FTIR spectra of **3**, **4**, **3a**, and **4a**.

ruling out the possibility of polymer chain cleavage under the reaction conditions employed for carbamate formation.

Table 2. Solubility[a] of Polymers 1–4 and 1a–4a

polymer	**1**	**1a**	**2**	**2a**	**3**	**3a**	**4**	**4a**
methanol	+	+	+	+	–	+	–	+
DMF	+	+	+	+	+	+	+	+
DMSO	+	+	+	+	+	+	–	+
acetone	±	+	+	+	+	+	–	+
THF	+	+	+	+	+	+	–	+
$CHCl_3$	+	+	+	+	±	+	–	+
toluene	+	+	±	+	–	+	–	+

[a] Symbols: +, soluble; ±, partly soluble; –, insoluble.

Solubility and Thermal Properties of Polymers. The solubility properties of ethyl cellulose (**1** and **2**), cellulose acetate (**3** and **4**), and their carbamate derivatives (**1a**–**4a**) are described in Table 2. **1** and **2** are soluble in polar protic solvents such as methanol and highly polar aprotic solvents like DMF and DMSO, and the same tendency was retained upon carbamoylation. The solubility behavior of the carbamate derivatives of ethyl cellulose, **1a** and **2a**, in THF and $CHCl_3$ was the same as that of the starting polymers, and only the two points of difference were the complete solubility of **1a** in polar aprotic solvent acetone (**1** is partly soluble) and that of **2a** in toluene (**2** is partly soluble). However, the solubility characteristics of cellulose acetate (**3** and **4**) got significantly tuned as a result of substitution of small hydroxy groups with polar carbamate linkages possessing a bulky alkyl periphery. For instance, **3** was insoluble in methanol and toluene, and partly soluble in $CHCl_3$, whereas **3a** was observed to be completely soluble in methanol due to the polar nature of the carbamate group, and in $CHCl_3$ and toluene owing to the presence of the bulky

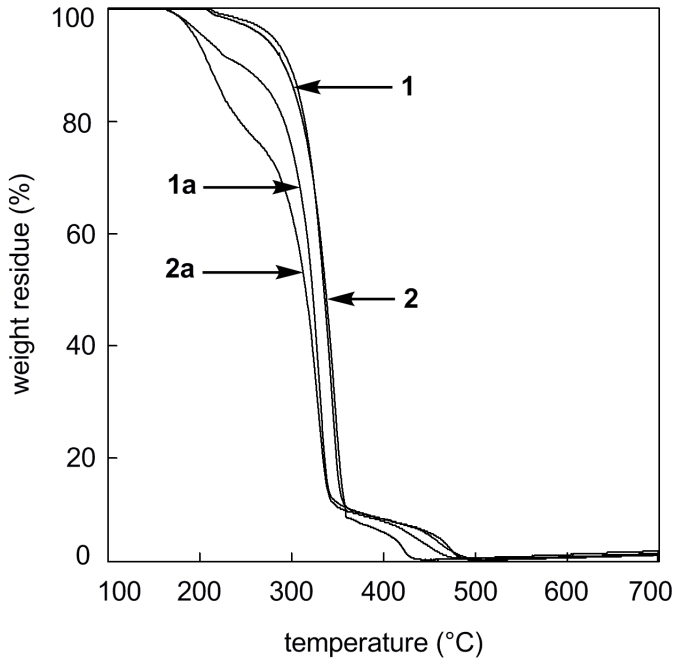

Figure 5. TGA curves of polymers **1**, **2**, **1a**, and **2a** (in air, heating rate 10 ºC min^{-1}).

t-butyl moiety. A striking change was witnessed in the solubility properties of **4**, soluble in DMF only, while its carbamate derivative **4a** displayed solubility in a variety of solvents including methanol, DMSO, acetone, THF, $CHCl_3$, and toluene because of the presence of polar carbamate linkages along with bulky *t*-butyl side groups, hence, overcoming the intramolecular hydrogen boding responsible for the insolubility of **4**. Thus it can be inferred that the incorporation of *t*-butylcarbamate group into various cellulose derivatives led to an overall improvement in the organosolubility of the polymers.

The thermal stability of polymers **1**–**4** and **1a**–**4a** was examined by thermogravimetric analysis (TGA) in air (Figures 5 and 6). The onset temperatures of weight loss (T_0) of **1**–**4** and **1a**–**4a** were in the ranges of 308–337 ºC and 177–204 ºC, respectively. The TGA curves of carbamate derivatives indicated a three step weight loss commencing at approximately 200 ºC, 300 ºC, and 350 ºC, respectively, whereas a two step weight loss was exhibited by the starting polymers. For **1a**–**4a**,

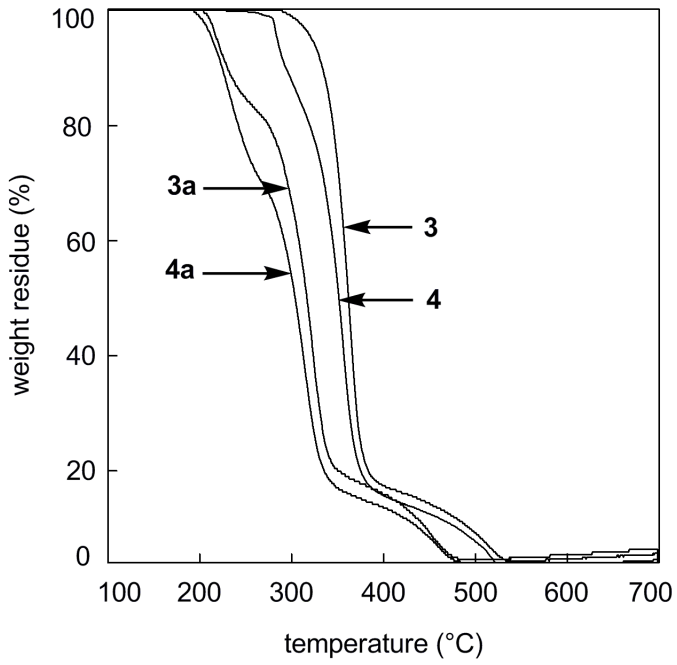

Figure 6. TGA curves of polymers **3**, **4**, **3a**, and **4a** (in air, heating rate 10 ºC min^{-1}).

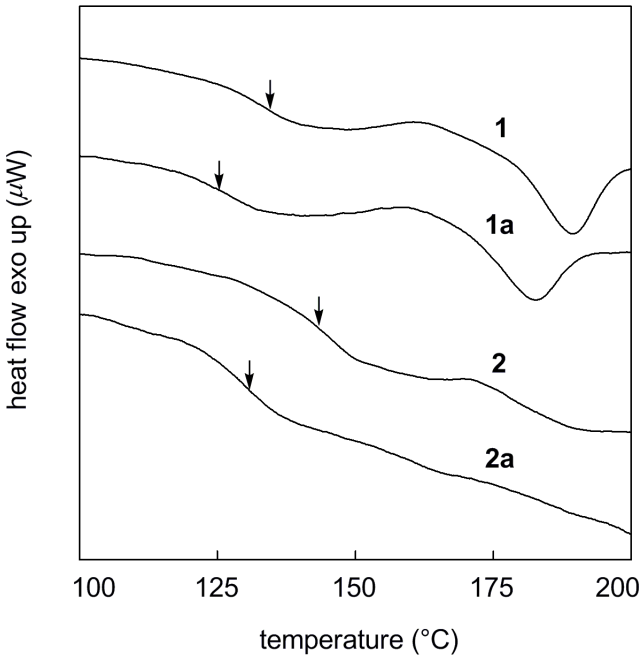

Figure 7. DSC thermograms of polymers **1**, **2**, **1a**, and **2a** (under N_2, second scan).

the first stage of decomposition should correspond to the cleavage of side groups as carbamate moieties are thermally labile and are known to undergo the elimination of isocyanate.[9]

The glass transition temperature (T_g) of polymers **1**–**4** and **1a**–**4a** were determined by the differential scanning calorimetric (DSC) analysis under nitrogen (Figures 7 and 8). The incorporation of *t*-butylcarbamoyl group was observed to accompany a slight decrease in the glass transition temperature (T_g); for instance, the T_g values of **2** and **4** were 142 ºC and 205 ºC while those for **2a** and **4a** were 127 ºC and 189 ºC, respectively (Table 3). The variation in the glass transition temperature of the polymeric materials is dramatically affected by the nature of side chains and the increased polarity entails enhanced T_g values and vice versa; on the other hand, the bulk and the shape of the substituents is of vital significance too and the presence of spherical bulky substituents augments the chain flexibility thus leading to the reduced T_g.[10] In previous studies concerning the derivatization of ethyl cellulose and cellulose acetate, the incorporation of nonpolar and bulky substituents has been

reported to lead to the decline in the glass transition temperature of the polymers.[11a,12]

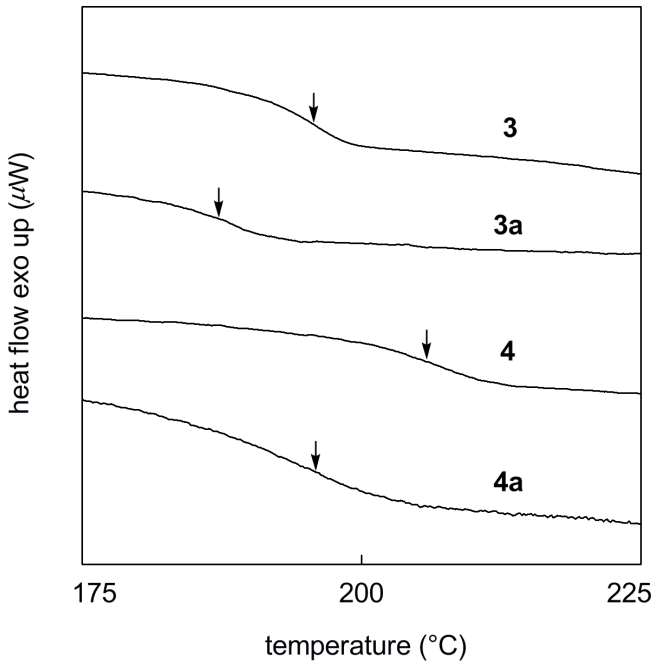

Figure 8. DSC thermograms of polymers **3**, **4**, **3a**, and **4a** (under N_2, second scan).

However, the present series of polymers (**1a**–**4a**) is characterized by the presence of polar carbamate linkages and the expected decrease in T_g resulting from the substitution of small hydroxy groups by bulkier carbamoyl functionalities is most probably offset by the polar nature of the carbamate moieties.

Gas Permeation Properties. The permeability coefficients of the membranes of **1**–**4** and **1a**–**4a** to various gases measured at 25 °C are shown in Table 4. The gas permeability coefficients (*P*) of the carbamate derivatives (**1a**–**4a**) were higher than those of the starting cellulose derivatives, and the most pronounced enhancement was observed for **4a**. In the case of ethyl cellulose derivatives (**1a** and **2a**) there was a slight increase in gas permeability without any significant change in permselectivity, *e.g.*, the P_{CO_2} and P_{CO_2}/P_{N_2} of **2a** were 89 and 22.8, whereas 80 barrers and 22.9 for **2**,

Table 3. Thermal Properties of Polymers 1–4 and 1a–4a

polymer	T_0[a] (°C)	T_g[b] (°C)
1	311	132
1a	177	124
2	308	142
2a	180	127
3	337	194
3a	204	185
4	319	205
4a	204	189

[a] T_0: Onset temperature of weight loss. Determined from TGA measurement in air.
[b] T_g: Glass transition temperature. Determined by DSC analysis under nitrogen.

respectively. On the other hand, the carbamoylation of cellulose acetate (**3** and **4**) resulted in a considerable increase in *P* values for all the gases; for instance, the P_{O_2} and P_{CO_2} of **3** being 0.67 and 4.6 while those for **3a** were 3.1 and 19 barrers, respectively, thus exhibiting a 4–5 times enhancement. Furthermore, the carbamate formation of **4** (DS_{Ac}, 1.80) accompanied the most extensive augmentation in gas permeability, probably due to the greatest extent of derivatization attained (**4a**, DS_{Ac}, 1.80; DS_{Carb}, 1.20); **4a** displayed the P_{O_2} and P_{CO_2} values of 5.5 and 38 barrers, respectively, representing a voluminous increase of ≥ 20 times.

The present study reveals the effect of the incorporation of carbamate appendages on the gas permeation characteristics of ethyl cellulose and cellulose acetate. There have been no systematic reports concerning the *t*-butylcarbamoylation of these membrane-forming cellulose derivatives and the transformation acquired in terms of gas permeability and permselectivity. It has been discerned that the substitution of small hydroxy groups of ethyl cellulose and cellulose acetate with polar carbamate linkages bearing a bulky and spherical periphery resulted in the increased permeability coefficients for all the gases. The present series of cellulose derivatives

Table 4. Gas Permeability Coefficients (*P*) of Polymer Membranes at 25 °C

polymer	*P* (barrer)[a]						P_{CO_2}/P_{N_2}	P_{CO_2}/P_{CH_4}
	He	H_2	O_2	N_2	CO_2	CH_4		
1	47	68	15	4.3	91	9.2	21.2	9.9
1a	57	75	17	4.7	100	10.5	21.2	9.5
2	41	59	13	3.5	80	7.5	22.9	10.7
2a	51	71	15	3.9	89	8.4	22.8	10.6
3	15	12	0.67	0.14	4.6	0.15	32.8	30.7
3a	27	26	3.1	0.66	19	0.83	28.8	22.9
4	8.4	5.7	0.28	0.044	1.7	0.045	38.6	37.8
4a	34	36	5.5	1.3	38	1.97	29.2	19.3

[a] 1 barrer = $1x10^{-10}$ cm^3 (STP) cm cm^{-2} s^{-1} $cmHg^{-1}$.

represents a clear manifestation of the dependence of the gas transport properties of membrane-forming materials upon the modification of two most important subtle structural features, *i.e*. interchain spacing and segmental mobility.

In polymeric membranes, the decrement of gas permeability emanating from the introduction of polar substituents due to the reduced free volume inside the polymer matrix is a well established concept;[13] on the contrary, the presence of spherical side groups is known to bring forth the augmentation in gas permeability owing to the increased excess free volume and/or enhanced local mobility.[14,15] The *t*-butylcarbamates of cellulose derivatives (**1a**–**4a**) possess both the aforementioned features and the local mobility of the side groups playing a dominant role resulted in the permeability enhancement which was quite substantial for cellulose acetate derivatives, especially for **4a**. These results are quite in compliance with the previous ones describing a two times increase in the *P* values to arise from the silylation of ethyl cellulose (DS_{Et}, 2.69), a four to five times enhancement for silylated cellulose acetate (DS_{Ac}, 2.46), and a magnanimous augmentation of more than 30 times to result from the silylation of cellulose acetate (DS_{Ac}, 1.80).[11b,12]

The most worth mentioning of the gas permeation characteristics of this series

of polymers is the fact that the CO_2 permselectivity was almost retained despite a considerable increase in permeability (Table 4). There was a fourfold increase in the CO_2 permeability of **3** upon carbamoylation (**3**, 4.6; **3a**, 19) but its P_{CO_2}/P_{N_2} selectivity underwent a relatively slight change (**3**, 32.8; **3a**, 28.8). Moreover, the carbamate derivative of **4** exhibited a 22 times enhancement in P_{CO_2} (**4**, 1.7; **4a**, 38), whereas its CO_2/N_2 permselectivity experienced a change from 38.6 to 29.2 only. The increased CO_2 permeability without any significant loss of permselectivity is probably a consequence of the increased CO_2 diffusivity and retained CO_2/N_2 solubility selectivity of these polymeric membranes; the latter being attributable to the presence of polar carbamate linkages.

Gas Diffusivity and Solubility. Gas permeability (*P*), which is the steady-state, pressure- and thickness-normalized gas flux through a membrane, can be expressed as the product of gas solubility (*S*) in the upstream face of the membrane and effective average gas diffusion (*D*) through the membrane, strictly in rubbery and approximately in glassy polymers:[1a–c,16]

$$P = S \times D$$

A detailed investigation of the gas permeation characteristics was carried out by determining the gas diffusion coefficients (*D*) and gas solubility coefficients (*S*) of the polymers. The plots of *S* versus *D* values of polymers **2**, **2a**, **4**, and **4a** for O_2 and CO_2 are illustrated in Figures 9 and 10, respectively. The gas permeability enhancement, as a consequence of the incorporation of polar carbamate linkages having spherical and bulky alkyl termini, has been revealed to stem from the amplification of the gas diffusion coefficients of the polymer membranes.

The *D* values of all the gases increased upon carbamoylation (**1a**–**4a**); for instance, **2** displayed the D_{O_2} value of 6.9, and that of **2a** was 9.1, in the units of 10^7 cm^2 s^{-1}. The gas diffusion coefficients, delineated as a complex interplay between fractional free volume and local mobility, tend to increase if accompanied by an

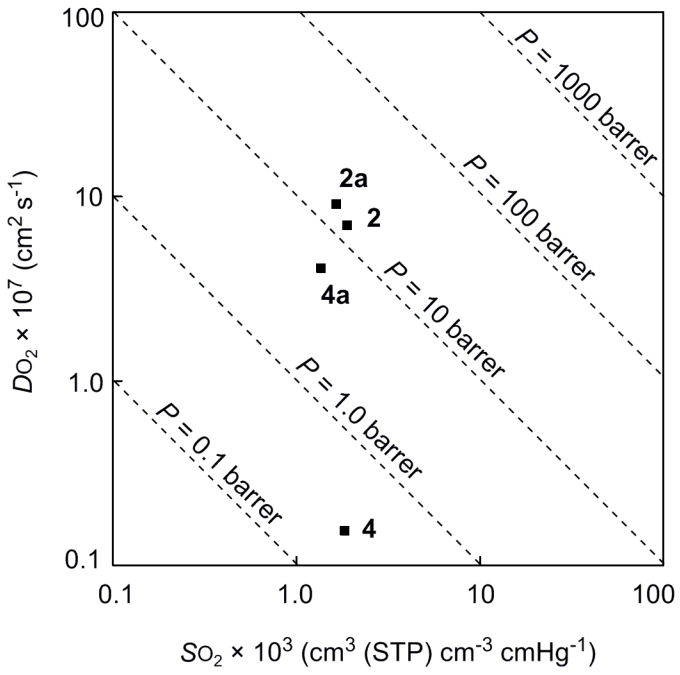

Figure 9. Plot of SO_2 vs DO_2 for polymers **2**, **4**, **2a**, and **4a**.

augmentation in either of these factors but are known to be more dependent on the latter. The increment in the gas diffusion coefficients finds its explanation in the enhanced segmental mobility of the carbamates of cellulose derivatives, attributable to the presence of spherical and bulky *t*-butyl moieties.[8,14] As with the gas permeability coefficients, the enhancement of the gas diffusivity was much more prominent for carbamates of cellulose acetate (**3a** and **4a**); the DCO_2 values of **2** and **2a** were 2.39 and 2.93 while those for **4** and **4a** were 0.023 and 1.05, respectively.

On the other hand, the carbamate formation accompanied a decrease in the gas solubility coefficients; *e.g.*, the SO_2 of **2** and **2a** were 1.89 and 1.65 while the SCO_2 values being 33.3 and 30.3, respectively, in the units of 10^3 cm^3 (STP) cm^{-3} cmHg^{-1}. The reduction in the *S* values can be accounted for by the attenuated fractional free volume of the derivatized polymers (**1a**–**4a**) because of the presence of polar carbamate linkages.[13]

In glassy polymeric membranes, generally the *D* value undergoes a decrease

with increasing critical volume of gases whereas the *S* value experiences an increase with increasing critical temperature of gases.[1a] Similar tendencies were observed in the *D* and *S* values of the polymer membranes of the starting (**1**–**4**) as well as the carbamoylated cellulose derivatives (**1a**–**4a**); *e.g.*, in the case of **4a**, the diffusivity of CH_4 was the lowest and that of O_2 was the highest (0.65 and 4.09 10^7 cm^2 s^{-1},

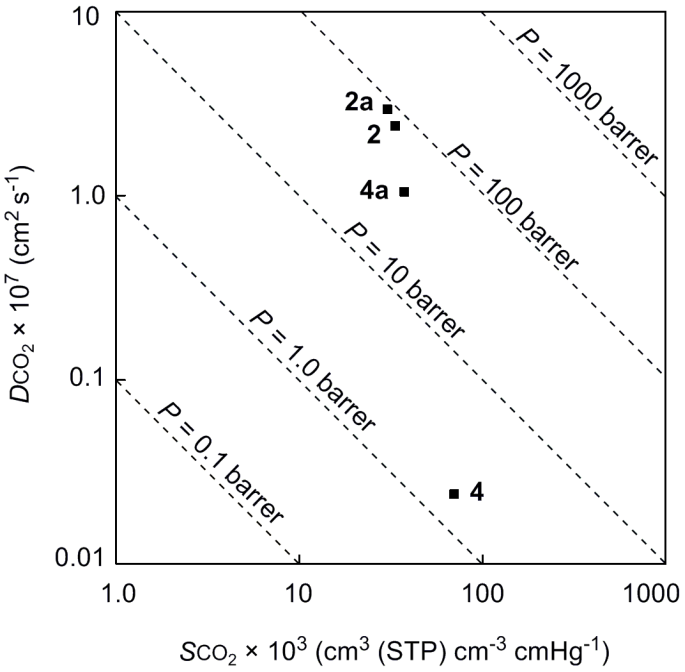

Figure 10. Plot of S_{CO_2} vs D_{CO_2} for polymers **2**, **4**, **2a**, and **4a**.

respectively) while CO_2 displayed the highest solubility and N_2 the lowest (37.5 and 0.72 10^3 cm^3 (STP) cm^{-3} $cmHg^{-1}$, respectively). The diffusion coefficients of these carbamate-functionalized cellulosics (**1a**–**4a**) were in the order $D_{O_2} > D_{N_2} > D_{CO_2} > D_{CH_4}$, the same as for the starting polymers, ethyl cellulose and cellulose acetate. Similarly, the *S* values of **1**–**4** and **1a**–**4a** were observed to follow the same trend ($S_{CO_2} > S_{CH_4} > S_{O_2} > S_{N_2}$).

It is noteworthy that the increase in the diffusion coefficients upon carbamoylation was more pronounced than the decrease in the solubility coefficients, thus leading to the net effect of enhanced permeability. Furthermore, these results

indicate the significance of bulky spherical groups to enhance gas permeability by affecting an increment in the gas diffusion coefficients of the polymer membranes.

Conclusions

The present study is concerned with the synthesis of a series of *t*-butylcarbamates of ethyl cellulose (**1a**: DS_{Et}, 2.69, DS_{Carb}, 0.31; and **2a**: DS_{Et}, 2.50, DS_{Carb}, 0.50) and cellulose acetate (**3a**: DS_{Ac}, 2.46, DS_{Carb}, 0.54; and **4**: DS_{Ac}, 1.80, DS_{Carb}, 1.20), and describes an approach to transform the gas permeation characteristics of these membrane-forming materials. The use of dibutyltin dilaurate as a catalyst has been demonstrated to accomplish the complete substitution of the residual hydroxy protons of ethyl cellulose (**1**: DS_{Et}, 2.69; **2**: DS_{Et}, 2.50) and cellulose acetate (**3**: DS_{Ac}, 2.46; **4**: DS_{Ac}, 1.80) by the *t*-butylcarbamoyl moiety as indicated by the ^{1}H NMR, and evidenced by the FTIR and elemental analysis. The carbamate derivatives displayed good solubility in common organic solvents and organosolubility of **4** was witnessed to undergo a remarkable improvement. Good thermal stability was revealed and initiation of degradation was elucidated to ensue from the loss of *t*-butylisocyanate around 180–200 °C under air. Free-standing membranes of all of the starting and resulting polymers, **1**–**4** and **1a**–**4a**, were fabricated by solution casting. Membranes of **1a**–**4a** exhibited increased gas permeability which was investigated to arise from the increment in the gas diffusion coefficients, presumably emanating from the enhanced local mobility in the polymer matrix. The increase in the gas permeability as well as gas diffusivity of polymer membranes was far more pronounced in the carbamate derivatives of cellulose acetate (**3a** and **4a**) than that observed upon carbamoylation of ethyl cellulose (**1a** and **2a**). Despite a considerable amplification of CO_2 permeability in **3a** and **4a**, the carbamate formation accompanied an almost retained CO_2/N_2 permselectivity and good separation performance was discerned for CO_2/N_2 and CO_2/CH_4 gas pairs.

References and Notes

1. (a) Yampolskii, Yu.; Pinnau, I.; Freeman, B. D. *Materials Science of Membranes for Gas and Vapor Separation*; Wiley: Chichester, 2006. (b) Pinnau, I.; Freeman, B. D. *Advanced Materials for Membrane Separations*; ACS Symposium Series 876; American Chemical Society: Washington, DC, 2004. (c) Baker, R. W. *Membrane Technology and Applications*, 2nd ed.; Wiley: New York, 2004. (d) Nagai, K.; Masuda, T.; Nakagawa, T.; Freeman, B. D.; Pinnau, I. *Prog. Polym. Sci.* **2001**, *26*, 721–798. (e) Nunes, S. P.; Peinemann, K.-V. *Membrane Technology in the Chemical Industry*; Wiley: New York, 2001. (f) Koros, W. J.; Mahajan, R. *J. Membr. Sci.* **2000**, *175*, 181–196. (g) Aoki, T. *Prog. Polym. Sci.* **1999**, *24*, 951–993. (h) Maier, G. *Angew. Chem. Int. Ed.* **1998**, *37*, 2961–2974.
2. (a) Alentiev, A. Y.; Shantarovich, V. P.; Merkel, T. C.; Bondar, V. I.; Freeman, B. D.; Yampolskii, Y. P. *Macromolecules* **2002**, *35*, 9513–9522. (b) Freeman, B. D.; Pinnau, I. *Trends Polym. Sci.* **1997**, *5*, 167–173. (c) Langsam, M. *Plastics Engineering* **1996**, *36*, 697–741. (d) Chung, I. J.; Lee, K. R.; Hwang, S. T. *J. Membr. Sci.* **1995**, *105*, 177–185. (e) Henis, J. M. S. *Commercial and Practical Aspects of Gas Separation Membranes*; CRC Press: Boca Raton, FL, 1994. (f) Koros, W. J. In *Membrane Separation Systems: Recent Developments and Future Directions*, Baker, R. W., Cuasler, E. L., Eykamp, W., Koros, W. J., Riley, R. L., Strathmann, H., Eds.; Noyes Data Corporation: Park Ridge, NJ, 1991; pp 189–241. (g) Spillman, R. W. *Chem. Eng. Prog*. **1989**, *85*, 41–62.
3. (a) Klemm, D.; Heublein, B.; Fink, H.-P.; Bohn, A. *Angew. Chem. Int. ed.* **2005**, *44*, 3358–3393. (b) Kosan, B.; Michels, C.; Meister, F. *Macromol. Symp*. **2005**, *223*, 1–12. (c) Crowley, M. M.; Schroeder, B.; Fredersdorf, A.; Obara, S.; Talarico, M.; Kucera, S.; McGinity, J. W. *Int. J. Pharm.* **2004**, *269*, 509–522. (d) Zugenmaier, P. *Macromol. Symp.* **2004**, *208*, 81–166. (e) Heinze, T.; Liebert, T. *Macromol. Symp.* **2004**, *208*, 167–237. (f) Li, X.-G.; Kresse, I.; Xu, Z.-K.; Springer, J. *Polymer* **2001**, *42*, 6801–6810. (g) Barton, D. H. R.; Nakanishi, K.; Meth-Cohn, O. *Comprehensive Natural Products Chemistry*; Elsevier Science: Oxford, 1999; Vol. 3. (h) Klemm, D.; Philipp, B.; Heinze, T.; Heinze, U.; Wagenknecht, W. *Comprehensive Cellulose Chemistry*; Wiley-VCH: Weinheim, 1998; Vol. 1, 2.
4. (a) Nakai, Y.; Yoshimizu, H.; Tsujita, Y. *J. Membr. Sci.* **2005**, *256*, 72–77. (b) Li, X.-G.; Huang, M.-R.; Gu, G.-F.; Qiu, W.; Lu, J.-Y. *J. Appl. Polym. Sci.* **2000**, *75*, 458–463. (c) Bai, S.; Sridhar, S.; Khan, A. A. *J. Membr. Sci.* **2000**, *174*, 67–79. (d) Ravindra, R.; Sridhar, S.; Khan, A. A.; Rao, A. K. *Polymer* **2000**, *41*, 2795–2806. (e) Wang, Y.; Easteal, A. J. *J. Membr. Sci.* **1999**, *157*, 53–61. (f) Li, X.-G.; Huang, M.-R.; Hu, L.; Lin, G.; Yang, P.-C. *Eur. Polym. J.* **1999**, *35*, 157–166. (g) He, Y.; Yang, J.; Li, H.; Huang, P. *Polymer* **1998**, *39*, 3393–3397. (h) Li, X.-G.; Huang,

M.-R. *J. Appl. Polym. Sci.* **1997**, *66*, 2139–2147. (i) Houde, A. Y.; Stern, S. A. *J. Membr. Sci.* **1997**, *127*, 171–183. (j) Suto, S.; Niimi, T.; Sugiura, T. *J. Appl. Polym. Sci.* **1996**, *61*, 1621–1630. (k) Houde, A. Y.; Stern, S. A. *J. Membr. Sci.* **1994**, *92*, 95–101. (l) Puleo, A. C.; Paul, D. R.; Kelley, S. S. *J. Membr. Sci.* **1989**, *47*, 301–332. (m) Minhas, B. S.; Matsuura, T.; Sourirajan, S. *Ind. Eng. Chem. Res.* **1987**, *26*, 2344–2348.

5. (a) Zugenmaier, P. In *Cellulosic Polymers, Blends and Composites*; Gilbert, R. D., Ed.; Hanser: Munich, 1994**;** pp 71–94. (b) Gilbert, R. D. *ACS Symp. Ser.* **1990**, *433*, 259–272. (c) Siekmeyer, M.; Zugenmaier, P. *Makromol. Chem.* **1990**, *191*, 1177–1196. (d) Vogt, U.; Zugenmaier, P. *Makromol. Chem. Rapid Commun.* **1983**, *4*, 759–765. (e) Zugenmaier, P.; Vogt, U. *Makromol. Chem.* **1983**, *184*, 1749–1760.
6. (a) Sato, T.; Shimizu, T.; Kasabo, F; Teramoto, A. *Macromolecules* **2003**, *36*, 2939–2943. (b) Okamoto, Y.; Yashima, E.; Yamamoto, C. *Top. Stereochem.* **2003**, *24*, 157–208. (c) Kubota, T.; Yamamoto, C.; Okamoto, Y. *Chirality* **2003**, *15*, 77–82. (d) Kubota, T.; Yamamoto, C.; Okamoto, Y. *Chirality* **2002**, *14*, 372–376. (e) Kubota, T.; Yamamoto, C.; Okamoto, Y. *J. Am. Chem. Soc.* **2000**, *122*, 4056–4059. (f) Spitzer, T.; Yashima, E.; Okamoto, Y. *Chirality* **1999**, *11*, 195–200. (g) Okamoto, Y.; Yashima, E. *Angew. Chem. Int. Ed.* **1998**, *37*, 1020–1043.
7. Bondar, V. I.; Freeman, B. D.; Pinnau, I. *J. Polym. Sci., Part B: Polym. Phys.* **2000**, *38*, 2051–2062.
8. Masuda, T.; Iguchi, Y.; Tang, B.-Z.; Higashimura, T. *Polymer* **1988**, *29*, 2041–2049.
9. Mormann, W.; Michel, U. *Carbohydr. Polym.* **2002**, *50*, 201–208.
10. Stevens, M. P. *Polymer Chemistry: An Introduction*, 3rd ed.; Oxford University Press: New York, 1999; pp 70–74.
11. (a) Khan, F. Z.; Sakaguchi, T.; Shiotsuki, M.; Nishio, Y.; Masuda, T. *Macromolecules* **2006**, *39*, 9208–9214. (b) Khan, F. Z.; Sakaguchi, T.; Shiotsuki, M.; Nishio, Y.; Masuda, T. *Macromolecules* **2006**, *39*, 6025–6030.
12. Morita, R.; Khan, F. Z.; Sakaguchi, T.; Shiotsuki, M.; Nishio, Y.; Masuda, T. *J. Membr. Sci.* **2007**, *305*, 136–145.
13. (a) Senthilkumar, U.; Reddy, B. S. R. *J. Membr. Sci.* **2007**, *292*, 72–79. (b) Kono, T.; Sakaguchi, T.; Hu, Y.; Shiotsuki, M.; Sanda, F.; Masuda, T. *J. Polym. Sci., Part A: Polym. Chem.* **2006**, *44*, 5943–5953. (c) Shida, Y.; Sakaguchi, T.; Shiotsuki, M.; Sanda, F.; Freeman, B. D.; Masuda, T. *Macromolecules* **2005**, *38*, 4096–4102. (d) Lin, H.; Freeman, B. D. *J. Mol. Struct.* **2005**, *739*, 57–74. (e) Ghosal, K.; Chern, R. T.; Freeman, B. D.; Daly, W. H. Negulescu, I. I.

Macromolecules **1996**, *29*, 4360–4369. (f) Simril, V. L.; Hershberger, A. *Mod. Plast.* **1950**, *27*, 95–102.

14. (a) Sakaguchi, T.; Shiotsuki, M.; Masuda, T. *Macromolecules* **2004**, *37*, 4104–4108. (b) Merkel, T. C.; Bondar, V. I.; Nagai, K.; Freeman, B. D. *J. Polym. Sci., Part B: Polym. Phys.* **2000**, *38*, 273–296. (c) Toy, L. G.; Nagai, K.; Freeman, B. D.; Pinnau, I.; He, Z.; Masuda, T.; Teraguchi, M.; Yampolskii, Y. P. *Macromolecules* **2000**, *33*, 2516–2524.
15. (a) Kanaya, T.; Tsukushi, I.; Kaji, K.; Sakaguchi, T.; Kwak, G.; Masuda, T. *Macromolecules* **2002**, *35*, 5559–5564. (b) Kanaya, T.; Tsukushi, I.; Kaji, K.; Teraguchi, M.; Kwak, G.; Masuda, T. *J. Phys. Soc., Suppl. A* **2000**, *70*, 332–334. (c) Kanaya, T.; Teraguchi, M.; Masuda, T.; Kaji, K. *Polymer* **1999**, *40*, 7157–7161.
16. (a) Graham, T. *J. Membr. Sci.* **1995**, *100*, 27–31. (b) Graham, T. *Philos. Mag.* **1866**, *32*, 401–420.

Chapter 5

Synthesis and Properties of Amino Acid Esters of Hydroxypropyl Cellulose

Abstract

The amino acid esters of hydroxypropyl cellulose [R' = H (**2a**), CH_3 (**2b**), $CH_2CH(CH_3)_2$ (**2c**), CH_2CONH_2 (**2d**), $CH_2CH_2CONH_2$ (**2e**), $CH_2CH_2CH_2CH_2NHOCOC(CH_3)_3$ (**2f**)] were synthesized in good yield by the reaction of *t*-butoxycarbonyl (*t*-Boc)-protected amino acids with hydroxy groups of hydroxypropyl cellulose (**1**; molar substitution (*MS*), 4.61). The amino acid functionalities displaying varied chemical nature, shape, and bulk were utilized and the bulk of the substituent on the α-carbon of amino acids was elucidated to be of vital significance for the observed degree of incorporation (DS_{Est}). The ^{1}H NMR spectra and elemental analysis were employed to determine the degree of incorporation of amino acid moiety (DS_{Est}) and almost complete substitution of the hydroxy protons was revealed for **2a**, **2b**, and **2f**. The presence of the peaks characteristic of the carbonyl group in the FTIR spectra furnished further evidence for the successful esterification of hydroxypropyl cellulose. The starting as well as the resulting polymers (**1** and **2a**–**f**) were soluble in polar organic solvents; however, the esterification of **1** with bulky organic moieties resulted in an increased hydrophobicity as all of the amino acid-functionalized polymers (**2a**–**f**) were insoluble in water. The onset temperatures of weight loss of **2a**–**f** were 175–230 °C, indicating fair thermal stability. The amino acid functionalization led to the enhanced polymer chain stiffness, and the glass transition temperatures of the derivatized polymers were 30–40 °C higher than that of **1** (T_g 3.9 °C; cf. T_g of **2a**–**f**, 35.1–43.3 °C).

Introduction

Cellulose, an inexhaustible natural polymeric material, endowed with a polyfunctional macromolecular structure and an environmentally benign nature, suffers from the lack of solubility emanating from its supramolecular architecture. On the other hand, water soluble cellulose derivatives are physiologically inert biocompatible materials characterized by a multitude of potential applications in the food, cosmetics, and pharmaceutical sectors. Hydroxypropyl cellulose (HPC), one of the commercially important cellulose ethers, is an odorless, thermoplastic, non-toxic polymer, displaying excellent solubility in water as well as polar organic solvents.[1] Owing to its ability to serve as a colloidal stabilizer, an emulsifier, and a coating agent, HPC finds a wide range of industrial applications in ceramics, paint, paper, or textile,[2] and has gained considerable interest as a speciality polymer in the electronic industry due to its remarkable biocompatibility. HPC has also been extensively employed in oral and topical pharmaceutical formulations as a tablet binder, a film-coating material, and a thickening agent etc.[3,3] However, the film formulations based on the biodegradable, biocompatible polysaccharides for the controlled delivery of hydrophobic drugs encounter the precipitation of the drug within the matrix of water-soluble polysaccharides.[4] Hydroxypropyl cellulose (HPC), being widely employed as a pharmaceutical excipient for various purposes, possesses three hydroxy groups per anhydroglucose unit capable to serve as the sites of chemical derivatization and offers the possibility to bring about the modification of solubility properties. The synthesis of HPC derivatives with hydrophobic side chains might be expected to increase the hydrophobicity of the resulting polymeric materials thus making them potentially more suitable carriers for hydrophobic drugs.

Amino acids are the basic building blocks of nature capable of accomplishing a variety of exquisite functions spanning the horizons of natural to synthetic materials, serving the multifarious domains of life including food, drugs, and fibers, playing a prominent role in the world of synthetic architectures as a chiral source for organic synthesis and optical resolution material. In the past few decades, synthesis of amino

acid- and peptide-containing polymers has attracted considerable attention, since a high degree of amino acid functionality and chirality can confer the polymers with the unique features of enhanced solubility, regulated higher order structures/helix formation, stimuli-responsiveness, and liquid crystalline arrangement.[5] Furthermore, amino acids and peptides are being widely used in the synthesis of biocompatible architectures, finding quite promising applications as controlled drug delivery systems, cell-adhesive structures, polyelectrolytes, chiral recognition materials, and medicines.[6]

Esterification is one of the facile means to exploit the hydroxy groups present in cellulose derivatives, and has been the most commonly used synthetic approach leading towards the preparation of cellulose-based materials capable of exhibiting cholesteric LC phase transitions.[7] Although the amino acid-containing polymers have engrossed substantial prominence as a new class of bioactive polymeric materials,[5,6] no significant research endeavor concerning the amino acid functionalization of cellulose derivatives has been reported so far. The hydroxy anchors of HPC and the carboxy termini of amino acids provide an ample opportunity of bringing about a successful conjunction of the two biocompatible families of materials. Our previous efforts to effect the derivatization of organosoluble cellulosic polymers with a variety of substituents are quite evident of the fact that the tailoring of pendants on the cellulosic backbone results in a significant alteration of solubility

Scheme 1. Synthesis of Amino Acid Esters of Hydroxypropyl Cellulose

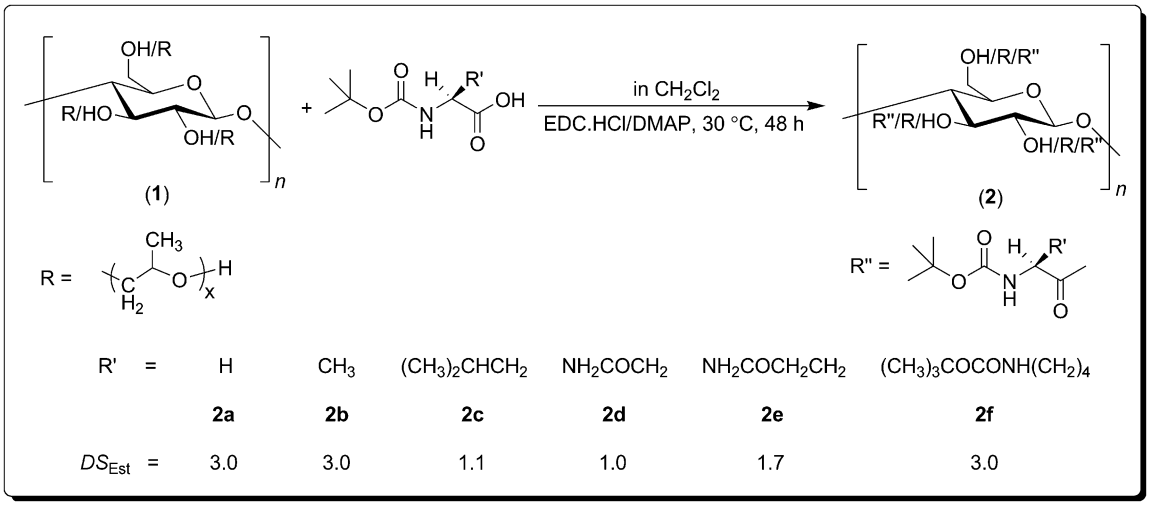

characteristics as desired for specific applications.[8] Hence, amino acid esterification of HPC is anticipated to lead to the modification of solubility and hydrophobicity of the derivatized counterparts, making these materials interesting candidates for hydrophobic drug carriers.

This chapter despicts the synthesis and characterization of amino acid-functionalized hydroxypropyl cellulose derivatives (**2a**–**f**) (Scheme 1). A clear dependence of degree of esterification (DS_{Est}) on the bulk of the substituent on the α-carbon of amino acids has been revealed. The solubility characteristics and thermal properties of the derivatized polymers were elucidated.

Experimental Section

Measurements. ^{1}H NMR spectra were recorded on a JEOL EX-400 spectrometer and the residual proton signal of the d_6-DMSO was used as internal standard. The samples for the NMR measurements were prepared at a concentration of approximately 10 mg/mL and chemical shifts are reported in parts per million (ppm). All of the spectra were recorded for 64 scans with a pulse delay of 37 s at 80 °C in order to obtain reliable integrations. Infrared spectra were recorded on a Jasco FTIR-4100 spectrophotometer and 64 spectra were accumulated at a resolution of 4 cm^{-1}, for each measurement. The elemental analyses were conducted at the Microanalytical Center of Kyoto University. The number- and weight-average molecular weights (M_n and M_w, respectively) and polydispersity indices (M_w/M_n) of polymers were determined by gel permeation chromatography (GPC) on a JASCO Gulliver system (PU-980, CO-965, RI-930, and UV-2075). All the measurements were carried out at 40 ºC using two TSK-Gel columns [α-M (bead size, 13 μm; molecular weight range > 1×10^7) and GMH_{XL} (bead size 9 μm; molecular weight range up to 4×10^8)] in series and LiBr solution (10 mM) in *N*,*N*-dimethylformamide as an eluent at a flow rate of 1.0 mL/min. The elution times were converted into molecular weights using a calibration curve based on polystyrene standards in combination with the information obtained from the refractive index detector.

Specific rotations ($[\alpha]_D$) were measured with a JASCO DIP-1000 digital polarimeter. Thermogravimetric analyses (TGA) were conducted in air with a Shimadzu TGA–50 thermal analyzer by heating the samples (5–7 mg) from 100–700 ºC at a scanning rate of 10 ºC min^{-1}. Differential scanning calorimetric (DSC) analyses were performed using a Seiko DSC6200/EXSTAR6000 apparatus and measurements were carried out by making use of 5–7 mg samples, under a nitrogen atmosphere, after calibration with an indium standard. The samples were first heated from ambient temperature (25 ºC) to 188 °C at a scanning rate of 20 ºC min^{-1} (first heating scan) and then immediately quenched to -100 °C at a rate of 100 ºC min^{-1}. The second heating scans were run from -100 to 188 °C at a scanning rate of 20 ºC min^{-1} to record stable thermograms. The data for glass transition temperature (T_g) were obtained from the second run and correspond to the midpoint of discontinuity in the heat flow.

Materials. Hydroxypropyl cellulose (**1**), 4-(dimethylamino)pyridine (Wako, Japan), and *N*-(3-Dimethylaminopropyl)-*N′*-ethylcarbodiimide hydrochloride (EDC·HCl; Eiweiss Chemical Corporation) were obtained commercially and used as received. *N*-*α*-*t*-Butoxycarbonyl-L-glycine, *N*-*α*-*t*-butoxycarbonyl-L-alanine, *N*-*α*-*t*-butoxycarbonyl-L-leucine, *N*-*α*-*t*-butoxycarbonyl-L-asparagine, *N*-*α*-*t*-butoxycarbonyl-L-glutamine, and *N*-*α*-,*N*-*ε*-di-*t*-butoxycarbonyl-L-lysine were purchased from Watanabe Chemical Ind. (Japan). Dichloromethane (CH_2Cl_2), used as the reaction solvent, and distilled water, used for polymer precipitation and washing, were purchased from Wako (Japan) and used without further purification.

The amino acid esters of hydroxypropyl cellulose (**2a**–**f**) were synthesized according to Scheme 1. The details of the synthetic procedure and analytical data are as follows:

***N*-*α*-*t*-Butoxycarbonyl-L-glycine Ester of Hydroxypropyl Cellulose (2a).** A 200 mL one-necked flask was equipped with a stopper and a magnetic stirring bar. Hydroxypropyl cellulose, **1**, (1.35 g, 3.13 mmol) was added into the flask and dissolved in CH_2Cl_2 (50 mL) at room temperature. 4-(Dimethylamino)pyridine (0.34 g, 2.82 mmol) was introduced followed by the addition of

N-*α*-*t*-Butoxycarbonyl-L-glycine (4.94 g, 28.17 mmol) and EDC·HCl (5.4 g, 28.17 mmol), respectively, and stirring was continued for 48 h at room temperature. The product was isolated by the precipitation in aqueous $NaHCO_3$ solution (1000 mL), filtered with a membrane filter, washed with water several times to ensure the complete removal of $NaHCO_3$, and dried under vacuum to constant weight to afford the desired product as a white solid. Yield 95%, ^{1}H NMR (400 MHz, d_6-DMSO, 80 ºC, ppm): 1.06–1.17 (m, 13.83H, OCHCH_3), 1.38 (s, 27.0H, OCOC(CH_3)$_3$), 3.21–4.45 (m, 18.83H, OCHCH_3, OCH, OCH_2, and 6.0H, NHCH_2CO), 4.91 (brs, 2H, OCHCH_3); IR (ATR, cm^{-1}): 3383, 2977, 2929, 2877, 1751, 1705, 1510, 1456, 1366, 1251, 1201, 1157, 1051, 959, 864, 782; $[\alpha]_D$ = –18.2° (*c* = 0.10 g/dL in CH_3OH); anal. calcd for $(C_{40.83}H_{70.66}N_{3.00}O_{18.61})_n$ $(901.3869)_n$: C, 54.40; H, 7.90; N, 4.66; O, 33.04, found: C, 53.89; H, 7.77; N, 4.83; O, 33.51.

***N*-*α*-*t*-Butoxycarbonyl-L-alanine Ester of Hydroxypropyl Cellulose (2b).** This derivative was prepared by following the same procedure as for **2a** using *N*-*α*-*t*-butoxycarbonyl-L-alanine (5.33 g, 28.17 mmol) instead of *N*-*α*-*t*-butoxycarbonyl-L-glycine. Yield 97%, white solid, ^{1}H NMR (400 MHz, d_6-DMSO, 80 ºC, ppm): 1.07–1.16 (m, 13.83H, OCHCH_3), 1.37 (s, 27.0H, OCOC(CH_3)$_3$), 1.50 (s, 9.0H, NHCH(CH_3)CO), 3.21–4.65 (m, 18.83H, OCHCH_3, OCH, OCH_2, and 3.0H, NHCHCO), 4.89 (brs, 2H, OCHCH_3); IR (ATR, cm^{-1}): 3368, 2978, 2936, 2877, 1755, 1712, 1505, 1454, 1366, 1303, 1250, 1213, 1161, 1091, 1055, 1020, 983, 950, 853, 778, 757; $[\alpha]_D$ = –28.3° (*c* = 0.10 g/dL in CH_3OH); anal. calcd for $(C_{43.83}H_{76.66}N_{3.00}O_{18.61})_n$ $(943.4666)_n$: C, 55.80; H, 8.19; N, 4.45; O, 31.56, found: C, 55.52; H, 7.92; N, 4.85; O, 31.71.

***N*-*α*-*t*-Butoxycarbonyl-L-leucine Ester of Hydroxypropyl Cellulose (2c).** This derivative was prepared by using *N*-*α*-*t*-butoxycarbonyl-L-leucine (6.52 g, 28.17 mmol) rather than *N*-*α*-*t*-butoxycarbonyl-L-glycine while the rest of the conditions and procedure were the same as those for the synthesis of **2a**. Yield 91%, white solid, ^{1}H NMR (400 MHz, d_6-DMSO, 80 ºC, ppm): 0.87 (brs, 6.6H, CH(CH_3)$_2$), 1.04–1.15 (m, 13.83H, OCHCH_3), 1.38 (s, 9.9H, OCOC(CH_3)$_3$), 1.48 (brs, 2.2H, NHCH(CH_2)CO),

1.66 (brs, 1.1H, NHCH($CH_2C\mathit{H}$)CO), 3.22–4.49 (m, 19.83H, $OC\mathit{H}CH_3$, OCH, OCH_2, and 1.1H, $NHC\mathit{H}CO$), 4.88 (brs, 1H, $OCHC\mathit{H}_3$); IR (ATR, cm^{-1}): 3441, 2969, 2877, 1752, 1708, 1521, 1456, 1367, 1328, 1271, 1161, 1114, 1047, 842; $[\alpha]_D$ = –37.8° (*c* = 0.10 g/dL in CH_3OH); anal. calcd for $(C_{31.93}H_{58.56}N_{1.1}O_{12.91})_n$ $(664.4862)_n$: C, 57.71; H, 8.88; N, 2.32; O, 31.09, found: C 57.74; H, 8.50; N, 1.99; O, 31.77.

***N*-*α*-*t*-Butoxycarbonyl-L-asparagine Ester of Hydroxypropyl Cellulose (2d).** The reaction of hydroxypropyl cellulose, **1**, (1.35 g, 3.13 mmol) with *N*-*α*-*t*-butoxycarbonyl-L-asparagine (6.54 g, 28.17 mmol) and the purification of the product were carried out in the same way as that for the synthesis of **2a**. Yield 90%, white solid, ^{1}H NMR (400 MHz, d_6-DMSO, 80 ºC, ppm): 1.04–1.18 (m, 13.83H, $OCHC\mathit{H}_3$), 1.40 (s, 9.0H, $OCOC(C\mathit{H}_3)_3$), 2.88–2.96 (m, 2.0H, $NHCH(C\mathit{H}_2CO)CO$), 3.21–4.45 (m, 19.83H, $OC\mathit{H}CH_3$, OCH, OCH_2, and 1.0H, $NHC\mathit{H}CO$), 4.91 (brs, 1H, $OCHC\mathit{H}_3$); IR (ATR, cm^{-1}): 3441, 2972, 2926, 2884, 1751, 1713, 1514, 1456, 1370, 1285, 1158, 1116, 1052, 887, 851, 790, 769, 668; $[\alpha]_D$ = –25.8° (*c* = 0.10 g/dL in CH_3OH); anal. calcd for $(C_{28.83}H_{51.66}N_{2.00}O_{13.61})_n$ $(644.1039)_n$: C, 53.76; H, 8.08; N, 4.35; O, 33.81, found: C, 53.32; H, 8.37; N, 4.01; O, 34.30.

***N*-*α*-*t*-Butoxycarbonyl-L-glutamine Ester of Hydroxypropyl Cellulose (2e).** It was synthesized by adopting the same procedure as for **2a** using *N*-*α*-*t*-butoxycarbonyl-L-glutamine (6.94 g, 28.17 mmol) instead of *N*-*α*-*t*-butoxycarbonyl-L-glycine. Yield 93%, white solid, ^{1}H NMR (400 MHz, d_6-DMSO, 80 ºC, ppm): 1.04–1.17 (m, 13.83H, $OCHC\mathit{H}_3$), 1.40 (s, 15.3H, $OCOC(C\mathit{H}_3)_3$), 1.93 (brs, 3.4H, $NHCH(CH_2C\mathit{H}_2CO)CO$), 2.65 (brs, 3.4H, $NHCH(C\mathit{H}_2CH_2CO)CO$), 3.21–4.50 (m, 19.13H, $OC\mathit{H}CH_3$, OCH, OCH_2, and 1.7H, $NHC\mathit{H}CO$), 4.93 (brs, 1.7H, $OCHC\mathit{H}_3$); IR (ATR, cm^{-1}): 3332, 2977, 2921, 1750, 1706, 1670, 1621, 1511, 1452, 1365, 1161, 1120, 1068, 1049, 834, 690; $[\alpha]_D$ = –25.7° (*c* = 0.10 g/dL in CH_3OH); anal. calcd for $(C_{36.83}H_{64.86}N_{3.4}O_{16.41})_n$ $(817.9020)_n$: C, 54.08; H, 7.99; N, 5.82; O, 32.11, found: C, 54.49; H, 7.67; N, 5.45; O, 32.39.

***N*-*α*-,*N*-*ε*-di-*t*-Butoxycarbonyl-L-lysine Ester of Hydroxypropyl Cellulose (2f).** The synthesis of **2f** was accomplished in the same way as that of **2a** by making

use of *N*-*α*-,*N*-ε-di-*t*-butoxycarbonyl-L-lysine (9.76 g, 28.17 mmol) instead of *N*-*α*-*t*-butoxycarbonyl-L-glycine. Yield 92%, white solid, ^{1}H NMR (400 MHz, d_6-DMSO, 80 ºC, ppm): 1.07–1.13 (m, 13.83H, OCHCH_3), 1.38 (s, 27.0H, OCOC(CH_3)$_3$), 1.49 (brs, 6.0H, NHCH(CH$_2$CH_2)CO), 1.63 (brs, 6.0H, NHCH(CH$_2$CH$_2$CH_2)CO), 2.11–2.15 (m, 6.0H, NHCH(CH_2)CO), 3.1 (brs, 6.0H, NHCH(CH$_2$CH$_2$CH$_2$CH_2NH)CO), 3.21–4.65 (m, 18.83H, OCHCH$_3$, OCH, OCH$_2$, and 3.0H, NHCHCO), 4.90 (brs, 2H, OCHCH_3); IR (ATR, cm^{-1}): 3375, 2978, 2930, 2866, 1750, 1706, 1689, 1599, 1517, 1456, 1399, 1365, 1249, 1163, 1043, 1024, 859, 778, 763; $[\alpha]_D$ = –25.6° (c = 0.10 g/dL in CH$_3$OH); anal. calcd for $(C_{67.83}H_{121.66}N_{6.00}O_{24.61})_n$ $(1415.0972)_n$: C, 57.57; H, 8.67; N, 5.94; O, 27.82, found: C, 57.15; H, 8.34; N, 6.17; O, 28.34.

Determination of the Degree of Substitution. The average number of hydroxypropyl substituents per anhydroglucose unit (molar substitution; *MS*) in hydroxypropyl cellulose (**1**) was determined by ^{1}H NMR by calculating the integration ratio of proton on the anomeric carbon of anhydroglucose unit (AGU) to those of the terminal methyl protons of hydroxypropyl group. On the other hand, the incorporation of amino acid moieties into hydroxypropyl cellulose has been accomplished through esterification and the extent of substitution of hydroxy protons of **1** by aminoalkanoyl pendants has been denoted by DS_{Est} throughout this contribution, which was determined by calculating the integration ratio of the peaks arising due to the methyl protons of hydroxypropyl pendants and those of *t*-Boc termini of the amino acid moieties.

Results and Discussion

Amino Acid Ester Synthesis. The amino acid esterification of hydroxypropyl cellulose was accomplished by coupling the hydroxy functionalities of hydroxypropyl cellulose (**1**) with the carboxy termini of amino acids; *N*-(3-dimethylaminopropyl)-*N*′-ethylcarbodiimide hydrochloride (EDC·HCl) was employed as a condensating agent and 4-(dimethylamino)pyridine (DMAP) as a base,

as shown in Scheme 1, and the results are summarized in Table 1. The amino acid esters (**2a**–**f**) were characterized by ^{1}H NMR and IR spectroscopy and elemental analysis. Each anhydroglucose unit (AGU) in HPC (**1**) possesses one anomeric proton and each hydroxypropyl group contributes three methyl protons thus its molar substitution (*MS*) could be calculated as (I_{CH3}/3)/ I_{H1}, where I_{CH3} (at 1.04 ppm, indicated as '*a*' in Figure 1) and I_{H1} (at 4.41 ppm, indicated as '*b*' in Figure 1) are the peak intensities of the methyl protons and anomeric proton, respectively. The ^{1}H NMR spectral data of amino acid esters of HPC (**2a**–**f)** were recorded to determine the degree of incorporation of aminoalkanoyl substituents (DS_{Est}) by making an estimation of the peak intensity ratios of the terminal methyl protons of hydroxypropyl group (at ≈ 1.04–1.17 ppm, indicated as '*a*' in Figure 1) and those of *t*-Boc moieties of the amino acid pendants (at ≈1.4 ppm, indicated as '*b*' in Figure 1). The ^{1}H NMR spectra of the starting (**1**) as well as derivatized polymers (**2c**–**e**) are shown in Figure 1 and complete substitution of three hydroxy protons was revealed for the *t*-Boc-protected

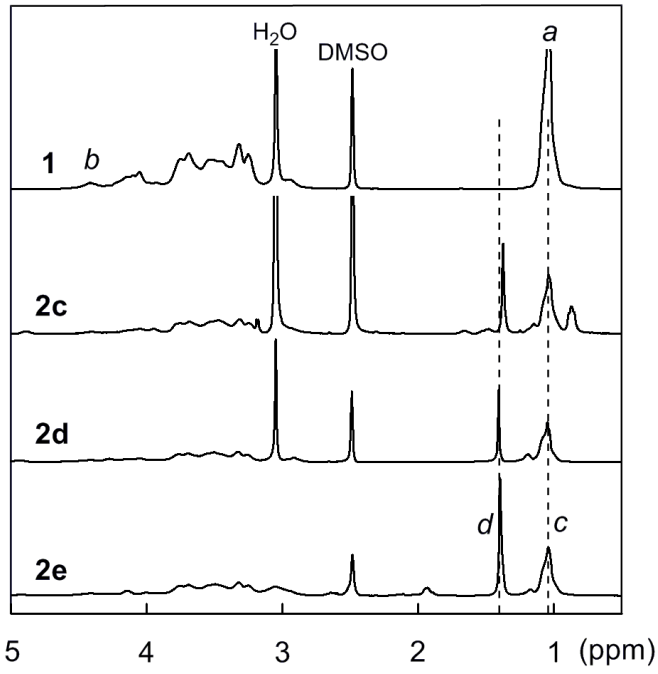

Figure 1. ^{1}H NMR spectra of polymers **1** and **2c**–**e**.
Labels: *a*, terminal methyl protons of hydroxypropyl cellulose; *b*, anomeric proton of hydroxypropyl cellulose; *c*, terminal methyl protons derived from the hydroxypropyl cellulose; *d*, terminal methyl protons of the *t*-butoxycarbonyl moiety.

glycine, alanine, and lysine derivatized polymers. Moreover, elemental analysis was carried out and the %N content of the polymers was exploited for the sake of confirmation of the exact degree of amino acid incorporation (DS_{Est}).

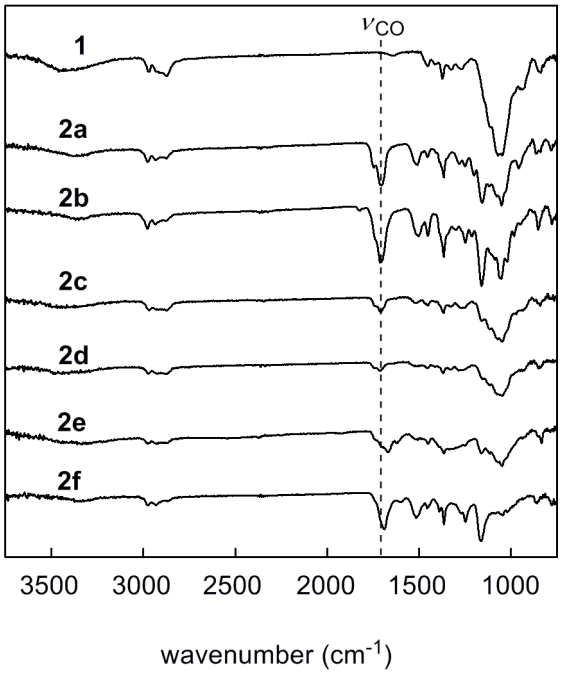

Figure 2. FTIR spectra of polymers **1** and **2a**–**f**.

Further evidence was acquired from the presence of the peaks characteristic of the carbonyl group of an ester (1755–1750 cm^{-1}) in the IR spectra of the amino acid-functionalized polymers (**2a**–**f**). The IR spectrum of **1** (Figure 2) displayed a broad band attributable to the hydroxy groups of HPC (3600–3200 cm^{-1}), which did not disappear upon derivatization as the NH bonds corresponding to the amino acid moiety absorb IR radiation in the same wavenumber region. Moreover, the peaks at 1713–1705 cm^{-1} and 1521–1505 cm^{-1} should correspond to the C=O stretching and NH-bending of the carbamate linkages present in the form of protected amino termini of the resulting polymers.

The molecular weights of the starting (**1**) as well as derivatized polymers (**2a**–**f**) were determined by the gel permeation chromatography and the data are listed

in Table 1. The molecular weight determination of hydroxypropyl cellulose (**1**; *MS*, 4.61) and its amino acid esters (**2a**–**f**) was carried out by making use of LiBr solution (0.01 M) in DMF as eluent because of good solubility of these polymeric materials in DMF. The esterification of HPC involving the substitution of small hydroxy protons with bulky organic moieties accompanied an increase in the molecular weight of the polymers; *e.g.*, the M_n of **1** was observed to be 71 000 while those for **2a**–**f** were 154 000–216 000, respectively. Moreover, the polydispersity indices (M_w/M_n) of the amino acid-functionalized polymers (**2a**–**f**) were not quite different from those of **1**; for instance, the M_w/M_n of **1** and **2a**–**f** were 4.3 and 4.2–5.7, respectively, thus ruling out the possibility of polymer chain cleavage under the mild reaction conditions employed for esterification.

Table 1. Degree of Esterification (DS_{Est}) and Molecular Weight of Polymers 1 and 2a–f

polymer	DS_{Est} [a]	M_n [b]	M_w [b]	M_w/M_n [b]
1	0.0	71 000	310 000	4.3
2a	3.0	154 000	883 000	5.7
2b	3.0	172 000	891 000	5.2
2c	1.1	216 000	905 000	4.2
2d	1.0	180 000	865 000	4.8
2e	1.7	183 000	871 000	4.7
2f	3.0	194 000	937 000	4.8

[a] Determined by ^{1}H NMR. [b] Determined by GPC (0.01 M LiBr in DMF as eluent).

Solubility and Thermal Properties of Polymers. The solubility characteristics of hydroxypropyl cellulose (**1**) and its amino acid esters (**2a**–**f**) are shown in Table 2. **1** is soluble in polar protic solvents such as methanol, highly polar aprotic solvents like DMF and DMSO, and moderately polar acetone. The same tendency was retained upon the incorporation of aminoalkanoyl substituents which can

reasonably be attributed to the presence of polar carbamate (protected amino) and ester linkages. Despite the introduction of polar substituents, the solubility behavior of derivatized polymers (**2a**–**f**) in THF and $CHCl_3$ was also the same as that of the starting polymer (**1**) presumably by the virtue of peripheral *t*-butyl groups. On the other hand, the amino acid-functionalized polymers (**2a**–**f**) were insoluble in low polarity solvents like toluene due to the incorporation of substituents having a number of polar moieties. A striking change was witnessed in the solubility of HPC (**1**) in water as all of the amino acid esters of hydroxypropyl cellulose (**2a**–**f**) displayed

Table 2. Solubility[a] of Polymers 1 and 2a–f

polymer	**1**	**2a**	**2b**	**2c**	**2d**	**2e**	**2f**
water	+	–	–	–	–	–	–
methanol	+	+	+	+	+	+	+
DMF	+	+	+	+	+	+	+
DMSO	+	+	+	+	+	+	+
acetone	+	+	+	+	+	+	+
THF	+	+	+	+	+	+	+
$CHCl_3$	+	+	+	+	+	+	+
toluene	–	–	–	–	–	–	–

[a] Symbols: +, soluble; –, insoluble.

insolubility in water ensuing from the loss of hydroxy protons and the introduction of bulky organic moieties. Thus it can be inferred that the amino acid esterification of hydroxypropyl cellulose has led to an overall increment in the hydrophobicity of polymers without having any effect on their organosolubility.

The thermal stability of the polymers (**1** and **2a**–**f**) was examined by thermogravimetric analysis (TGA) in air (Figure 3). The onset temperature of weight loss (T_0) of **1** was 311 ºC while those for **2a**–**f** were in the range of 175–230 ºC, respectively. The TGA curves of all of the amino acid esters (**2a**–**f**) indicated an

almost same pattern of three-step weight loss commencing at approximately 200 ºC, 300 ºC, and 350 ºC, respectively, whereas a two-step weight loss was exhibited by the starting cellulosic (**1**). For **2a**–**f**, the first stage of decomposition should correspond to the cleavage of peripheral *t*-butoxycarbonyl (*t*-Boc) groups as *t*-butyl moieties are thermally labile (above 180 ºC) and are known to undergo the elimination of isobutene.[9]

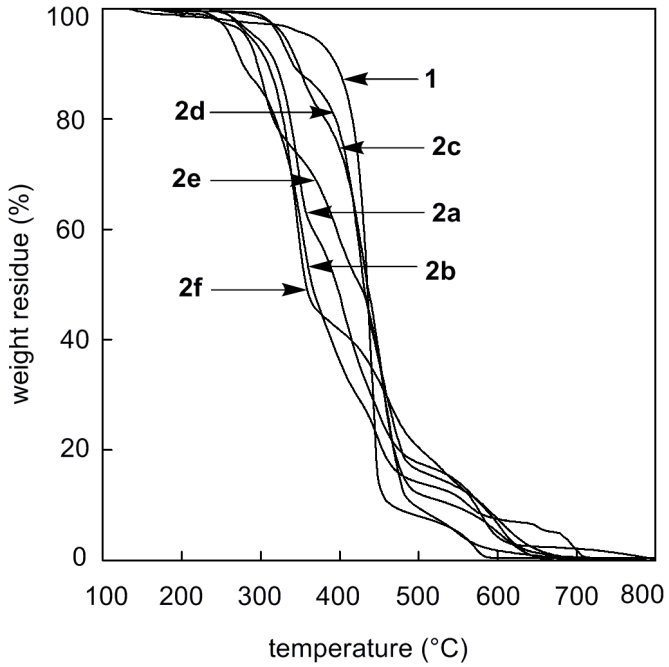

Figure 3. TGA curves of polymers **1** and **2a**–**f** (in air, heating rate 10 ºC min^{-1}).

The glass transition temperatures (T_g) of polymers (**1** and **2a**–**f**) were determined by the differential scanning calorimetric (DSC) analysis under nitrogen (Figure 4). The incorporation of *t*-Boc protected amino acid pendants was observed to accompany an increase in the glass transition temperature (T_g) of polymers; for instance, the T_g of **1** was 3.9 ºC whereas those for **2a–f** were 35.1–43.3 ºC, respectively (Table 3). The variation in the glass transition temperature of the polymeric materials is dramatically affected by the nature of side chains and the increased polarity entails enhanced T_g values and vice versa. On the other hand, the bulk and shape of the substituents are also of vital significance and the presence of spherical bulky

substituents augments the chain flexibility and thus ensues the reduced T_g.[10] In previous studies concerning the derivatization of other organosoluble cellulosics like ethyl cellulose and cellulose acetate, the incorporation of bulky nonpolar substituents has been reported to lead to the decline in the glass transition temperature of the polymers.[8b,c] However, the present series of polymers (**2a**–**f**) is characterized by the presence of polar amino and ester linkages along with spherical peripheries, probably the former being more dominant in the determination of T_g. Hence, the substitution of small hydroxy groups by bulkier aminoalkanoyl functionalities has led to the increment in T_g resulting in the transition from rubbery (**1**) to glassy (**2a**–**f**) polymeric materials.

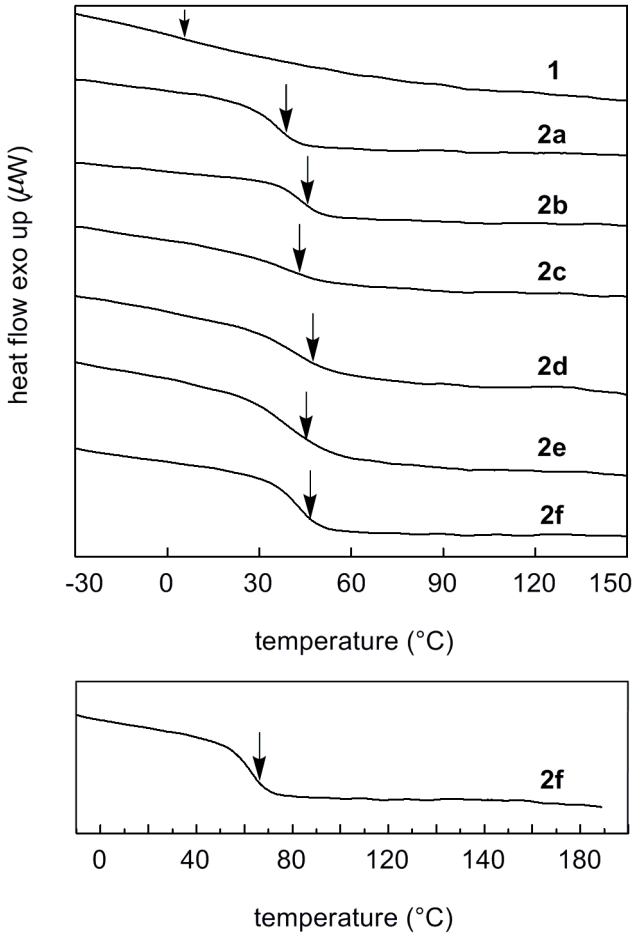

Figure 4. DSC thermograms of polymers **1** and **2a**–**f** (under N_2, second scan)[a].
[a] The lower portion delineates the DSC trace for **2f** (derivative with the lowest T_0 value), indicating the absence of the commencement of weight loss under N_2 until 188 °C.

Table 3. Thermal Properties of Polymers 1 and 2a–f

polymer	T_0[a] (°C)	T_g[b](°C)
1	311	3.9
2a	222	35.1
2b	180	43.3
2c	230	36.9
2d	212	42.0
2e	184	39.5
2f	175	43.2

[a] T_0: Onset temperature of weight loss. Determined from TGA measurement in air.
[b] T_g: Glass transition temperature. Determined by DSC analysis under nitrogen.

Conclusions

The present study is concerned with the synthesis of a series of *t*-Boc protected amino acid esters of hydroxypropyl cellulose (**2a**: DS_{Est}, 3.0; **2b**: DS_{Est}, 3.0; **2c**: DS_{Est}, 1.1; **2d**: DS_{Est}, 1.0; **2e**: DS_{Est}, 1.7; and **2f**: DS_{Est}, 3.0) delineating an approach to transform the hydrophobicity and thermal characteristics of an organosoluble cellulosic. The use of EDC·HCl as a condensating agent in the presence of DMAP has been demonstrated to accomplish a facile mode of amino acid esterification of **1** without any polymer chain cleavage in the course of the reaction. The bulk of the substituent on the α-carbon of the amino acid pendants was revealed to be the most significant parameter effecting the extent of substitution of the hydroxy protons of hydroxypropyl cellulose (**1**: *MS*, 4.61). The complete incorporation of amino acid functionalities ($DS_{Est} \approx 3.0$) was observed for *t*-Boc protected glycine, alanine, and lysine groups as evidenced by the ^{1}H NMR and confirmed by elemental analysis. The derivatized polymers displayed good solubility in common organic solvents and were insoluble in water. Good thermal stability was revealed and initiation of weight loss was elucidated to ensue from for the degradation of *t*-butyl moieties around 175–230 °C under air. The amino acid functionalization of HPC accompanied a

considerable amplification of glass transition temperature and all of the ester derivatives were glassy at room temperature (T_g, 35.1–43.3 °C).

References and Notes

1. (a) Klemm, D.; Heublein, B.; Fink, H. -P.; Bohn, A. *Angew. Chem. Int. ed.* **2005**, *44*, 3358–3393. (b) Barton, D. H. R.; Nakanishi, K.; Meth-Cohn, O. *Comprehensive Natural Products Chemistry*; Elsevier Science: Oxford, 1999; Vol. 3. (c) Klemm, D.; Philipp, B.; Heinze, T.; Heinze, U.; Wagenknecht, W. *Comprehensive Cellulose Chemistry*; Wiley-VCH: Weinheim, 1998; Vol. 1, 2.
2. (a) Kibbe, A. H. *Handbook of Pharmaceutical Excipients*, 3rd ed.; American Pharmaceutical Association and Pharmaceutical Press: Washington, 2000. (b) Dönges, R. *Br. Polym. J.* **1990**, *23*, 315–326. (c) Brandt, L. In *Ullmann's Encyclopedia of Industrial Chemistry*; Campbell, F. T., Pfefferkorn, R., Rounsaville, J. F., Eds.; VCH-Verlagsgesellschaft: Weinheim, 1986; p 461–488.
3. (a) Bajdik. J.; Regdon, Jr. G.; Marek, T.; Eros, I.; Suvegh, K.; Pintye-Hodi, K. *Int. J. Pharm.* **2005**, *301*, 192–198. (b) Rowe, R. C.; Sheskey, P. J.; Weller, P. I. *Handbook of Pharmaceutical Excipients*, 4th ed.; Pharmaceutical Press: London, 2003. (c) Jian-Hwa Guo; Skinner, G. W.; Harcum, W. W.; Barnum, P. E. *Pharm. Sci. Technol. Today* **1998**, *1*, 254–261.
4. Jackson, J. K.; Skinner, K. C.; Burgess, L.; Sun, T.; Hunter, W. L.; Burt, H. M. *Pharm. Res.* **2002**, *19*, 411–417.
5. (a) Baughman, T. W.; Wagener, K. B. *Adv. Polym. Sci.* **2005**, *176*, 1–42. (b) Okoshi, K.; Sakajiri, K.; Kumaki, J.; Yashima, E. *Macromolecules* **2005**, *38*, 4061–4064. (c) Vriezema, D. M.; Kros, A.; de Gelder, R.; Cornelissen, J.; Rowan, A. E.; Nolte, R. J. M. *Macromolecules* **2004**, *37*, 4736–4739. (d) Vriezema, D. M.; Hoogboom, J.; Velonia, K.; Takazawa, K.; Christianen, P. C. M.; Maan, J. C.; Rowan, A. E.; Nolte, R. J. M. *Angew. Chem. Int. Ed.* **2003**, *42*, 772–776. (e) Katsarava, R. *Macromol. Symp.* **2003**, *199*, 419–429. (f) Vandermeulen, G. W. M.; Tziatzios, C.; Klok, H.-A. *Macromolecules* **2003**, *36*, 4107–4114. (g) Checot, F.; Lecommandoux, S.; Gnanou, Y.; Klok, H.-A. *Angew. Chem. Int. Ed.* **2002**, *41*, 1339–1343. (h) Klok, H.-A.; Langenwalter, J. F.; Lecommandoux, S. *Macromolecules* **2000**, *33*, 7819–7826. (i) Sanda, F.; Endo, T. *Macromol. Chem. Phys.* **1999**, *200*, 2651–2661. (j) Cornelissen, J. J. L. M.; Fischer, M.; Sommerdijk, N. A. J. M.; Nolte, R. J. M. *Science* **1998**, *280*, 1427–1430.
6. (a) Scholl, M.; Nguyen, T. Q.; Bruchmann, B.; Klok, H.-A. *J. Polym. Sci. Part A: Polym. Chem.* **2007**, *45*, 5494–5508. (b) Deng, C.; Chen, X.; Sun, J.; Lu, T.; Wang,

W.; Jing, X. *J. Polym. Sci. Part A: Polym. Chem.* **2007**, *45*, 3218–3230. (c) Biagini, S. C. G.; Parry, A. L. *J. Polym. Sci. Part A: Polym. Chem.* **2007**, *45*, 3178–3190. (d) Sinaga, A.; Ravi, P.; Hatton, T. A.; Tam, K. C. *J. Polym. Sci. Part A: Polym. Chem.* **2007**, *45*, 2646–2656. (e) Carrillo, A.; Yanjarappa, M. J.; Gujraty, K. V.; Kane, R. S. *J. Polym. Sci. Part A: Polym. Chem.* **2006**, *44*, 928–939. (f) Ayres, L.; Hans, P.; Adams, J.; Löwik, D. W. P. M.; van Hest, J. C. M. *J. Polym. Sci. Part A: Polym. Chem.* **2005**, *43*, 6355–6366. (g) Klok, H.-A. *J. Polym. Sci. Part A: Polym. Chem.* **2005**, *43*, 1–17. (h) Maynard, H. D.; Okada, S. Y.; Grubbs, R. H. *J. Am. Chem. Soc.* **2001**, *123*, 1275–1279. (i) Maynard, H. D.; Okada, S. Y.; Grubbs, R. H. *Macromolecules* **2000**, *33*, 6239–6248. (j) Biagini, S. C. G.; Coles, M. P.; Gibson, V. C.; Giles, M. R.; Marshall, E. L.; North, M. *Polymer* **1998**, *39*, 1007–1014.

7. (a) Huang, B.; Ge, J. J.; Li, Y.; Hou, H. *Polymer* **2007**, *48*, 264–269. (b) Greiner, A.; Hou, H.; Reuning, A.; Thomas, A.; Wendorff, J. H.; Zimmermann, S. *Cellulose* **2003**, *10*, 37–52. (c) Wojciechowski, P. *J. Appl. Polym. Sci.* **2000**, *76*, 837–844. (d) Hou, H.; Reuning, A.; Wendorff, J. H.; Greiner, A. *Macromol. Chem. Phys.* **2000**, *201*, 2050–2054. (e) Guittard, F.; Yamagishi, T.; Cambon, A.; Sixou, P. *Macromolecules* **1994**, *27*, 6988–6990. (f) Bhadani, S. N.; Tseng, S.-L.; Gray, D. G. *Macromol. Chem.* **1983**, *184*, 1727–1731. (g) Tseng, S.-L.; Laivins, G. V.; Gray, D. G. *Macromolecules* **1982**, *15*, 1262–1264. (h) Tseng, S.-L.; Valente, A.; Gray, D. G. *Macromolecules* **1981**, *14*, 715–719.
8. (a) Khan, F. Z.; Shiotsuki, M.; Nishio, Y.; Masuda, T. *Macromolecules* **2007**, *40*, 9293–9303. (b) Morita, R.; Khan, F. Z.; Sakaguchi, T.; Shiotsuki, M.; Nishio, Y.; Masuda, T. *J. Membr. Sci.* **2007**, *305*, 136–145. (c) Khan, F. Z.; Sakaguchi, T.; Shiotsuki, M.; Nishio, Y.; Masuda, T. *Macromolecules* **2006**, *39*, 9208–9214. (d) Khan, F. Z.; Sakaguchi, T.; Shiotsuki, M.; Nishio, Y.; Masuda, T. *Macromolecules* **2006**, *39*, 6025–6030.
9. (a) Zhang, C.; Price, L. M.; Daly, W. H. *Biomacromolecules* **2006**, *7*, 139–145. (b) Newkome, G. R.; Weis, C. D.; Abourahma, H. *ARKIVOC* **2000**, *1*, 210–217. (c) Depuy, C. H.; King, R. W. *Chem. Rev.* **1960**, *60*, 431–457.
10. Stevens, M. P. *Polymer Chemistry: An Introduction*, 3rd ed.; Oxford University Press: New York, 1999; pp 70–74.

List of Publications

Chapter 1

Synthesis, Characterization, and Gas Permeation Properties of Silylated Derivatives of Ethyl Cellulose

Khan, F. Z.; Sakaguchi, T.; Shiotsuki, M.; Nishio, Y.; Masuda, T.

Macromolecules **2006**, *39*, 6025–6030.

Chapter 2

Perfluoroacylated Ethyl Cellulose: Synthesis, Characterization, and Gas Permeation Properties

Khan, F. Z.; Sakaguchi, T.; Shiotsuki, M.; Nishio, Y.; Masuda, T.

Macromolecules **2006**, *39*, 9208–9214.

Chapter 3

Synthesis and Properties of Amidoimide Dendrons and Dendronized Cellulose derivatives

Khan, F. Z.; Shiotsuki, M.; Nishio, Y.; Masuda, T.

Macromolecules **2007**, *40*, 9293–9303.

Chapter 4

Synthesis, Characterization, and Gas Permeation Properties of *t*-Butylcarbamates of Cellulose Derivatives

Khan, F. Z.; Shiotsuki, M.; Nishio, Y.; Masuda, T.

J. Membr. Sci. Submitted.

Chapter 5

Synthesis and Properties of Amino Acid Esters of Hydroxypropyl Cellulose

Khan, F. Z.; Shiotsuki, M.; Sanda, F.; Nishio, Y.; Masuda, T.

J. Polym. Sci. Part A: Polym. Chem. In Press.

Publications Not Included in the Thesis

1. Synthesis, Characterization, and Gas Permeation Properties of the Silyl Derivatives of Cellulose Acetate

   Morita, R.; Khan, F. Z.; Sakaguchi, T.; Shiotsuki, M.; Nishio, Y.; Masuda, T.

   J. Membr. Sci. **2007**, *305*, 136–145.

2. Synthesis and Properties of Poly(phenylacetylene)s Carrying Siloxy, Hydroxy and Carbonate Groups

   Saeed, I.; Shida, Y.; Khan, F. Z.; Shiotsuki, M.; Masuda, T.

   Macromolecules Submitted.

3. Cellulose-Based Organic Radical Battery: Synthesis and Charge/Discharge Properties of Free Radical Carrying Cellulose Derivatives

   Qu, J.; Khan, F. Z.; Satoh, M.; Wada, J.; Hayashi, H.; Mizoguchi, K.; Masuda, T.

   Polymer Submitted.

4. Amino- and Carbamate-Substituted Poly(phenylacetylene)s: Synthesis and Properties

   Saeed, I.; Khan, F. Z.; Shiotsuki, M.; Masuda, T.

   To be Submitted.

5. Synthesis, Characterization, and Gas Permeation Properties of Amino Acid-Functionalized Ethyl Cellulose

   Ikeuchi, Y.; Khan, F. Z.; Shiotsuki, M.; Sanda, F.; Nishio, Y.; Masuda, T.

   To be Submitted.

Acknowledgments

While submitting this doctoral thesis and looking back at the events which have gone by, I realize that my supervisor, Professor Toshio Masuda earns most of the credit given the fact that he gave me such an amazing research project which brought forth the best in me. His candid advice, suggestions and behavior injected this faith in me that I can surmount such a challenging task.

I am indeed indebted to Assistant Professor Masashi Shiotsuki, whom I found exceptionally patient for inculcating the fundamental techniques for my project, which were outstandingly conducive during the research. Associate Professor Fumio Sanda also deserves my heartiest gratitude for his helpful suggestions and enriching discussions. I am also very grateful to all the members of the Masuda research group for their cheerful company and cooperation, whose words have always been a source of encouragement, which kindled my heart and aroused in me the will to make rapid strides.

My earnest feelings of reverence are due to Professor Yoshiyuki Nishio without whose valuable suggestions, comments and discussions, I would not have been able to explore multiple dimensions of my research theme. He is the one who accompanied me in making my way through various obstacles which I confronted during the completion of my doctoral degree. I would also like to express my sincere regards for the group members in his lab, especially Mr. Takahiro Ohno, Mr. Dan Aoki, and Mr. Ryosuke Kusumi who made me feel at home by sharing their ideas which developed into an in-depth understanding and knowledge about my research topic. I am highly obligated to Professor Yoshiki Chujo and Professor Shunsaku Kimura for their pragmatic suggestions and enriching comments. One of my seniors, Mr. Toshikazu Sakaguchi, also deserves my heart-felt regards. I thank him for his patience as I always turned to him, at times repeatedly, for the problems I encountered in the initial yet the most stressful stages of my research work.

My parents' relentless faith in the accomplishment of this task and their unfaltering support has always provided me solace through every ordeal I went through. Their constant prayers made me resolute in maximizing the results which I can derive from this research work. I would like to express my heartfelt and veracious gratitude for my ever-loving Filza, Faiza, and Awais, who have helped me all the way along, providing me immense help and courage when confronted to a perilous brink.

On a more personal note, a special acknowledgment of thanks and gratitude must be given to my husband, Irfan, who has felt through all the unfathomable moments of my life along with me. He gauged the intensity of my feelings and grew inside me as an entity without which this task would have never sought completion. He has transformed into the love of my life by selflessly backing up my love for chemistry.

Finally, I am grateful to the Ministry of Education, Culture, Sports Science and Technology (MEXT), Japan for the award of MEXT scholarship.

Fareha Zafar Khan

January 2008

Synthesis, Characterization, and Gas Permeation Properties of Novel Cellulose Derivatives **Fareha Zafar KHAN** **2008**